



Università degli Studi di Firenze  
Facoltà di Scienze Matematiche, Fisiche e Naturali  
Dottorato di Ricerca in Scienze Chimiche  
XXI Ciclo

**Modified Glycopeptides to Investigate Antigen-Antibody  
Interaction in Multiple Sclerosis**

Feliciana Real Fernández

Tutor  
Prof. Anna Maria Papini

PhD Supervisor  
Prof. Gianni Cardini

31th December 2008



<b>Introduction .....</b>	<b>5</b>
Antigen-Antibody interaction.....	5
Molecular mechanisms of autoimmune diseases.....	8
Antibodies as biomarkers of autoimmune diseases.....	11
From Radio-Immuno Assay to Enzyme-Linked Immunosorbent Assay	12
From peptide-epitope discovery to peptide-based immunoassays .....	13
Epitope discovery by a “Chemical Reverse Approach”	
in autoimmune diseases .....	15
Multiple Sclerosis and the glucosylated peptide CSF114(Glc)	
as mimetic of protein autoantigens.....	16
<b><u>PART A: Glycopeptide antigen-antibody interaction</u></b>	
<b><u>in Multiple Sclerosis .....</u></b>	<b>21</b>
<b>1. Characterisation of the epitope of the glycopeptide mimetic</b>	
<b>antigen: role of the sugar moiety and of its configuration linking</b>	
<b>to asparagine side chain .....</b>	<b>21</b>
1.1 Synthesis of <i>N</i> - $\alpha$ -glucosylated asparagine building block Fmoc-	
Asn( $\alpha$ GlcAc4)-OH .....	23
1.2 Synthesis of glycopeptide mimetics.....	30
1.3 Immunochemical assays of CSF114(Glc) analogues.....	31
<b>2. Modification of the glycopeptide antigen CSF114(Glc)</b>	
<b>with electrodetectable molecules to improve antibody detection .....</b>	<b>35</b>
2.1 Ferrocenyl derivatives as electrochemical probes.....	36
2.2 Synthetic strategy to labelled peptides.....	38
2.3 Immunoenzymatic assays of ferrocenyl peptides.....	40
2.4 Electrochemical measurements.....	43
<b>3. Identification of antibodies by Surface Plasmon Resonance .....</b>	<b>49</b>
3.1 Synthetic biotinylated glycopeptides	
for autoantibody recognition in Multiple Sclerosis patients’ serum.....	49
3.2 Antigen-antibody interaction study in Multiple Sclerosis	
patients’ serum by Surface Plasmon Resonance .....	51
<b>4. Real-time measurements of antigen-antibody force interactions</b>	
<b>in Multiple Sclerosis by Optical Tweezers.....</b>	<b>57</b>
4.1 Design and synthesis of optically labelled CSF114(Glc)-	
glycopeptide analogues for Optical Tweezers measurement. ....	58
4.2 Functionalization of the microscopic beads .....	59
4.3 Real-time antigen-antibody interaction measurements .....	60
4.4 Rupture force statistic study of CSF114(Glc)-anti-CSF114(Glc)	
IgG antibodies .....	65

## SUMMARY

<b><u>PART B: Study on molecular mechanisms of autoantibody recognition in Multiple Sclerosis.....</u></b>	<b><u>67</u></b>
<b>5. Bilayers mimicking biological membranes.....</b>	<b>67</b>
5.1 Cells natural barrier .....	67
5.2 Why mimicking a biological membrane?.....	69
5.3 Biomimetic membranes: model systems .....	69
<b>6. Role of <math>\beta</math>-turn structures in membrane permeability.....</b>	<b>73</b>
6.1 CSF114(Glc) a $\beta$ -turn structure-based designed glycopeptide.....	74
<b>7. Mimetic antigens in a membrane model environment .....</b>	<b>75</b>
7.1 The tethered Bilayer Lipid Membrane (tBLM) system.....	76
7.2 Behaviour of glucosylated peptides CSF114(Glc) (I) and Scramble CSF114(Glc) (VI) in biomimetic membrane .....	78
7.3 Behaviour of unglucosylated peptides CSF114 (I') and Scramble CSF114 (VI') in biomimetic membrane .....	79
<b><u>Experimental Part.....</u></b>	<b><u>89</u></b>
<b>8. Experimental Part A.....</b>	<b>89</b>
8.1 Materials and methods.....	89
8.2 Synthesis of glucosyl amino acid derivatives.....	90
8.3 Solid Phase Peptide Synthesis .....	100
8.4 Immunoassays .....	106
8.5 Ferrocenyl electrochemical studies .....	109
8.6 Optical Tweezers procedures.....	110
<b>9. Experimental Part B.....</b>	<b>111</b>
9.1 Materials and methods.....	111
9.2 Peptide and glycopeptide synthesis .....	114
9.3 Bilayer preparation .....	115
9.4 Liposomes-peptide incubation.....	116
<b>10. Description of the techniques.....</b>	<b>119</b>
10.1 Surface plasmon resonance .....	119
10.2 Optical Tweezers .....	120
10.3 AC Voltammetry .....	123
10.4 Cyclic Voltammetry .....	124
10.5 Electrochemical impedance spectroscopy .....	125
<b><u>Abbreviations .....</u></b>	<b><u>127</u></b>

## Introduction

Protein-protein, protein-peptide, and peptide-peptide interactions are intrinsic to virtually most of cellular processes. Any listing of major research topics in biology — i.e., DNA replication, transcription, translation, splicing, secretion, cell cycle control, signal transduction, and intermediary metabolism — is also a listing of processes in which protein complexes have been implicated as essential components. As a consequence, the analysis of interactions between these complexes is no longer the exclusive domain of developmental biologists or molecular biologists; in fact chemical biologists and biophysicists have gotten by necessity into the act. Therefore, protein-protein interactions play an essential role for any process in a living cell in any different competence scientific field. Amplifying knowledge about these interactions could possibly allow to better understand protein-based disease conditions and could provide the basis for new therapeutic approaches.

The main purpose of this study performed during my PhD research project was to apply both classical and recent methods to identify and characterize antigen-antibody interactions, and to assess the strength of these interactions in the particular case study of Multiple Sclerosis.

### **Antigen-Antibody interaction**

The **antigen** (Ag) is usually a protein molecule that often protrudes from the surface of a cell inducing an immune response and producing specific antibodies. The modern definition encompasses all substances that can be recognized by the adaptive immune system. In a strict sense, antigens are those substances eliciting a response from the immune system, whereas antigens are all those defined molecules binding to specific antibodies.

Cells present antigens to the immune system via **Major Histocompatibility Complex (MHC)**. Depending on the antigen presented and the type of histocompatibility molecule, several types of immune cells can be activated.

## INTRODUCTION

**Antibodies** (Abs), also known as immunoglobulins, are used by the immune system to identify and neutralize foreign objects, such as bacteria and viruses. Antibodies can bind to different targets, allowing the immune system to recognize an equally wide diversity of antigens.

The specific association of antigens and antibodies is strongly dependent on hydrogen bonds, hydrophobic interactions, electrostatic, and Van der Waals forces. All antigen-antibody binding is reversible, and follows the basic thermodynamic principles of any reversible bimolecular interaction.

While B lymphocytes become stimulated, by those macromolecules (i.e. protein antigens) triggering a humoral response, the specific affinity of an antibody is not for the entire macromolecular antigen but for a particular portion or site of the protein antigen, which could be mimicked by a peptide. Small dimensions molecules cannot induce an adaptive immune response by themselves. These small molecules can be recognized by antibodies only after their conjugation to some macromolecules. In this case the small molecule is termed **hapten**, while the macromolecule is the carrier. Therefore the complex hapten-carrier is able to work as an immunogen. Moreover, relative low mass peptides are usually not immunogenic and need to be coupled to carriers to induce or augment an anti-peptide humoral immune response. This is the case for human little gastrin where conventional gastrin/carrier protein conjugates prepared via classical crosslinking reactions generally lead to strong anti-gastrin responses in terms of antisera titers.<sup>1</sup>

An antibody binds only a determinant or an epitope region of a macromolecule, which can also contain multiple determinants. Globular proteins generally do not contain identical repeated epitopes. While, in the case of polysaccharides and nucleic acids numerous identical determinants to regular intervals can be found again.

---

<sup>1</sup> Moroder, L.; Kocher, K.; Papini, A.M.; Dufresne, M. *Chemistry of peptides and proteins*, **1993**, 783-791.

## INTRODUCTION

The epitopes composed by linear (closed) amino acid sequences are termed **linear epitopes**. Usually, the binding site of an antibody can lodge an antigenic epitope of approximately 6 amino acids. Linear epitopes can be accessible to antibodies if they are exposed on the external surface of the antigen or in a conformationally extended region in the folded native protein. Differently, in **conformational epitopes**, the antibody interacts with amino acids not sequentially linked but spatially close one to each other, because of the protein folding. The variety of possible binding sites is huge with each potential binding site having its own structural properties derived by covalent bonds, ionic bonds, hydrophilic, and hydrophobic interactions characteristics of amino acid side-chains (Figure 1).

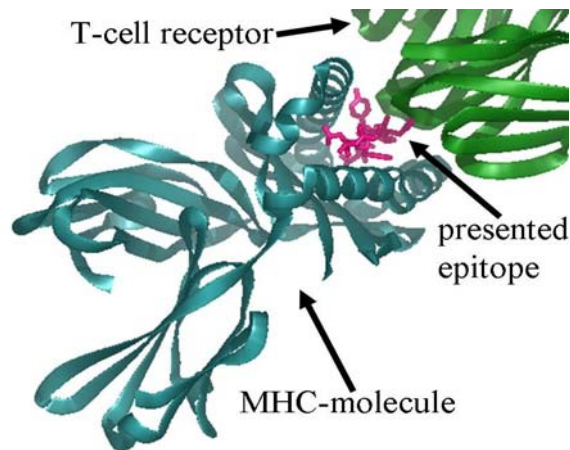


*Figure 1. MHC-I bound epitope is scanned by T-cell receptor.*

T cell recognition of glycopeptides may be important in the immune defense against microorganisms due to the fact that many microbial antigens are glycosylated. Evidences about T cell recognition of protein glycans may be crucial also for T cell responses to autoantigens in the course of autoimmune diseases.<sup>2</sup> Therefore, glycopeptides with simple sugars can be suitable tools to investigate the antigen fine specificity of glycoprotein-specific T cells.

---

<sup>2</sup> Bäcklund, J., Carlsen, S., Höger, T., Holm, B., Fugger, L., Kihlberg, J., Burkhardt, H. & Holmdahl, R. *Proc. Natl. Acad. Sci. USA* **2002**, *99*, 9960–9965.

## INTRODUCTION

Therefore, co- or post-translational modifications, e.g. glycosylation, as well as proteolysis can alter the native protein covalent structure generating new epitopes. These modified regions are termed neo-antigenic epitopes and can be recognized by different specific antibodies.

### **Molecular mechanisms of autoimmune diseases**

Autoimmune diseases affect at least 5% of the whole population and have a high social impact, because patients have a long expectation of life during which they are subordinated to the follow up of the disease by means of very invasive techniques, e.g. Magnetic Resonance Imaging (MRI), that are not suitable for a routine use.

In order to investigate the molecular mechanisms of autoimmune diseases, it is necessary to introduce the immune system, which is based on the ability to distinguish foreign molecules from self molecules. After the introduction of an unknown agent that is potentially pathogenic (antigen), the organism can reply to the attack by two different reactions of the immune system: the antibody (Ab) or humoral response and the cell-mediated immune response.

- Humoral responses involve antibodies that are produced by B-lymphocytes and are able to bind specifically to the foreign antigen. B-lymphocytes create an antigen/antibody complex to neutralize and kill the foreign, dangerous molecule. B-cells are programmed to produce a single antibody class, especially receptors for proteins or peptide fragments that present a high affinity (epitopes).
- Cell-mediated immune responses involve the production of specialized cells that react with foreign antigens on the surface of other host cells. T-lymphocytes, employed in cell-mediated responses, stimulate B-lymphocytes and fight against foreign substances by using a composite mechanism. T-lymphocytes kill infected cells and expose fragments on the membrane surface. The Antigen Presenting Cell (APC) exposes peptide fragments, derived from



hydrolysis of all the proteins being into the cell, by a special class of cell-surface glycoproteins, e.g. the MHC molecules.

Foreign molecules can substitute self peptides and cause the reaction of the immune system. T-cells use a specific T-cell Receptor and induce the formation of the MHC/peptide antigen complex. This trimolecular complex induces immune responses.

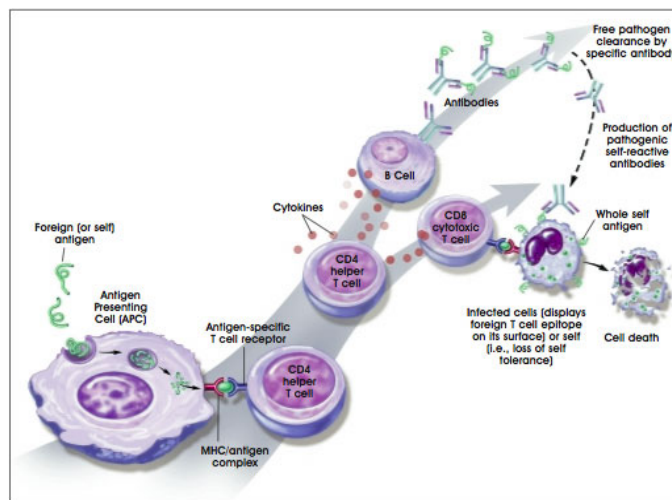


**Figure 2.** Mechanism of the immune response.

Autoimmune diseases are due to a "mistake of evaluation" of the immune system, which no more recognizes self-antigens.<sup>3</sup> The immune system can occasionally attack self-antigens triggering an autoimmune response, with damages to the tissues on which these antigens are expressed. Autoimmune disorders are up to now considered as triggered by T lymphocytes further inducing an autoantibody response.

In some autoimmune disorders a pathologic immune response is localised to specific antigens confined to a particular organ system. Alternatively, systemic autoimmune diseases are characterized by an immune response to ubiquitous

<sup>3</sup> N. Rose, I. Mackay, *The Autoimmune Diseases*, 2006, Elsevier Academic Press, 4<sup>th</sup> edition.

## INTRODUCTION

intracellular antigens in which the relationship between immune specificity and disease manifestations may not be obvious.

It is now accepted that autoimmune diseases have a multifactorial origin including genetic predisposition, endogenous, and exogenous elements. Many infectious bacteria and viruses contain surface carbohydrates with a very similar molecular structure and/or conformation to mammalian surface glycoproteins and glycolipids. **Molecular mimicry** is the process by which viruses or bacteria activate an immune response because of a cross-reaction with self-antigens (Figure 3).<sup>4</sup> Moreover, such homology should involve a self-determinant displaying an important biological activity so that the immune attack injures tissues and cause a disease. As an example, in Guillain Barré syndrome (GBS), which is considered a prototype of post-infectious autoimmune disease, molecular mimicry has been considered responsible of triggering the disease. Clinically, GBS is characterized by an acute ascending flaccid paralysis that is often generated by a preceding viral or bacterial infection. The most commonly identified triggering agents are pathogens having carbohydrate sequences (considered the antigens) in common with peripheral nervous tissue.

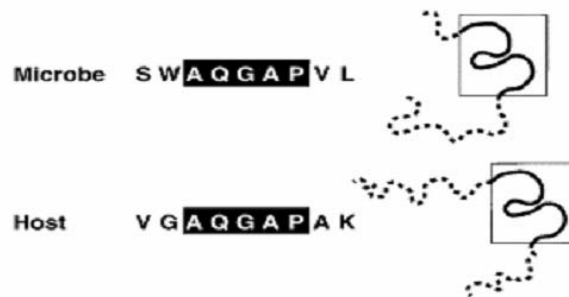


*Figure 3. Molecular mimicry.*

In other autoimmune diseases in which the antigens have not yet been characterised, possibly not only carbohydrates can modify by a covalent bond

---

<sup>4</sup> Oldstone, M. B. A. *Cell* **1987**, *50*, 819-820.

a self-protein antigen, which will become a non-self one triggering an abnormal antibody response.<sup>5</sup> Therefore, aberrant glycosylation of self-antigens (proteins) can be responsible of influencing the level of epitope production, and the generation of neoepitopes, leading to autoimmune responses.

It is evident that different hypotheses have been proposed to explain autoimmune processes to dissect the intricate pathogeneses of such diseases in the natural complexity of the biochemical mechanisms.

### **Antibodies as biomarkers of autoimmune diseases**

A biomarker is an anatomical, physiological, and/or biochemical parameter, which should be easily determined and used as indicator of normal physiological or pathogenic processes. Molecules present in tissues and biological fluids can be identified as biomarkers and used to set up diagnostic/prognostic tools. Moreover, biomarkers can be used also for monitoring the efficacy of a therapeutic treatment. Sera from patients suffering from autoimmune disorders often contain multiple types of autoantibodies. Some autoantibodies can be exclusive of a disease and used as biomarkers. In particular, if they fluctuate with disease exacerbations or remissions, autoantibody detection is extremely valuable in the follow up of patients. Consequently, the antibodies present in patients' serum can be used as disease biomarkers.<sup>6, 7</sup> Therefore, evaluation of antibodies as disease specific biomarkers is extremely important not only for diagnosis, follow-up, and prevention of autoimmune diseases, but also for "theragnostics", i.e. evaluation of efficacy of specific therapeutic treatments.<sup>8,9</sup>

---

<sup>5</sup> S. Mouritsen, M. Meldal, I. Christiansen-Brams, H. Elsner, O. Werdelin, *Eur. J. Immunol.*, **1994**, *24*, 1066-1072.

<sup>6</sup> D. Leslie, P. Lipsky, A. L. Notkins, *J Clin Invest* **2001**, *108*, 1417-1422.

<sup>7</sup> Alcaro, M.C.; Lolli, F.; Migliorini, P.; Chelli, M.; Rovero, P.; Papini, A.M. *Chemistry Today* **2007**, *25* (5), 14-16.

<sup>8</sup> P. Roland, P.; Atkinson, J.A.; Lesko, L.J. *Clin. Pharm. Ther.* **2003**, *73*, 284-291.

## INTRODUCTION

Native proteins formulate antigens and have been exploited to raise antibodies for different purposes. This characteristics was translated in their use to identify autoantibodies that was traditionally achieved using directly damaged patients' tissues containing triggering agents in different immunoassays. Biological fluids containing autoantibodies have replaced the use of damaged tissues as a non-invasive alternative. Unfortunately, in autoimmune diseases only very low specific antibodies were demonstrated to be detected in serum, possibly because proteins used in the assays were not reproducing the real autoantigen. Moreover, an entire protein should contain more than one epitope specific for different autoantibodies. Yet, growing evidences indicate that post-translational modifications, either native or aberrant, may play a fundamental role for specific autoantibody recognition in autoimmune diseases.<sup>10</sup> These observations account, at least in part, for the limited success got in the discovery of biomarkers for autoimmune diseases using proteomic analysis and/or protein microarrays.

### **From Radio-Immuno Assay to Enzyme-Linked Immunosorbent Assay**

Over the past years, autoimmunity diagnosis has gone through a very dynamic period, associated with the introduction of new tests deriving from the identification of various new families of autoantibodies and the demonstration of their usefulness in clinic. A better knowledge of autoantigen molecules has been associated with the very rapid growth of molecular biology technologies. In the field of autoimmune diseases, a number of autoantibody detection techniques have been developed. Radio-Immuno Assay (RIA) has been traditionally used in autoantibody detection and it is based on labelled targets providing a radioactive signal. In fist versions of RIA, a radioactive-labelled

---

<sup>9</sup> Baker, M.; *Nature Biotech.* **2005**, 23, 297-304.

<sup>10</sup> Doyle, H.A.; Mamula, M.J. *Trends Immunol.* **2001**, 22, 443-449.

substance, or isotopes of the substance, was mixed with antibodies and inserted in a sample containing patient's tissue. The same non-radioactive substance in these tissues took the place of the isotope in the antibodies, thus leaving the radioactive substance free, generating a signal. Up to now, autoantibodies detection in assays is usually performed using recombinant native protein antigens as non-invasive protocols. Moreover, RIA also requires special radioactivity instrumentation and precautions. Therefore, today RIA was largely supplanted by the Enzyme-Linked Immunosorbent Assay (ELISA) when possible, because in ELISA the antigen-antibody reaction is measured using a colorimetric signal instead of a radioactive signal.

Even more recently, the application of proteomic technologies for the diagnosis of autoimmune diseases has opened new diagnostic scenarios, which could revolutionize diagnostic procedures in future suggesting some interesting opportunities.

### **From peptide-epitope discovery to peptide-based immunoassays**

In autoimmune diseases, characterization of autoantibodies by protein antigens isolated from biological material or reproduced by recombinant technologies has sometimes turned out as an unrealistic approach. In fact the big limit in using such material is a mistake in epitope recognition because of mutations and/or unfolded sequences, or lack of post-translational modifications.

The most logical alternative could be the use of peptides derived from native protein sequences and reproducing specific epitopes including the hapten. In some instances, antibody recognition by peptides could be even more effective and specific than by native proteins.

Peptides are particularly useful when the epitope sequence has been discovered inside the total protein. In fact, native protein antigens (particularly if underexpressed) can be difficult to be fully sequenced or cannot often be successfully reproduced using recombinant techniques. In any case protein

## INTRODUCTION

folding can be also a difficult task. Moreover, proteins may be difficult to isolate with correct co- or post-translational modifications. On the contrary, epitope discovery by peptides as synthetic antigens requires only identifying an amino acid sequence limited in length. Exposition of the epitope is a challenge to optimise antibody recognition. Moreover, peptide antigens can display enhanced recognition specificity eliminating or minimizing potential cross-reactivity between structurally homologous protein epitopes.

Peptides have several advantages: they are relatively easy to produce and may retain chemical stability over time. Moreover, reproduction of co- or post-translational modifications in peptides, synthetically speaking, is a quite easy task compared to recombinant techniques.<sup>11</sup> Therefore theoretical ability to understand the immune response with defined peptide epitopes can have important advantages. Nowadays these hypotheses are confirmed by a limited number of peptide-based assays widely expanding for characterization of antibodies in different infectious diseases, i.e. Scheriacoli, Salmonella,<sup>12</sup> Chlamydia trachomatis,<sup>13</sup> etc.

In the particular case of Reumathoid Arthritis (RA), several aberrant modifications of proteins (such as Arg deimination leading to citrulline formation and/or methylation) have been associated with its pathogenesis and lead to the development of different synthetic modified antigens used in simple ELISA.<sup>10</sup> A key step in setting up the commercially available ELISA for RA was represented by identification of deiminated sequences of filaggrin that are recognized in a high percentage of RA sera.<sup>14,15</sup> Sensitivity of the assay was

---

<sup>11</sup> Papini, A.M. "Peptide-based Immunoassays for Biomarkers Detection: a Challenge for Translational Research" *Zervas Award Lecture 30<sup>th</sup> European Peptide Symposium*, August 31-September 5 2008, Helsinki, Finland.

<sup>12</sup> Kulagina, N. V.; Shaffera, K.M.; Anderson, G.P.; Liglera, F.S.; Taitt, C. R. *Anal. Chim. Acta*, **2006**, 575, 9-15.

<sup>13</sup> Morré, S.; Munk, C.; Persson, K.; Krüger-Kjaer, S.; Van Dijk, R.; Meijer, C.; Van den Brule, A. *J Clin Microbiol.* **2002**, 40(2), 584-587.

<sup>14</sup> Sebbag, M.; Simon, M.; Vincent, C.; Masson-Bessiere, C.; Girbal, E.; Durieux, J.J.; Serre, G.; *J. Clin. Invest.* **1995**, 95, 2672-2679

increased modifying the peptide structure to optimally expose the citrulline moiety. In fact a cyclic citrullinated peptide allows detection of antibodies in up to 70% RA patients.<sup>16</sup> This ELISA is now considered a gold standard for RA diagnosis and follow up.

### **Epitope discovery by a “Chemical Reverse Approach” in autoimmune diseases**

In order to develop optimised synthetic peptides as antigenic probes for fishing out autoantibodies from biological fluids as biomarkers, an innovative “Chemical Reverse Approach” has been developed for the first time in the Laboratory of Peptide and Protein Chemistry and Biology (PeptLab). This approach was defined “Reverse” because the screening of the synthetic antigenic probe is guided by autoantibodies circulating in autoimmune disease patients’ blood. “Chemical” because autoantibody recognition drives selection and optimisation of the “chemical” structure from defined peptide libraries.<sup>17</sup>

Thus, autoantibodies circulating in patients’ biological fluids allow the selection of synthetic post-translationally modified peptides mimicking new epitopes in antigens. Peptide epitopes identified by this approach, if selectively and specifically recognizing autoantibodies in a statistically significant number of patients, can be used as antigenic probes in immunoenzymatic assays to detect disease biomarkers in an efficient synthetic way.

The screening of focused libraries of unique modified peptide molecules is a valuable strategy to obtain optimised peptide antigens containing the minimal epitope with the correct modification to detect at the best autoantibodies

---

<sup>15</sup> Serre, G. *Joint Bone Spine* **2001**, 68, 103-105

<sup>16</sup> Schellekens, G.A.; de Jong, B.A.; van den Hoogen, F.H.; van de Putte, L.B.; van Venrooij, W.J. *J. Clin. Invest.* **1998**, 101, 273-281

<sup>17</sup> Papini, A.M. “A Chemical Reverse Approach to Modified Peptides as Synthetic Antigenic Probes to detect autoantibodies as Biomarkers of Multiple Sclerosis”. *1st Dimitrios Theodoropoulos Memorial Lecture Award*. 6<sup>th</sup> Hellenic Forum on Bioactive Peptides, May 18, **2008**, Patras, Greece.

## INTRODUCTION

specific of the autoimmune disease under investigation.<sup>18</sup> As a proof-of-concept this approach has been successfully applied for the identification of autoantibodies as biomarkers of an autoimmune mediated form of Multiple Sclerosis, the most difficult disease because protein antigens are localized in the central nervous system.

### **Multiple Sclerosis and the glucosylated peptide CSF114(Glc) as mimetic of protein autoantigens**

Multiple Sclerosis (MS) is an autoimmune, chronic, inflammatory, demyelinating disease of the central nervous system (CNS), which represents a group of very heterogeneous disorders. Distinctive neuropathological features are present in the disorder suggesting different pathophysiological mechanisms leading to the formation of myelin lesions.<sup>19,20</sup> Several data suggest that the disease pathogenesis is linked to an autoimmune mechanism against the prominent CNS myelin antigens,<sup>21</sup> possibly triggered by a viral or bacterial infection. The target antigens are not definitively defined because of their difficult localization. Multiple Sclerosis lesions are characterized by large sharply, demarcated areas of demyelination, with macrophage infiltration and accumulation of T lymphocytes. Different self-proteins of myelin have been investigated as potent targets for T or B cells in Multiple Sclerosis, e.g. Myelin Oligodendrocyte Glycoprotein (MOG).

---

<sup>18</sup> Lolli, F.; Rovero, P.; Chelli, M.; Papini, A.M. *Expert Rev. Neurotherapeutics* **2006**, 6 (5), 781-794.

<sup>19</sup> Lucchinetti C, Bruck W, Rodriguez M, Lassmann H. *Brain Pathol* **1996**, 6, 259-274.

<sup>20</sup> Lassmann H: *Multiple Sclerosis* **1998**, 4, 93-98.

<sup>21</sup> Martin, R.; McFarland, H. *Crit. Rev. Clin. Lab. Sci.* **1995**, 32, 121-182.



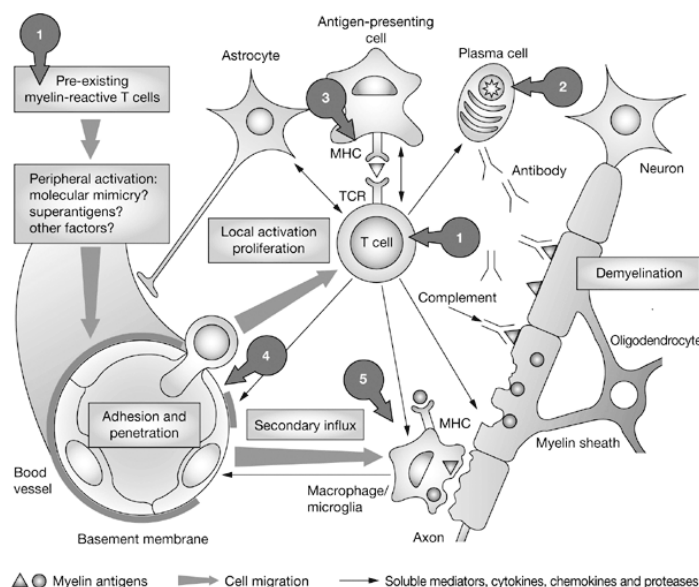


**Figure 4.** Possible therapeutic targets: (1) depletion or inhibition of T cells, (2) depletion or inhibition of plasma cells, (3) interference with the molecular mechanisms of T-cell activation, (4) inhibition of lymphocyte migration, and (5) inhibition of soluble mediators, such as cytokines and chemokines. MHC, major histocompatibility complex; TCR, T-cell receptor.

In particular, in the Laboratory of Peptide & Protein Chemistry & Biology of the University of Florence, it was demonstrated that the glucosylated peptide [Asn<sup>31</sup>(Glc)hMOG(30-50)] is able to detect autoantibodies in Multiple Sclerosis patients' sera by ELISA experiments.<sup>22</sup> It was observed that the ability of the glucosylated peptide to detect autoantibodies in Multiple Sclerosis was linked to characteristics other than conformation and that the specific autoantibody binding site on MOG glycopeptide was related to the *N*-linked glucosyl moiety.<sup>23</sup>

<sup>22</sup> Mazzucco, S.; Mata, S.; Vergelli, M.; Fioresi, R.; Nardi, E.; Mazzanti, B.; Chelli, M.; Lolli, F.; Ginanneschi, M.; Pinto, F.; Massacesi, L.; Papini, A. M. *Bioorg. Med. Chem. Lett.* **1999**, *9*, 167-172.

<sup>23</sup> Carotenuto, A.; D'Ursi, A.M.; Nardi, E.; Papini, A.M.; Rovero, P. *J. Med.Chem.* **2001**, *44*, 2378-2381.

## INTRODUCTION

Hence, the recognition properties of the molecule were optimized through the design and screening of focused libraries of glycopeptides by a “Chemical Reverse Approach”. The family of specific antigenic probes, **CSF114(Glc)**, was developed to identify autoantibodies, as biomarkers of Multiple Sclerosis correlating with disease activity. The glycopeptides based on CSF114(Glc), a structure-based designed glucosylated peptide as first Multiple Sclerosis Antigenic Probe (MSAP),<sup>24,25</sup> are able to measure accurately high affinity autoantibodies in sera of a statistically significant patients’ population.<sup>26,27</sup> The glycopeptides are characterised by different types of  $\beta$ -turn structures bearing as minimal epitope a  $\beta$ -D-glucopyranosyl moiety linked to an Asn residue on the tip of the turn possibly reproducing an aberrant *N*-glucosylation of myelin proteins fundamental for autoantibody recognition.<sup>22,28</sup>

---

<sup>24</sup> Lolli, F.; Mulinacci, B.; Carotenuto, A.; Bonetti, B.; Sabatino, G.; Mazzanti, B.; D’Ursi, A. M.; Novellino, E.; Pazzagli, M.; Lovato, L.; Alcaro, M. C.; Peroni, E.; Pozo-Carrero, M. C.; Nuti, F.; Battistini, L.; Borsellino, G.; Chelli, M.; Rovero, P.; Papini, A.M. *Proc. Natl. Acad. Sci., U.S.A.* **2005** *102*(29), 10273-10278.

<sup>25</sup> Lolli, F.; Mazzanti, B.; Pazzagli, M.; Peroni, E.; Alcaro, M.C.; Sabatino, G.; Lanzillo, R.; Brescia Morra, V.; Santoro, L.; Gasperini, C.; Galgani, S.; D’Elios, M.M.; Zipoli, V.; Sotgiu, S.; Pugliatti, M.; Rovero, P.; Chelli, M.; Papini, A.M. *J Neuroimmunol.* **2005**, *167*, 131-137

<sup>26</sup> Carotenuto, A.; D’Ursi, A. M.; Mulinacci, B.; Paolini, I.; Lolli, F.; Papini, A. M.; Novellino, E.; Rovero P. A. *J. Med. Chem.* **2006**, *49*, 5072-5079.

<sup>27</sup> Carotenuto, A.; Alcaro, M.C.; Saviello, M.R.; Peroni, E.; Nuti, F.; Papini, A.M.; Novellino, E.; Rovero, P. *J. Med. Chem.*, **2008**, *51*, 5304–5309.

<sup>28</sup> Nuti, F.; Paolini, I.; Cardona, F.; Chelli, M.; Lolli, F.; Brandi, A.; Goti, A.; Rovero, P.; Papini, A.M. *Bioorg. Med. Chem.* **2007**, *15*, 3965-3973.

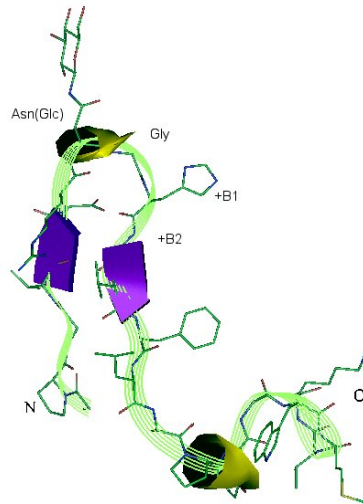


**Figure 5.** Calculated structures of CSF114(Glc). Ribbon diagram of the lowest energy conformer of 200 calculated structures of CSF114(Glc) derived from NMR data.

Up to now, N-glycosylation, a post-translational modification not common in eukaryotic proteins, has been detected only in bacterial glycoproteins.<sup>29</sup> Putative glycosylation of myelin proteins, by a still unknown mechanism, could transform self-antigens in non-self ones and triggering an autoimmune response. More than one protein could be aberrantly glycosylated creating a family of new autoantigens. Our hypothesis is that an aberrant N-glycosylation of myelin proteins could generate neoantigens no more recognized as self and for that reason triggering an autoimmune response. More than one protein could be aberrantly glycosylated and CSF114(Glc) could be a mimetic of all those glycosylated proteins.

---

<sup>29</sup> Wieland, F.; Heitzer, R.; Schaefer, W. *Proc. Natl. Acad. Sci. U.S.A.* **1983**, *80*, 5470-5474.



## **PART A: Glycopeptide antigen-antibody interaction in Multiple Sclerosis**

### ***1. Characterisation of the epitope of the glycopeptide mimetic antigen: role of the sugar moiety and of its configuration linking to asparagine side chain***

Carbohydrates play an important role in biological function of glycoproteins. They can be involved in recognition signal, in cell adhesion, cell growth regulation, etc. Moreover, glycosylation is the most common co- or post-translational modification of proteins in eukaryotic cells. Two main forms of protein glycosylation are naturally found: *O*- and *N*-glycosylation. Naturally occurring *N*-glycoproteins and *N*-glycopeptides are usually reported to present as first sugar an *N*-acetyl glucosamine *N*- $\beta$ -linked to Asn side chain into the specific consensus sequence Asn-Xaa-Ser/Thr (where Xaa is any amino acid except Pro). The *N*-glycosidic bond links the glycan portion and the side chain of an asparagine residue. One exception is represented by nephritogenoside, a glycopeptide able to induce glomerulonephritis in its animal models,<sup>30</sup> where the *N*-terminal sequence Asn-Pro-Leu is modified by a trisaccharide consisting of three *O*-linked glucosyl (Glc) residues, with *N*- $\alpha$ -Glc as the first sugar moiety linked to the Asn residue.<sup>31</sup>

Following the hypothesis that an aberrant glycosylation could trigger autoantibodies in Multiple Sclerosis, different families of autoantibodies to proteins aberrantly glycosylated with different sugar moieties might be related to disease activity.<sup>24</sup> Moreover, some authors reported of specific anti-Glc( $\alpha$ 1,4)Glc( $\alpha$ ) identified in different MS patients suggesting an important

---

<sup>30</sup> Shibata, S., Sakaguchi, H., and Nagasawa, T.; *Nephron*, **1976**, 16, 241-245.

<sup>31</sup> (a) Shibata, S.; Takeda, T.; Natori, Y. *J. Biol. Chem.* **1988**, 263, 12483-12485. (b) Takeda, T.; Sawaki, M.; Ogihara, Y.; Shibata, S. *Chem. Pharm. Bull.* **1989**, 37, 54-56.

## PART A

role for glucose-based modifications in the pathogenesis of MS.<sup>32</sup> These data have not yet been confirmed by other authors.

In previous studies performed at PeptLab, we selected CSF114( $\beta$ -Glc), as optimal Multiple Sclerosis Antigenic Probe (MSAP). CSF114( $\beta$ -Glc) was developed by a screening of a CSF114-type glycopeptide library based on O- and N- $\beta$ -glycosyl amino acid diversity (Glc, Man, Glc $\beta$ Glc, Gal, GlcNAc, etc) tested in ELISA.<sup>33,28</sup> Up to now, the role of different configuration, i.e. the  $\alpha$ -N-glycosyl moiety, has not been yet investigated, particularly because Fmoc-Asn( $\alpha$ GlcAc<sub>4</sub>)-OH had never been synthesized before (Figure 1.1). For that reason, we devoted some efforts to the synthesis of this new building block useful for solid phase synthesis of CSF114( $\alpha$ -Glc).

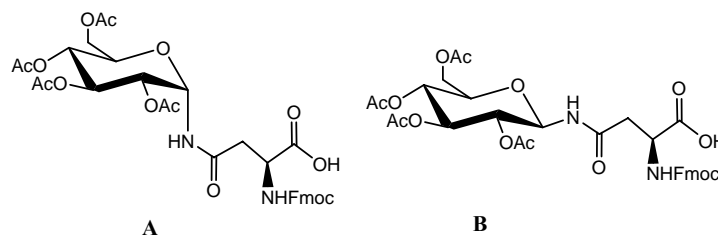


**Figure 1.1.** N-glycosylated asparagine building blocks Fmoc-Asn( $\alpha$ GlcAc<sub>4</sub>)-OH (A) and Fmoc-Asn( $\beta$ GlcAc<sub>4</sub>)-OH (B) orthogonally protected for Solid Phase Peptide Synthesis.

---

<sup>32</sup> Schwarz, M.; Spector, L.; Gortler, M.; Weisshaus, O.; Glass-Marmor, L.; Arnon Karni, L.; Dotan, N.; Miller, A. *Journal of the Neurological Sciences*, **2006**, 244 59 – 68.

<sup>33</sup> (a) Nuti, F.; Cicchi, S.; Peroni, E.; Pozo-Carrero, M. C.; Mazzanti, B.; Pazzagli, M.; Lolli, F.; Chelli, M.; Papini, A. M.; Brandi, A. *Peptides* **2002**, E. Benedetti; C. Pedone (Eds.), Edizioni Ziino, Castellammare di Stabia, Italy, 238-239. (b) Nuti, F.; Paolini, I.; Mulinacci, B.; Pozo-Carrero, M. C.; Mazzanti, B.; Pazzagli, M.; Lolli, F.; Chelli, M.; Cordero, F. M.; Brandi, A.; Papini, A. M. *Peptide Revolution: Genomics, Proteomics & Therapeutics*. M. Chorev & T.K. Sawyer (Eds), American Peptide Society, San Diego, CA, USA **2004**, 77-78.

## 1.1 Synthesis of *N*- $\alpha$ -glucosylated asparagine building block Fmoc-Asn( $\alpha$ GlcAc<sub>4</sub>)-OH

### 1.1.1 *State of the art*

In glycopeptide synthesis, much attention has to be paid to the stereoselective formation of the glycosidic bond which should survive during all the steps of peptide synthesis. The building block approach is up to now the most convenient one and therefore the most commonly used. In this case preformed glycosylated amino acid building blocks<sup>34</sup> can be employed in the stepwise assembly of the peptide backbone. The use of anomerically pure glycosylated amino acid building blocks in Solid-Phase Glycopeptide Synthesis (SPGPS) guarantees the presence of a selective sugar linkage to the amino acid side chain in the glycopeptide.

A variety of syntheses leading to  $\beta$ -N-linked amino acid building blocks are reported in the literature.<sup>35</sup> In particular, in previous studies performed in PeptLab we optimized large-scale synthesis of  $\beta$ -linked glycans to Asn and Gln side chains for a series of sugar moieties. In particular, thanks to microwave energy, the building block Fmoc-Asn( $\beta$ GlcAc<sub>4</sub>)-OH [useful in the glycopeptide synthesis of CSF114( $\beta$ -Glc)] was synthesized in a shorter time and in high yield compared to conventional approaches (Scheme 1).<sup>36</sup>

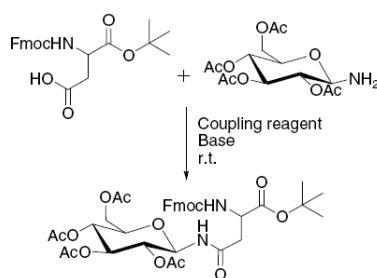
---

34 (a) M. Meldal, In: *Neoglycoconjugates: Preparation and Application*, ed. Y. C. Lee and R. T. Lee, Academic Press, Orlando, **1994**, 145-198; (b) M. Meldal, *Curr. Opin. Struct. Biol.*, **1994**, 4, 710-718; (c) M. Meldal, K. Bock, *Glycoconjugate J.*, **1994**, 11, 59-63.

35 (a) Christiansen-Brams, I.; Meldal, M.; Bock, K.; *J. Chem. Soc. Perkin Trans. 1*, **1993**, 1461-1471. (b) Van Ameijde, J.; Albada, H.B.; Liskamp, R.; *J. Chem. Soc. Perkin Trans. 1*, **2002**, 1042-1049. (c) Venkataramanarao, R.; Sureshbabu, V. *SYNLETT*, **2007**, 16, 2492-2496. (d) Toshuki, I. **1994**, patent JP 93-77583 19930311. (e) Ying, L.; Liu, R.; Zhang, J.; Lam, K.; Lebrilla, C. B.; Gervay-Hague, J. *J. Comb. Chem.*, **2005**, 7, 372-384.

36 Paolini, I.; Nuti, F.; Pozo-Carrero, M.C.; Barbetti, F.; Kolesinska, B.; Kaminski, Z.J.; Chelli, M.; Papini, A.M. *Tetrahedron*, **2007**, 48, 2901-2904.

## PART A



**Scheme 1.** Synthetic strategy to *Fmoc-L-Asn(βGlcAc<sub>4</sub>)-OtBu*

On the other hand, the interest in developing a stereoselective synthesis of  $\alpha$ -N-linked glycosylated asparagine prompted us to investigate several strategies. In fact, up to now very few ones have been reported and none for this anomeric building block orthogonally protected for both Fmoc/tBu and Boc/Bzl SPGPS.

Recently, the use of glycosylazides as starting reagent has replaced the traditional glycosylamines, classically used in the synthesis of the  $\beta$ -anomer, as a consequence of poor final stereoselectivity.<sup>37</sup> A method for the stereoselective synthesis of *N*-glycosylated asparagine, based on the traceless Staudinger ligation of glycosyl azide with pre-functionalized phosphines, has been reported.<sup>38</sup> In this case, the  $\alpha$ -glycosyl amide could be obtained only when hydroxyl functions of the glycosyl moiety were benzyl-protected. This synthetic strategy required two more steps to change sugar hydroxyl protecting groups from benzyl to acetate.

Damkaci and DeShong proposed a straightforward strategy to obtain acetylated *N*- $\alpha$ -glucosyl asparagine by controlling the stereochemistry of the carbohydrate anomeric center *via* an isoxazoline intermediate.<sup>39</sup> In this approach, the stereochemistry of the isoxazoline intermediate should control

<sup>37</sup>(a) Staudinger, H.; Meyer, J. *Helv. Chim. Acta* **1919**, 2, 635-646. (b) Gololobov, Y. G.; Kasukhin, L. F. *Tetrahedron*, **1992**, 48, 1353-1407. (c) Kovács, L.; Ösz, E.; Domokos, V.; Holzer, W.; Györgydeák, Z. *Tetrahedron* **2001**, 57, 4609-4621.

<sup>38</sup> Bianchi, A.; Bernardi, A.; *J. Org. Chem.*, **2006**, 71 (12), 4565-4577.

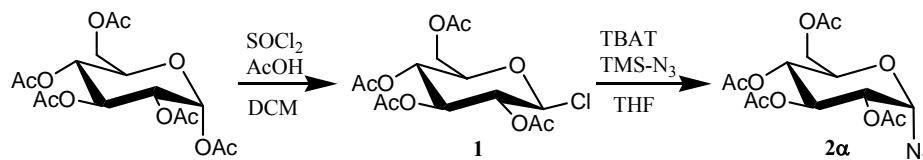
<sup>39</sup> Damkaci, F.; DeShong, P. *J. Am. Chem. Soc.* **2003**, 125, 4408-4409.



stereochemistry at the newly formed anomeric center. We followed this strategy to try to obtain the desired building block Fmoc-Asn( $\alpha$ -GlcAc<sub>4</sub>)-OH orthogonally protected for SPGPS.

**1.1.2 Synthesis of Fmoc-Asn( $\alpha$ -GlcAc<sub>4</sub>)-OH via 3,4,6-tri-O-acetyl- $\alpha$ -D-glucopyranosyl isoxazoline intermediate.**

Damkaci and DeShong previously reported that treatment of either  $\alpha$ - and  $\beta$ -glucopyranosyl azides with Ph<sub>3</sub>P in refluxing 1,2-dichloroethane in the presence of 4Å molecular sieves for 15 h gave exclusively  $\alpha$ -isoxazoline. During preparation of the isoxazoline (**3**) (Scheme 3), both  $\alpha$ - and  $\beta$ -glucopyranosylazide anomers (**2**) were used. Compound **2a** was previously synthesized as reported in Scheme 2 and compound **2b** is commercially available.



**Scheme 2.** Synthesis of  $\alpha$ -glucopyranosylazide derivative **2a**.

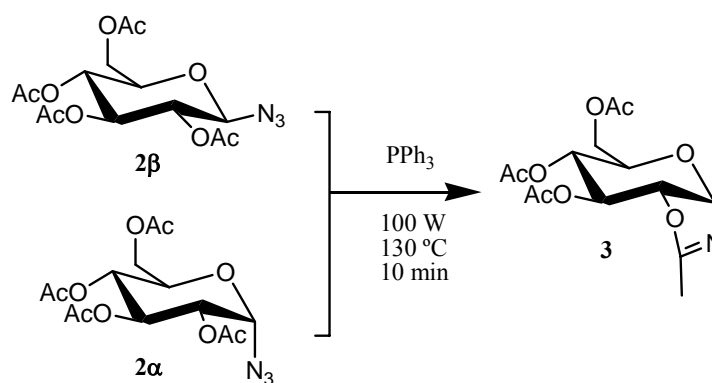
First of all, we tried to improve the synthesis of the isoxazoline **3** by microwave (MW) technology.

While MW-assisted synthesis is widely applied in other domains of organic synthesis, in the field of glycopeptide synthesis very few examples have been reported possibly because of the low stability of carbohydrates to thermal degradation.<sup>40</sup> Several results in other fields show enhanced reaction rates and

<sup>40</sup> (a) Das, S. K.; Reddy, K. A.; Abbineni, C.; Roy, J.; Rao, K. V. L. N.; Sachwani, R. H.; Iqbal, J. *Tetrahedron Lett.* **2003**, *44*, 4507. (b) Oliveiva, R. N.; Filho, J. R. F.; Srivastava, R. M. *Tetrahedron Lett.* **2002**, *43*, 2141. (c) Das, S. K.; Reddy, K. A.; Roy, J. *Synlett* **2003**, 1607. (d) Mathew, F.; Jayaprakash, K. N.; Fraser-Reid, B.; Mathew, J.; Scicinski, J. *Tetrahedron Lett.* **2003**, *44*, 9051.

## PART A

higher product yields as compared to conventional approaches.<sup>41</sup> Generally speaking, the MW energy should mainly be related to heat effects, and many reports have focused on “improvement of reactions”. We applied our expertise in the microwave-assisted synthesis of the  $\beta$ -glucosyl anomer linked to the Asn side chain orthogonally protected for SPGPS, Fmoc-Asn( $\beta$ GlcAc<sub>4</sub>)-OH,<sup>36</sup> to the synthesis of the corresponding  $\alpha$ -anomer Fmoc-Asn( $\alpha$ GlcAc<sub>4</sub>)-OH. The isoxazoline **3** was successfully synthesized under MW conditions at 100W and 130°C (Scheme 3). Thanks to MWs, the reaction time could be reduced from 15 h to only 10 min.



**Scheme 3.** Synthesis of 3,4,6-tri-O-acetyl- $\alpha$ -D-glucopyranosyl isoxazoline **3**.

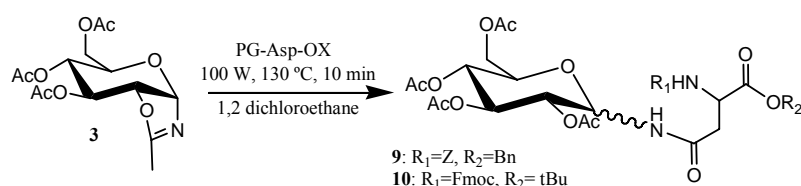
In the literature, it was previously reported the synthesis of Z-Asn( $\alpha$ GlcAc<sub>4</sub>)-OBn via acylation of the isoxazoline derivative **3** leading to *N*- $\alpha$ -peracetylated glucosyl asparagine protected at the  $\alpha$ -amino function with a benzyloxycarbonyl group (Z) and at the  $\alpha$ -carboxyl function as benzyl ester (Bn). In particular, Z-Asn( $\alpha$ GlcAc<sub>4</sub>)-OBn, was obtained using the asparagine residue modified on the side chain with mercaptopyridine, Z-Asp(SPy)-OBn (**6**), and  $\text{CuCl}_2 \cdot 2\text{H}_2\text{O}$  as an additive at 30°C in 24h.<sup>39</sup>

Unluckily, Z-Asn( $\alpha$ GlcAc<sub>4</sub>)-OBn is not an useful tool for solid phase synthesis of glycopeptides. Moreover, Z and Bn are not orthogonal for SPPS. These

<sup>41</sup> (a) Kappe, C.O. *Angew. Chem. Int. Ed.* **2004**, 43 6250. (b) Kappe, C.O.; Dallinger, D. *Nat. Rev. Drug Disc.* **2006**, 5, 51.

observations prompted us to perform several reactions to obtain *N*- $\alpha$ -glycosylated amino acids orthogonally protected for SPGPS, in particular Fmoc-Asn( $\alpha$ GlcAc4)-OtBu (**10a**). Finally, we succeeded in performing MW-assisted coupling reactions on differently protected aspartic acid derivatives (PG-Asp-OX) as acylating reagents (Table 1.1.1) with the isoxazoline derivative **3** (Scheme 4).

In fact, by MW irradiation (100 W), the reaction was complete in less than 10 min. maintaining the vessel temperature at 130 °C.



**Scheme 4.** Coupling reaction of 3,4,6-tri-O-acetyl- $\alpha$ -D-glucopyranosyl isoxazoline **3** with PG-Asp-OX..

**Table 1.1.1. Coupling reaction conditions and reagents.<sup>a</sup>**

PG-Asp-OX	equiv	$\alpha/\beta$ <sup>b</sup>	MW Protocol	Yield <sup>c</sup>
	3	No product	P = 100W T = 130°C Time = 10min	-
	3	53/47	P = 100W T = 130°C Time = 10min	32 %
	1	52/48	P = 100W T = 130°C Time = 10min	28%
	1.3 <sup>d</sup>	73/27	P = 100W T = 130°C Time = 10min	78%
	1.3 <sup>d</sup>	56/44	P = 100W T = 130°C Time = 10min	43%

<sup>a</sup>All reactions were performed in a sealed vessel specific for the monomode microwave synthesizer CEM EXPLORER 48® in 1,2-dichloroethane using NMM, the coupling reagent DMT-NMM/BF<sub>4</sub>, and the acylating reagent PG-Asp-OX. Detailed protocol is reported in the Experimental Part A. <sup>b</sup>Calculated by HPLC analysis. <sup>c</sup>For isolated product. <sup>d</sup>CuCl<sub>2</sub>·2H<sub>2</sub>O was added as an additive. Syntheses of PG-Asp-OX **4**, **6**, and **7** are described in details in the Experimental Part A.

## PART A

While Z-Asp(Spy)-OBn in the coupling reaction maintained a good stereoselectivity also under MW conditions, the use of the Fmoc-protected aspartic acid derivative, Fmoc-Asp(Spy)-OtBu, significantly decreased stereoselectivity and reaction yield. For this reason, we developed a new strategy to obtain Fmoc-Asn( $\alpha$ GlcAc<sub>4</sub>)-OH.

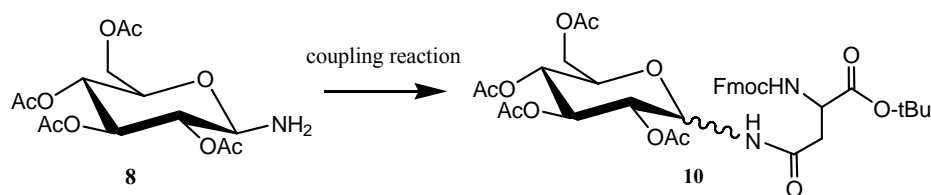
### 1.1.3 New synthetic strategy to Fmoc-Asn( $\alpha$ GlcAc<sub>4</sub>)-OH (11)

We previously reported a MW-assisted synthesis of Fmoc-Asn( $\beta$ GlcAc<sub>4</sub>)-OtBu coupling glucosylamine (1 equiv) to aspartic acid side chain (1 equiv) in the presence of NMM (1 equiv) and the new efficient triazine-based coupling reagent DMT-NMM/BF<sub>4</sub> [4-(4,6-dimethoxy-1,3,5-triazin-2-yl)-4-methylmorpholinium tetrafluoroborate] displacing the equilibrium of the coupling reaction and favouring formation of the final product (Scheme 1).<sup>42</sup>

Therefore, we developed a new strategy for the synthesis of the corresponding  $\alpha$ -glucosyl derivative Fmoc-Asn( $\alpha$ GlcAc<sub>4</sub>)-OH orthogonally protected for Fmoc/tBu SPGPS. We performed a series of coupling reactions changing different parameters (i.e., MW power, temperature, and reaction time) to set up the optimal conditions leading to the *N*- $\alpha$ -linked glucosyl derivative **10a**. To the best of our knowledge, up to now no data were reported on temperature effect influencing stereoselectivity of *N*-glycosidic bond formed between amino sugars and the side-chain carboxyl function of Asp.

---

<sup>42</sup> (a) Kaminski, Z.J.; Kolesinska, B.; Kolesinska, J.; Sabatino, G.; Chelli, M.; Rovero, P.; Blaszczyk, M.; Glowka, M.L.; Papini, A.M. *J. Am. Chem. Soc.* **2005**, 127, 16912. (b) "Process for the preparation of *N*-triazinylammonium salts". Filing date 07/11/2005. Applicant: Italvelluti S.p.a. Inventors: Z. Kaminski, A. M. Papini, B. Kolesinska, J. Kolesinska, K. Jastrzabek, G. Sabatino, R. Bianchini. PCT/EP2005/055793, **2005**. (c) Kamiński, Z.J. *Int. J. Pept. Protein Res.*, **1994**, 43, 312-319



**Scheme 5.** Coupling reaction between 1-glucosylamine **8** and Fmoc-Asp-OtBu (**5**)

The results are summarized in Table 1.1.2. The coupling reaction monitored by NMR and HPLC showed that in 5 min, at 70°C, and 100 W the *N*- $\beta$ -glucosyl derivative **10 $\beta$**  could be obtained and purified as a unique product (Table 1.1.2, entry 1). When temperature and MW power were increased, the  $\alpha$ -anomer **10 $\alpha$**  started to form, with a maximum of  $\alpha/\beta$  ratio 87/13 at 150°C and 100 W (entry 8). Moreover, when MW power was increased from 100 W to 200 W (see entry 9) the  $\alpha/\beta$  ratio reached 92/8. By decreasing coupling reaction time to 1 min, it was possible to avoid  $N^{\alpha}$ -Fmoc deprotection because of high temperature.

**Table 1.1.2 Comparative study of different coupling conditions for amide bond formation between 1-glucosylamine and aspartic acid side chain to obtain *N*- $\alpha$ - and/or *N*- $\beta$ -glucosyl derivatives 10 $\alpha$ /10 $\beta$ .**

Entry	Temp <sup>b</sup> (°C)	Time <sup>c</sup> (min)	Power (W)	Yield <sup>d</sup> (%)	10 $\alpha$ /10 $\beta$ <sup>e</sup>
1	70	5	100	80	6/94
2	70	5	30	37	8/92
3	70	1	300	52	26/74
4	100	3	100	58	45/55
5	100	3	150	63	50/50
6	130	1	100	52	72/28
7	130	1	200	58	85/15
8	150	1	100	69	87/13
9	150	1	200	76	92/8

<sup>a</sup>All reactions were performed in a sealed vessel specific for the monomode microwave synthesizer CEM EXPLORER 48® in acetonitrile using Fmoc-L-Asp-OtBu, NMM, and the coupling reagent DMT-NMM/BF<sub>4</sub> as starting materials. Protocol is described in details the Experimental Part A. <sup>b</sup>For coupling reaction. <sup>c</sup>At the temperature described. <sup>d</sup>For isolated product. <sup>e</sup>Calculated by HPLC analysis.

## PART A

All reaction conditions reported in Table 1.1.2 were also performed without microwave energy (data not shown). In that case only the *N*- $\beta$ -glucosyl anomer **10 $\beta$**  could be obtained. Considering that we achieved in a limited number of steps, with a very good yield Fmoc-Asn( $\alpha$ GlcAc<sub>4</sub>)-OH by microwave irradiation, we can hypothesize that the  $\alpha$ -anomer is the thermodynamically favoured compound (Figure 1.1.3).

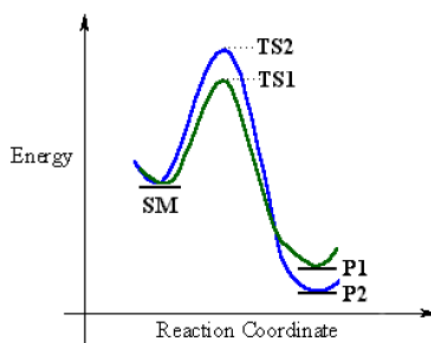


**Figure 1.1.3.** Formation of the kinetic product *P1* occurs under the faster reaction since it has a more stable transition state, *TS1*, and therefore a lower activation barrier. Thermodynamic product *P2* is the more stable product since it is formed at lower energy than *P1*.

In any case, playing with microwave energy, we can decide to obtain the  $\alpha$  or the  $\beta$ -anomer<sup>36</sup> in high yield and short reaction time.

In conclusion, the *N*-glucosyl asparagine derivatives **10 $\alpha$**  and **10 $\beta$**  could be successfully purified independently by Flash Column Chromatography. After deprotection of the  $\alpha$ -carboxyl function by a TFA solution in DCM we obtained the two anomerically pure building blocks useful for SPGPS, Fmoc-Asn( $\alpha$ GlcAc<sub>4</sub>)-OH (**11 $\alpha$** ) and Fmoc-Asn( $\beta$ GlcAc<sub>4</sub>)-OH (**11 $\beta$** ) orthogonally protected for Fmoc/*t*Bu strategy.

## 1.2 Synthesis of glycopeptide mimetics

Fmoc-Asn( $\alpha$ GlcAc<sub>4</sub>)-OH (**11 $\alpha$** ) and Fmoc-Asn( $\beta$ GlcAc<sub>4</sub>)-OH (**11 $\beta$** ) were employed in the stepwise solid phase synthesis of the  $\beta$ -turn structure CSF114 at position 7 (Table 1.2.1).

**Table 1.2.1. Glycopeptide sequences**

<b>Glycopeptide</b>	<b>Sequence</b>
CSF114( $\alpha$ Glc) ( <b>I<math>\alpha</math></b> )	TPRVERN( $\alpha$ Glc)GHSVFLAPYGWMVK
CSF114( $\beta$ Glc) ( <b>I<math>\beta</math></b> )	TPRVERN( $\beta$ Glc)GHSVFLAPYGWMVK

Glycopeptides **I $\alpha$**  and **I $\beta$**  were synthesized on an automatic Prelude® instrument, starting from a Wang resin, according to the General Procedure for the SPPS described in details in the Experimental Part and using commercially available Fmoc-protected amino acids and HOBt/TBTU/NMM activation. The new building block Fmoc-L-Asn( $\alpha$ GlcAc<sub>4</sub>)-OH (**11 $\alpha$** ) and Fmoc-L-Asn( $\beta$ GlcAc<sub>4</sub>)-OH (**11 $\beta$** ) were manually added using HOBt/TBTU/NMM activation. After cleavage of the glycosylated peptides from the resin and deprotection of amino-acid side chains, deprotection of the hydroxyl functions of sugars was performed as described in details in the Experimental Part using MeONa/MeOH. The glycopeptides were purified by semi-preparative HPLC and characterized by ESI-MS. Analytical data are reported in Table 1.2.2

**Table 1.2.2. Analytical data of glycopeptides.**

<b>Peptide</b>	<b>HPLC (R<sub>t</sub>,min)<sup>a</sup></b>	<b>ESI-MS [M+2H]<sup>2+</sup> Calc (found)</b>
I $\alpha$	14.82	1303.0 (1303.6)
I $\beta$	14.83	1303.0 (1302.8)

<sup>a</sup>Analytical HPLC gradients at 1 mL min<sup>-1</sup>, 20-60% B in 20 min, solvent system A: 0.1% TFA in H<sub>2</sub>O, B: 0.1% TFA in CH<sub>3</sub>CN;

### 1.3 Immunochemical assays of CSF114(Glc) analogues

The antibody recognition using the CSF114(Glc) glycopeptide analogues **I $\alpha$**  and **I $\beta$**  was evaluated by solid phase and competitive-ELISA on Multiple Sclerosis patients' sera. The unglycosylated peptide CSF114 was employed as negative control.

We evaluated, by SP-ELISA, serum antibodies (IgM and IgG class) to the glycopeptides **I $\alpha$**  and **I $\beta$**  in a group of MS patients and compared the results with Normal Blood Donors' sera (NBDs). IgM and IgG responses were

## PART A

detected using as secondary antibodies anti-human IgMs and anti-human IgGs conjugated to alkaline phosphatase.

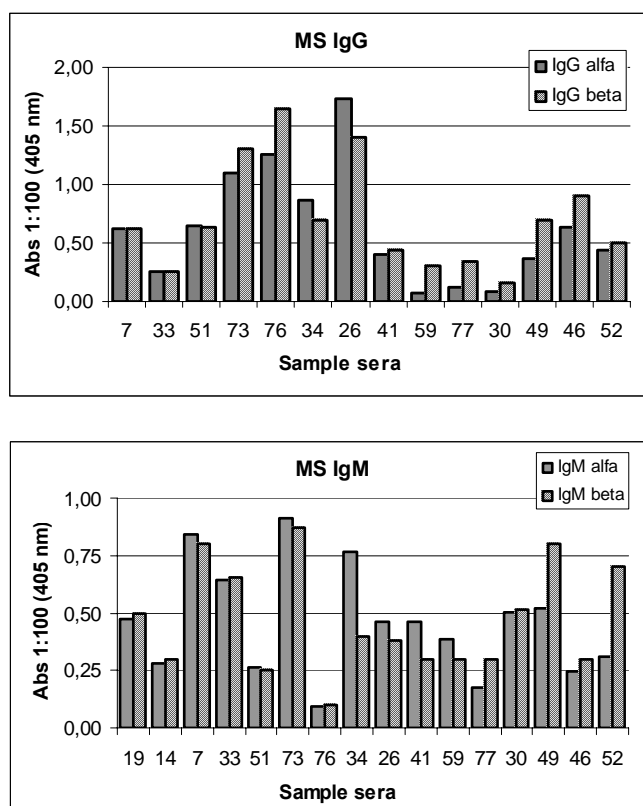


**Figure 1.3.1.** Antibody titre in MS patients to glycopeptides CSF114( $\alpha$ Glc) and CSF114( $\beta$ Glc).

It is accepted that the glycopeptide **I $\beta$**  CSF114( $\beta$ Glc) detects specific antibodies in MS patients' sera.<sup>24</sup> In fact, as reported in Figure 1.3.1, the glycopeptide **I $\beta$**  displays high antibody recognition, and the glycopeptide **I $\alpha$**  is always able to detect antibodies showing a relative similar activity.



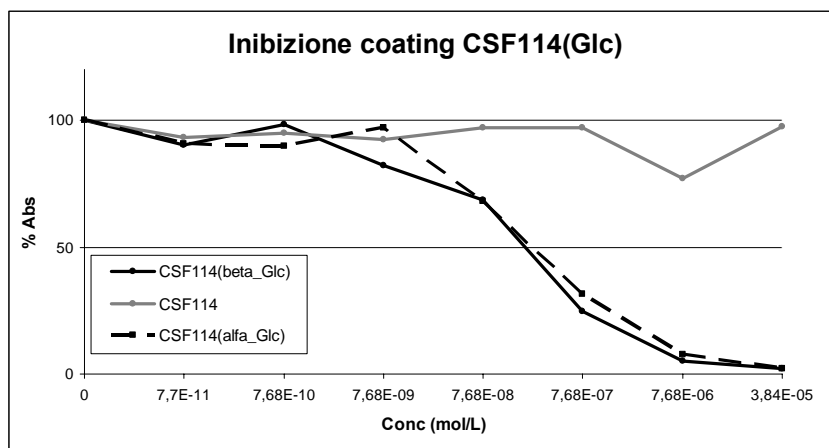


**Figure 1.3.2.** Inhibition curves of anti-CSF114(Glc) antibodies with the glycopeptides **I $\alpha$**  and **I $\beta$** . Results are expressed as % of a representative Multiple Sclerosis positive serum (y axis). Concentrations of peptides as inhibitors are reported on the x axis.

In competitive ELISA, the two glycopeptides displayed inhibitory activity at the same concentration. As reported in Figure 1.3.2, the two glycosylated peptides present similar IC<sub>50</sub> value (concentration required for 50% inhibition). In conclusion, the glycopeptides containing the Asn(Glc) residue, independently of the anomeric configuration of the glucosyl moiety, showed similar high affinity to autoantibodies present in Multiple Sclerosis patients' sera.

Further NMR studies of glycopeptides **I $\alpha$**  and **I $\beta$**  could confirm the real configuration of the glucosyl moiety once linked into the peptide sequence. Cleavage and deacetylation conditions could modify the anomeric configuration or this could change because of possibly tautomeric forms. This hypothesis is supported by recent results reporting that in the case of glycosylated peptides tautomerization of the sugar moiety could be kinetically driven allowing less stable tautomers formation.<sup>43</sup>

<sup>43</sup> Carganico, S.; Rovero, P.; Halperin, J.A.; Papini, A.M.; Chorev, M. *J Pept Sci*, **2008**, published online 11 November 2008.



## ***2. Modification of the glycopeptide antigen CSF114(Glc) with electrodetectable molecules to improve antibody detection***

In order to help clinicians to follow up Multiple Sclerosis patients by a simple blood test to detect autoantibodies, different problems have to be solved. In fact, the development of reliable and efficient diagnostic/prognostic assays for autoimmune diseases requires:

- 1) Selection of the antigen recognising specific autoantibodies in a statistically significant number of patients (sensitivity) compared to other autoimmune diseases and normal controls;
- 2) Selection of the diagnostic technique to detect autoantibodies (ELISA, radioimmunoassay, immunofluorescence, SPR, etc).

In the case of Multiple Sclerosis, patients accumulate myelin lesions, but also axonal loss leading to permanent neurological dysfunctions. Magnetic Resonance Imaging (MRI) is up to now the most reliable technique to help clinicians not only in diagnosis, but also in prognosis because no gold standard simple immunoassays are available. However, it is evident that MRI cannot be considered a routine technique and that efficient autoantibody detection could be useful as signal of disease progression when the clinical symptoms are not still visible to guide a targeted MRI checkup.<sup>44</sup>

Other diagnostics techniques exploit the capability of antibodies to detect analytes with high sensibility, specificity, and adaptability at very low levels. Therefore, immunoassays are based on an antigen/antibody interaction to identify a target compound or a class of compounds, as in the ELISA. Immunoassays take advantage of the ability of antibodies to bind selectively a target antigen present in a sample matrix and characterized by a specific chemical structure. Working like a key and lock, the binding sites on an

---

<sup>44</sup> Vossenaar, E.R.; van Venrooij, W.J. *Clin. Appl. Immunol. Rev.* **2004**, 4, 239-262

## PART A

antibody attach precisely and non covalently to the corresponding target antigens.

ELISA offers advantages, such as allowing simultaneous analyses of a large number of samples. To avoid non-reproducible or non-interpretable results because based on operator-dependent procedures, there is a need of diagnostics industry involved in the field of autoimmunity, not only for fast, but also for sensitive and more consistent techniques particularly for quantitative determination of autoantibodies to follow up disease activity.

Electrochemistry as detection technique of biological and clinical assays is extremely interesting because it can shorten time analyses, increasing reliability.

### **2.1 Ferrocenyl derivatives as electrochemical probes**

Glycopeptide analogues of CSF114(Glc), properly modified at N-terminus with new ferrocenyl and ferrocenyl-thiophosphine derivatives as “Electrochemical Probes”, were used in Cyclic Voltammetry measurements in solution and/or grafting peptides on a gold electrode. At this purpose, in the context of the cooperation with the Institut de Chimie Moléculaire (ICMUB) of the University of Burgundy (Dijon, France), new electrodetectable molecules have been designed. In particular, ferrocenyl and thiophosphine derivatives were selected as biosensors.

Availability of a large variety of ferrocenyl derivatives and their favourable electrochemical properties (undergoing a reversible oxidation in aqueous solution) make ferrocene and its derivatives very trendy molecules for biological applications and for conjugation with biomolecules.<sup>45</sup> Furthermore, ferrocenyl and thiophosphine derivatives are a new class of linkers useful for electrochemical and optical bio-detections. In this context, we decided to use

---

<sup>45</sup> Van Staveren, D.R.; Metzler-Nolte, *N. Chem. Rev.* **2004**, 104, 5931-5985.

ferrocenyl carboxylic acid and a new ferrocenylthiophosphine derivative of butyric acid (Figure 2.1).

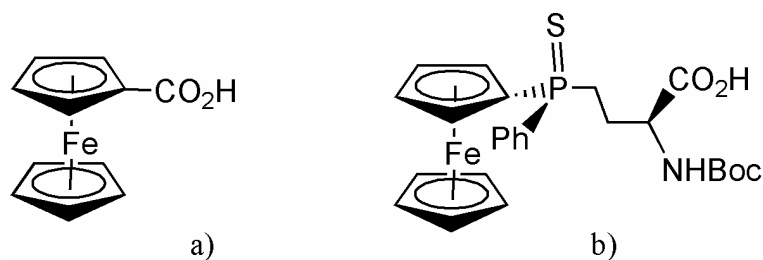


**Figure 2.1.** Structure of ferrocenyl derivatives used for SPPS. a) Ferrocenyl carboxylic acid [**Fc-COOH**] and b) (*Sp,S*)-(+)-2-(tert-butoxycarbonylamino)-4-(ferrocenylphenylthiophosphino)butanoic acid [**4-FcPhP(S)Abu**].

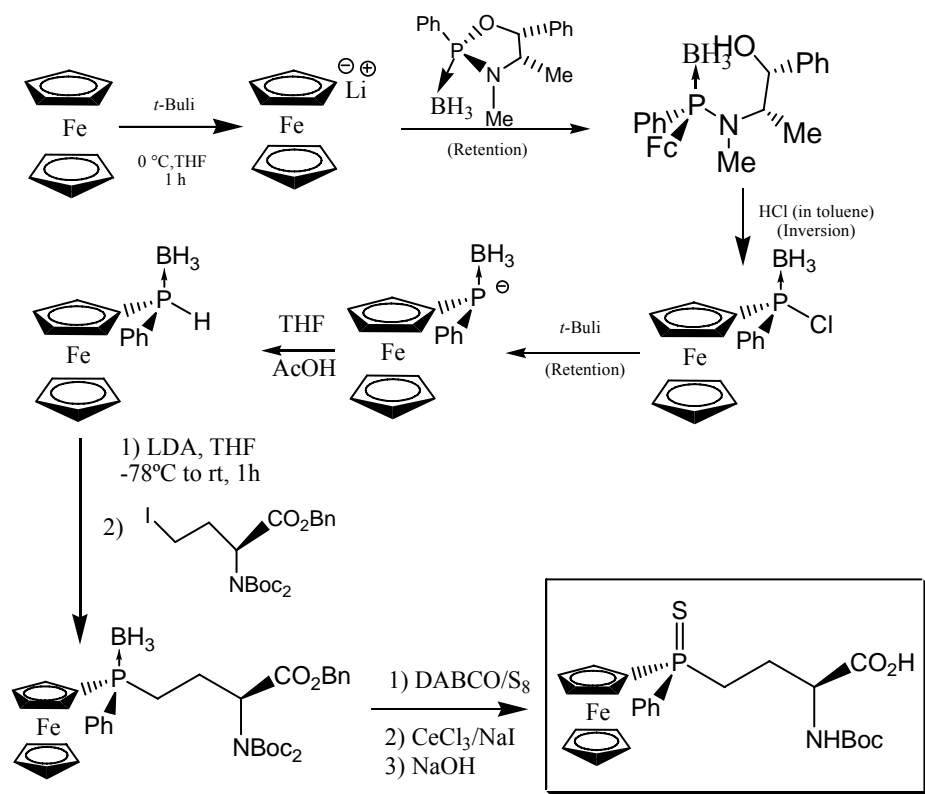
The electrochemical properties of ferrocene coupled to thiophosphine ability to build simple monolayers on gold surfaces will let peptides anchoring on the working electrode used for detection. The possibility of grafting the synthetic probe directly on the electrode surface will enable to obtain an innovative strategy to develop new techniques for antibody detection opening new strategies in the analysis of antibody profiles in MS patients' sera, possibly improving detection of a panel of antibodies as specific biomarkers for different forms of the disease.

The new unnatural amino acid 4-FcPhP(S)Abu, protected for SPPS, was synthesized following the strategy previously developed at the University of Burgundy.<sup>46</sup> The ferrocenyl-thiophosphine derivative 4-FcPhP(S)Abu was obtained from ferrocene in 10 steps with global yield of 48% by reaction of (*S*)-ferrocenylphenylphosphine borane with the (*S*)-(-)-2-[bis(tert-butoxycarbonyl)amino]-4-iodobutanoate<sup>47</sup> and then subsequent sulfuration and deprotection gave desired amino acid derivative 4-FcPhP(S)Abu (Scheme 2.1).

<sup>46</sup> Colson, A.; Bayardon, J.; Rémond, E.; Lauréano, H.; Nuti, F.; Meunier-Prest, R.; Kubicki, M.; Darcel, C.; Papini, A.M.; Jugé, S. *J. Org. Chem.* Submitted.

<sup>47</sup> The benzyl (*S*)-(-)-2-[bis(tert-butoxycarbonyl)amino]-4-iodobutanoate was prepared according a modified following procedure described in: Adamczyk, M.; Johnson, D.D.; Reddy, R. E. *Tetrahedron: Asymmetry* **2000**, 11, 3063-3068.

## PART A



**Scheme 2.1.** Synthesis of the modified amino acid (*Sp,S*)-(+)-2-(tert-butoxycarbonylamino)-4-(ferrocenylphenylthiophosphino)butanoic acid [4-FcPhP(S)Abu].

## 2.2 Synthetic strategy to labelled peptides

A collection of labelled peptides was prepared by solid phase peptide synthesis (SPPS) using the Fmoc/tBu strategy (Table 2.2). The novel ferrocenyl peptides were synthesized modifying CSF114(Glc) and the corresponding unglucosylated sequence, both containing the original 21 amino acids and the designed ferrocenyl derivatives (Figure 2.1). The N<sup>α</sup> amino function of the amino acid 4-FcPhP(S)Abu was Boc protected and the α-carboxylic functions of both derivatives were free to be used directly in SPPS.

Only few studies reported on the solid-phase synthesis of organometallic derivatives of peptides. In fact, decomposition of organometallic peptides and

secondary products of SPPS have usually affected final yield.<sup>48</sup> Taking into account that microwave technology applied to SPPS is proposed as a valid support for enhancement of efficiency of coupling reactions in short times, this strategy was applied to synthesize the peptide sequences performing the syntheses with a microwave-assisted automatic solid phase peptide synthesizer. Microwave technology decreases chain aggregation during the syntheses, improves the coupling rates, and prevents side reactions in particularly difficult peptide sequences.<sup>49</sup>

At the end of the peptide synthesis, Boc-protected organometallic unnatural amino acids were manually introduced at the N-terminus of the resin-bound glycopeptide **I** and unglucosylated peptide **I'** to obtain the peptide collection reported in Table 1.

**Table 2.2. Analytical data from Ultra Performance Liquid Chromatography (UPLC).**

Peptide name	$R_t$ (min)	Calculated mass	Observed mass [M+2H] <sup>2+</sup>
CSF114(Glc) ( <b>I</b> )	2.07 <sup>a</sup>	2606.3	1303.6
Fc-CSF114(Glc) ( <b>IV</b> )	1.872 <sup>b</sup>	2820.2	1411.2
4-FcPhP(S)Abu-CSF114(Glc) ( <b>V</b> )	1.833 <sup>b</sup>	3015.5	1508.3
CSF114 ( <b>I'</b> )	1.96 <sup>a</sup>	2444.2	1222.6
Fc-CSF114 ( <b>IV'</b> )	1.813 <sup>b</sup>	2655.3	1329.8
4-FcPhP(S)Abu-CSF114 ( <b>V'</b> )	1.863 <sup>b</sup>	2853.5	1427.4

Gradients at 0.45 mL min<sup>-1</sup>: <sup>a</sup> 10-60% B in 3.5 min, <sup>b</sup> 20-70% B in 3.5 min (solvent system, A: 0.1% TFA in H<sub>2</sub>O, B: 0.1% TFA in CH<sub>3</sub>CN).

The metallocene moieties were demonstrated to be stable during Fmoc-deprotection, cleavage, and in the deacetylation conditions (pH=12) requested for deprotection of the hydroxyl groups of the sugar. However, the final

<sup>48</sup> Chantson, J.T.; Verga Falza, M.V.; Sergio Crovella, S.; Metzler-Nolte, N. *Chem. Med. Chem.* **2006**, 1, 1268–1274.

<sup>49</sup> Rizzolo, F.; Sabatino, G.; Chelli, M.; Rovero, P.; Papini, A.M. *International Journal of Peptide Research and Therapeutics* **2007**, 13, 203-208.

## PART A

ferrocenyl peptides could be safely obtained when phenol rather than water was used as scavenger in the final cleavage mixture for resin and amino acid side chains deprotection.<sup>48</sup>

All the compounds were analyzed by UPLC-ESIMS and HPLC-ESIMS and purified by RP-HPLC (>95%) to be used for autoantibody detection.

### 2.3 Immunoenzymatic assays of ferrocenyl peptides

The glycopeptide CSF114(Glc) (**I**), designed as a type I'  $\beta$ -turn around the minimal epitope Asn(Glc), guarantees an optimal exposure of the epitope for antibody recognition in the solid phase conditions of the ELISA plate on sera of MS patients. In fact, the CSF114(Glc)-based ELISA allows to recognize both IgM and IgG in sera of 30% of MS patients' sera.<sup>26</sup>

We evaluated, by ELISA, serum antibodies (IgM and IgG class) to the new organometallic peptides and glycopeptides (Table 2.2) in a group of MS patients and compared the results with Normal Blood Donors' sera (NBDs). IgM and IgG responses were detected using as secondary antibodies anti-human IgMs and anti-human IgGs conjugated to alkaline phosphatase.

The antibody recognition to CSF114(Glc) (**I**) was compared versus the ferrocenyl glycopeptides **IV** and **V** and the corresponding unglycosylated sequences **I'**, **IV'**, and **V'** in a first group of patients' sera affected by clinically definite MS using SP-ELISA. It is accepted that the glycopeptide CSF114(Glc) (**I**) detects specific antibodies in MS patients' sera.<sup>24</sup> In fact, as it can be observed in Figure 2.3.1, the glycopeptide **I** presented the highest antibody recognition, but the new ferrocenyl glycopeptides **IV-V** are always able to detect antibodies showing only a relative lower biological recognition. As expected unglycosylated peptides **I'**, **IV'**, **V'** are always inactive.



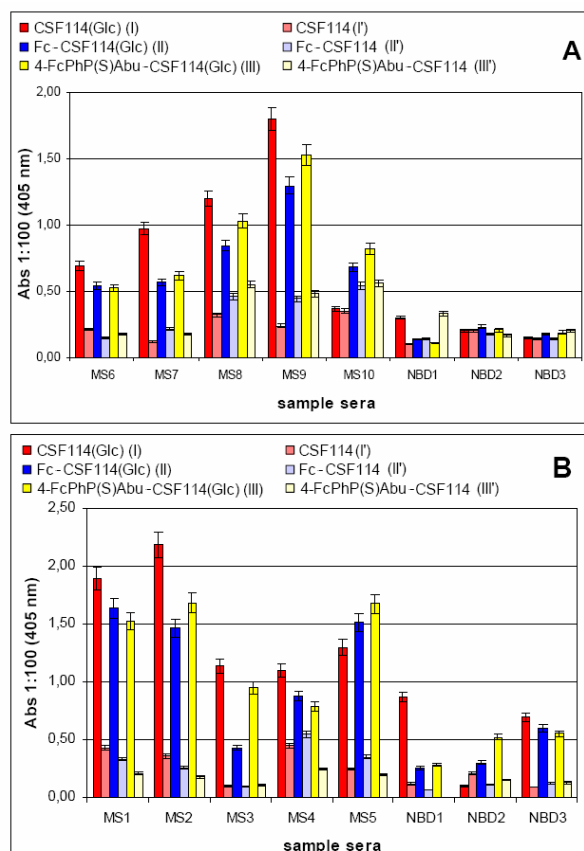


**Figure 2.3.1.** Autoantibody recognition in MS patients' sera and NBDs sera. IgM (A) and IgG (B) classes versus the ferrocenyl glycopeptides (IV–V) and the corresponding unglycosylated ones (I', IV', V') compared to the glycopeptide CSF114(Glc) I. Data are reported as absorbance at 405 nm of sera diluted 1:100.

Considering that SP-ELISA reflects essentially the relative affinity, which depends on the exposure of the minimal epitope in the solid phase conditions of the assay, we also investigated the absolute antibody affinity in a competitive ELISA based on inhibition of autoantibodies in solution. In a set of MS positive sera, ferrocenyl glycopeptides **IV** and **V** inhibited binding of autoantibodies to CSF114(Glc) (**I**), giving rise to similar inhibition curves. The data of a representative serum (Figure 2.3.2) show that the two modified glycopeptides **IV** and **V** exhibited equivalent affinity in competitive ELISA,

## PART A

despite the differences of apparent affinity detected in SP-ELISA (Figure 2.3.1). These findings indicated that the new ferrocenyl glycopeptides share an epitope similar to the one presented by CSF114(Glc), and the presence of ferrocenyl and/or thiophosphine moiety at the N-terminus doesn't influence antibody recognition.

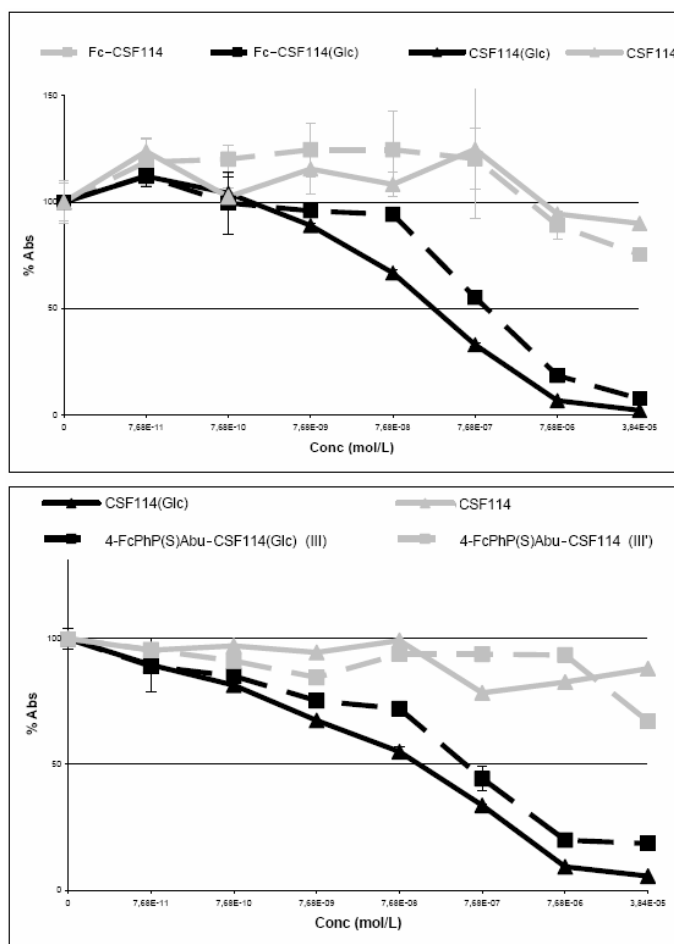


**Figure 2.3.2.** Inhibition curves of anti-CSF114(Glc) Abs with ferrocenyl glycopeptides II-III and with unglycosylated peptides I', IV', V', in comparison with I in a competitive ELISA. The results are expressed as the percentage of absorbance of a representative MS serum (ordinate axis).

Therefore the glycopeptide **CSF114(Glc)** modified with the ferrocenyl amino acids is still able to detect and inhibit autoantibodies in MS patients' sera and cannot detect any antibody titre in NBDs' sera.

## 2.4 Electrochemical measurements

### 2.4.1 Grafting peptides on gold electrode

The glucosylated ferrocenyl peptide 4-FcPhP(S)Abu-CSF114(Glc) (**V**) and the unglucosylated one 4-FcPhP(S)Abu-CSF114 (**V'**) were adsorbed on gold surface to form a self-assembled monolayer (SAM) via the sulphur atom. A mixture of 11-mercaptoundecanoic acid and decanethiol was used to block the uncovered surface. The modified electrodes are denoted **Au-V** for the electrode grafted with **V** and **Au-V'** for the electrode grafted with **V'**. The electrochemical response of the ferrocenyl group was performed by Cyclic Voltammetry.  $\text{Fe}(\text{CN})_6^{4-}$  was used as catalyst to increase the electrochemical current.<sup>50,51,52,53</sup> Figure 2.4.1 shows the electrochemical response of **Au-V** in a tween solution of  $\text{Fe}(\text{CN})_6^{4-}$ . When a solution of purified anti-CSF114(Glc) antibodies is added, the electrochemical response is shifted towards more positive potentials. The peak potential appears 46 mV more positive than that of the same solution without antibodies.

---

<sup>50</sup> Creager, S. E.; Radford, P. T. *J. Electroanal. Chem.* **2001**, 500, 21-9.

<sup>51</sup> Radford, P. T.; French, M.; Creager, S. E. *Anal. Chem.* **1999**, 71, 5101-8.

<sup>52</sup> Radford, P. T.; Creager, S. E. *Anal. Chim. Acta.* **2001**, 449, 199-209.

<sup>53</sup> Bergren, A. J.; Porter, M. D. *J. Electroanal. Chem.* **2006**, 591, 189-200.

## PART A

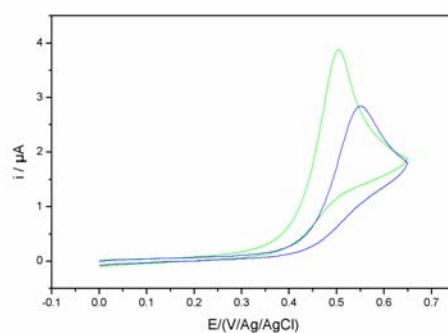


**Figure 2.4.1.** Cyclic Voltammetry of **Au-V** in a tween solution containing  $\text{LiClO}_4$  0.1 M and  $\text{Fe}(\text{CN})_6^{4-}$   $9 \times 10^{-4} \text{ M}$  (green curve) without antibodies and with a solution of purified anti-CSF114(Glc) antibodies at a final dilution of 1:1000 (blue curve). Scan rate  $50 \text{ mV}^{\text{s}^{-1}}$ .

When the same experiment is repeated with **Au-V'**, i.e. with the electrode modified by unglucosylated peptide **V'**, which is not able to recognize autoantibodies, the results are completely different (Figure 2.4.2). The electrochemical response of **Au-V'** doesn't change significantly after addition of a solution of purified anti-CSF114(Glc) antibodies. The potential peak is even shifted by few millivolts toward more negative potentials.

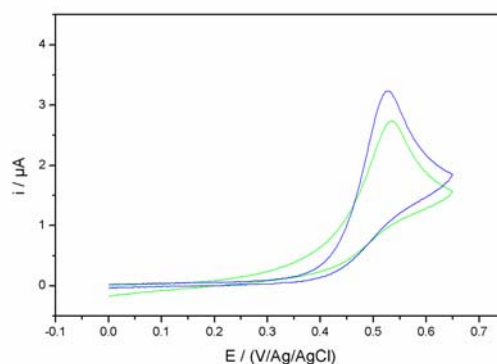


**Figure 2.4.2.** Cyclic Voltammetry of **Au-V'** in a tween solution containing  $\text{LiClO}_4$  0.1 M and  $\text{Fe}(\text{CN})_6^{4-}$   $9.10^{-4} \text{ M}$  (green curve) without antibodies and with a solution of purified anti-CSF114(Glc) antibodies at a final dilution of 1:1000 (blue curve). Scan rate  $50 \text{ mV}^{\text{s}^{-1}}$ .

### 2.4.2 In solution measurements

The detection of interactions between autoantibodies and the ferrocenyl peptide, Fc-CSF114(Glc) (**IV**), i.e. without P=S anchor, was realized in solution. The gold electrode properly modified with 11-mercaptopundecanoic acid to avoid non specific interactions with the biological medium, was introduced in a tween solution containing both  $\text{LiClO}_4$  0.1 M and  $\text{Fe}(\text{CN})_6^{4-}$   $9 \times 10^{-4} \text{M}$  and the ferrocenyl glycopeptide **IV**. Figure 2.4.3 shows the cyclic voltammograms before and after addition of purified anti-CSF114(Glc) antibodies.

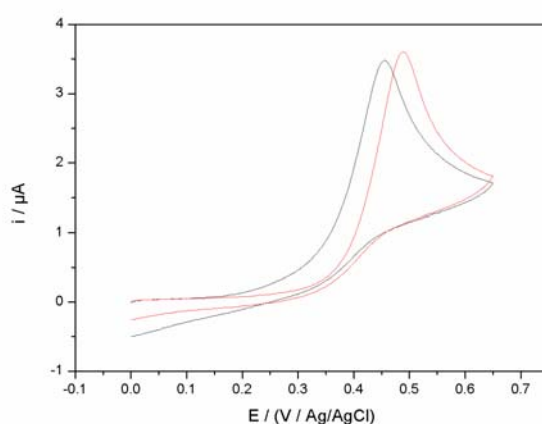


**Figure 2.4.3.** Cyclic Voltammetry of **IV**,  $1.77 \cdot 10^{-4} \text{M}$  in a tween solution containing  $\text{LiClO}_4$  0.1 M and  $\text{Fe}(\text{CN})_6^{4-}$   $9 \cdot 10^{-4} \text{M}$  (black curve) without antibodies and (red curve) with a solution of purified anti-CSF114(Glc) antibodies at a final dilution of 1:1000. Scan rate  $50 \text{ mV}^{\text{s}^{-1}}$ .

In the case of the glucosylated ferrocenyl peptide **IV**, the peak potential is shifted of 34 mV towards positive values by addition of anti-CSF114(Glc) antibodies. However, in this case, a study of the nature of the protective monolayer should be investigated to confirm the interest of the glycopeptide **IV** for autoantibody detection.

Figure 2.4.4 summarizes the results. The glucosylated biosensor **Au-V** and the glucosylated ferrocenyl peptide **IV** in solution, shift of more than 30mV

## PART A

towards positive values by addition of anti-CSF114(Glc) antibodies. This is indicative of detection of antigen-antibody interaction, and therefore of the presence of autoantibodies in the tested MS patients' sera. The negative control realized with the unglucosylated biosensor (**Au-V'**) shows a very small potential shift in the opposite direction.

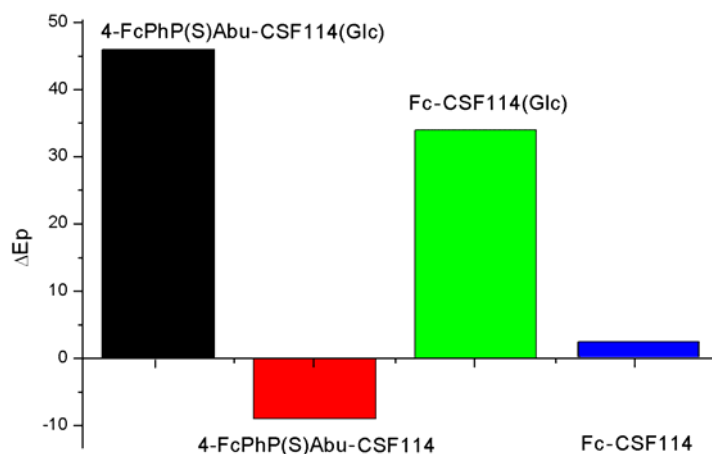


**Figure 2.4.4.** Electrochemical immunoassay: Potential difference between the electrochemical response with and without purified anti-CSF114(Glc) antibodies at a final dilution of 1:1000 for (black) the biosensor **Au-V**, (red) its negative control **Au-V'**, (green) the ferrocenyl glycopeptide **IV** in solution and (blue) its negative control **IV'** in solution.

In conclusion, the new ferrocenyl peptides containing the unnatural amino acid 4-FcPhP(S)Abu are able to detect specific anti-CSF114(Glc) antibodies by electrochemical technique. Moreover, thanks to the presence of thiophosphine, the modified glycopeptide 4-FcPhP(S)Abu-CSF114(Glc) (**V**) is able to build simple monolayers on gold surfaces and it can be useful for antibody detection and quantitative determinations. The possibility of grafting these new ferrocenyl glycopeptides, as synthetic antigenic probes, directly on the electrode surface (as a valid alternative analytical method to detect autoantibodies in sera of MS patients) is currently under investigation in our laboratories.

We demonstrated the possibility of detecting isolated antibodies by Cyclic Voltammetry in samples containing 1:1000 diluted antibodies. This detection limit is in any case lower compared to the one set up in our validated ELISA on sera.<sup>24,25</sup> Therefore, we are confident that this new voltammetry-based technique could be useful in detecting antibodies in sera of Multiple Sclerosis patients.





### ***3. Identification of antibodies by Surface Plasmon Resonance***

The most commonly applied techniques for antibody detection exploit the characteristic of antibodies to bind selectively to a target antigen. These are Enzyme-Linked ImmunoSorbent Assay (ELISA), RadioImmunoAssay (RIA), or Fluorescent ImmunoAssay (FIA)

An attractive and complementary method for measuring antigen-antibody interactions is **Surface Plasmon Resonance (SPR)**. The SPR response is correlated to changes in refractive index at a sensor chip surface, caused by concentration changes, e.g. resulting from binding of an antibody to an immobilised antigen. Study of interactions between biomolecules can be monitored continuously allowing real-time measurements. The on-line monitoring may facilitate information regarding for example the specificity of the interaction between an immobilised antigen and its target molecule. Furthermore, information regarding the kinetics of the interaction, the strength of the interaction, and the concentration of the interacting species can also be obtained.<sup>54</sup>

Therefore we investigated antigen-antibody interaction in Multiple Sclerosis by Surface Plasmon Resonance, using Biacore T100 instrument for real-time detection of anti-CSF114(Glc) antibodies in serum.

#### **3.1 Synthetic biotinylated glycopeptides for autoantibody recognition in Multiple Sclerosis patients' serum**

In order to improve signal response in SPR studies, the glycopeptide probe CSF114(Glc) and the unglucosylated one CSF114, as synthetic antigens, were

---

<sup>54</sup> Malmqvist, M.; Karlsson, R. *Current Opinion in Chemical Biology*, **1997**, 1(3), 378-383.

## PART A

modified at the N-terminus with a biotinylated residue. Immobilization of peptide antigens via the biotin/avidin complex apparently represents an approach superior to the direct adsorption of low mass antigens on a surface.<sup>55</sup>. At this purpose, biotinylated peptides CSF114(Glc) and CSF114 were synthesized by Fmoc/tBu SPPS. Peptides were synthesized in an automatic Prelude® instrument starting from a Wang resin, according to the General Procedure for SPPS described in details in the Experimental Part and using Fmoc-amino acids and HOBt/TBTU/NMM activation. The peptide sequences were modified at the N-terminus introducing manually biotinyl-6-aminoesanoic acid in SPPS by HOBt/TBTU/NMM activation.

**Table 3.1. Analytical data of biotinylated peptides.**

Peptide	HPLC (R <sub>t</sub> ,min) <sup>a</sup>	ESI-MS [M+3H] <sup>3+</sup> Calc (found)
Biotin-CSF114(Glc) ( <b>II</b> )	14.7	982.6 (982.83)
Biotin-CSF114 ( <b>II'</b> )	18.4	929.3(929.7)

<sup>a</sup>Analytical HPLC gradients at 1 mL min<sup>-1</sup>, 20-60% B in 20 min, solvent system A: 0.1% TFA in H<sub>2</sub>O, B: 0.1% TFA in CH<sub>3</sub>CN.

Both Peptides **II** and **II'** were contemporary cleaved from the resin and deprotected on the amino-acid side chains by using a mixture of TFA/ethanedithiole/thioanisole/H<sub>2</sub>O/phenol (92:2:2:2:2). In the case of glycopeptide **II** deprotection of the hydroxyl functions of the glucosyl moiety was performed as described in details in the Experimental Part using MeONa/MeOH. The peptides were purified by semi-preparative HPLC and characterized by ESI-MS. Analytical data are reported in Table 3.1.

---

<sup>55</sup> Moroder, L.; Papini, A.M.; Sigmuller, G.; Kocher, K.; Dorrer, E.; Schneider, C. *Biol. Chem. Hoppe-Seyler*, **1992**, 373, 315-321.

### 3.2 Antigen-antibody interaction study in Multiple Sclerosis patients' serum by Surface Plasmon Resonance

BIAcore monitors in real time, with a microfluidic system on a sensor surface, binding interactions between molecular partners such as antigen-antibody. A sensor surface was prepared by immobilising the synthetic glycopeptide CSF114(Glc) using two different strategies: direct immobilisation on dextran CM5 chip [amino coupling of CSF114(Glc)] and immobilisation on a previously activated streptavidin dextran CM5 chip with biotin-CSF114(Glc) (II) (Table 3.2).

Traditionally, BIAcore is considered an inappropriate technology for serum diagnostics because it is extremely difficult to subtract unspecific adsorption (with no relevant recognition properties) from the immunosensor surface. This is a particular critical point in the case of complex biological systems, e.g. sera samples. The difficulties in setting up of a reference surface with similar physical-chemical properties were overcome using the unglucosylated peptide CSF114, which lacks of activity. Therefore, all the unglucosylated peptide sequences were used on the reference surface for subtraction of unspecific binding or buffer effects. Unglycosylated peptides were captured on the reference channels (Fc1 and Fc3) and the corresponding glycosylated peptide sequences at the same level on active channels (Fc2 and Fc4).

**Table 3.2. Summary of immobilization procedures.**

<b>Immobilisation</b>	<b>Flow cell</b>	<b>Immobilised ligand</b>	<b>Absolute response</b>
Direct amino coupling	FC1	CSF114	1063 RU
	FC2	CSF114(Glc)	950 RU
Biotin/streptavidin	FC3	biotin-CSF114	453 RU
	FC4	biotin-CSF114(Glc)	766 RU

A first study was realized with specific anti-CSF114(Glc) antibodies, previously purified as described in the Experimental Part and characterised in

## PART A

ELISA to establish their antigen recognition properties. The antibodies were hence used for optimisation of the sensor. Purified antibodies solution was fluxed on the channels for 3 min at 30 $\mu$ l/min. Immunosensor surface regeneration was carried out using solutions of glycine in HCl at pH = 2.0 at different concentrations. Antigen-antibody recognition is reported as relative response in Figure 3.2.1.

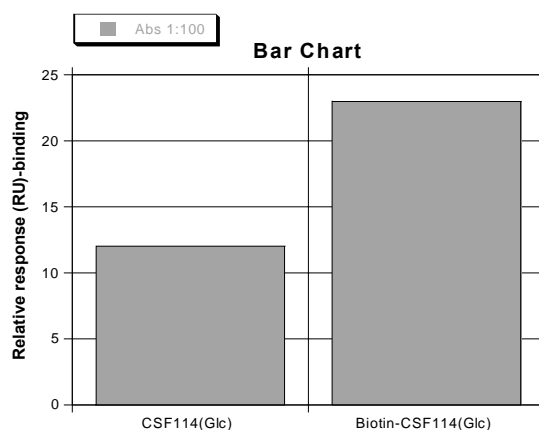


**Figure 3.2.1.** Bar chart reporting the relative response of the purified antibodies interacting with CSF114(Glc) (**I**) and its biotinylated derivative (**II**)(dilution 1:100).

If the CSF114(Glc)-immobilization absolute response is higher using the amino coupling procedure, the relative signal response in the presence of antibodies is lower than expected. On the contrary, biotinylated peptides allowed to observe an increase of the signal by using the streptavidin-biotin immobilisation. This effect was likely because of a favoured CSF114(Glc) exposition on the sensor surface, improving the signal response in the biotin-streptavidin system.<sup>56</sup> The amino coupling binding to the activated dextran layer might occur in two different positions. In fact, CSF114(Glc) presents two free amino functions, one at the N-terminus and the other on Lys-21 side chain.

---

<sup>56</sup> Bulukin, E. *Biosensor Development for Food and Environmental Applications*, 2006, PhD Thesis, Università degli Studi di Firenze.

Consequently, the minimal fundamental epitope Asn<sup>7</sup>(Glc) might not be optimally exposed for antibody interaction. Moreover, surface capacity in the two cases is different since streptavidin could bind up to four biotinylated antigen molecules. The different binding capacity in the two cases might significantly influence the sensitivity of recognition.

The chip containing Biotin-CSF114(Glc) (**II**) was then used for the analysis of MS patients' sera. Single sample serum from one MS patient, MS14, resulting positive in ELISA, was used to optimize the signal at dilution 1:100. We tested both directly injected serum MS14, and anti-human IgG (1:100) after MS14 serum injection (Figure 3.2.2).

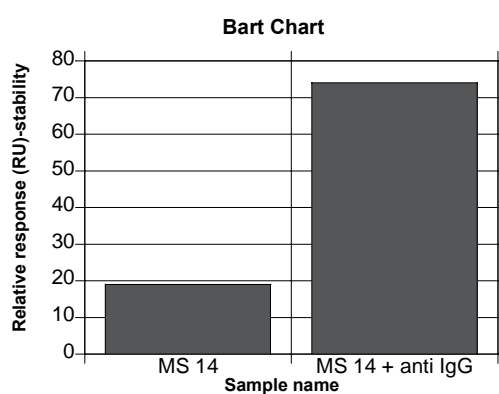


**Figure 3.2.2.** Comparison of relative responses of the immunosensor in absence and in presence of anti-human IgG (to enhance antibody recognition signal).

Time per assay was 20 min, hence a rapid screening. Signal was optimized thanks to injection of anti-human IgG after the serum sample. In fact, we obtained a four times increased recognition signal.

After set-up of injection conditions, a series of analyses of Multiple Sclerosis patients' sera (MS, 12) and normal blood donors (NBD, 20) was performed. Samples sera were diluted 1:100 before injection on the modified chip surface. The signal for each serum was obtained as difference between the control

PART A

channel with immobilised Biotin-CSF114 (flow cell 3) and Biotin-CSF114(Glc) channel (flow cell 4).

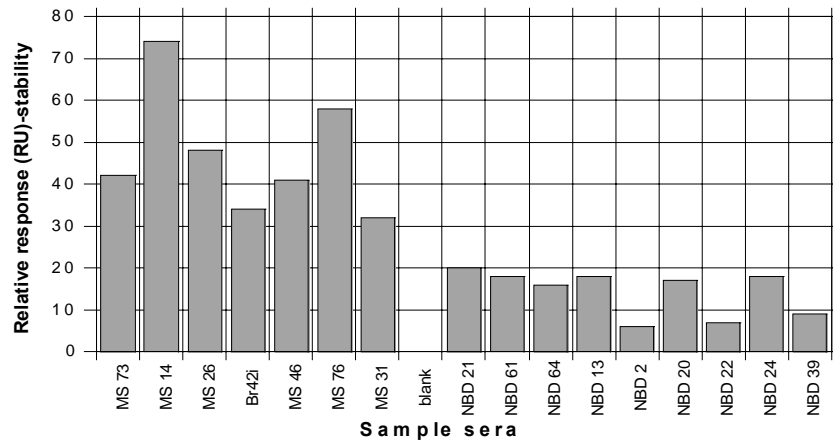


**Figure 3.2.3.** Analyses of MS patients sera and normal blood donors (NBD).

Results reported in Fig. 3.2.3 indicate that the system is able to distinguish between MS patients and NBDs. Differences between positive and negative samples were significant and allowed to establish a cut-off value.

Moreover, results obtained with the immunosensor we developed in this study were compared with the ones obtained in ELISA. Comparison between BIAcore and ELISAs was carried out using the relative response and the IgG absorbance values respectively, on sera diluted 1:100 (Figure 3.2.4).

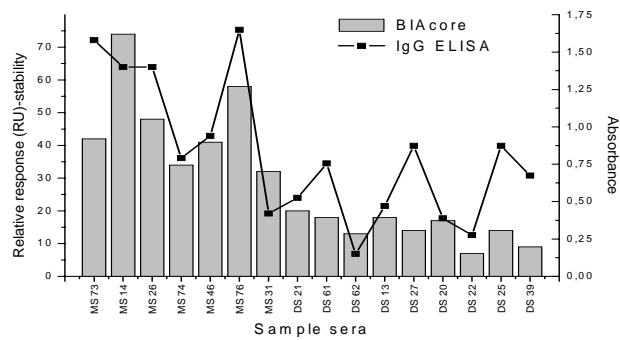


**Figure 3.2.4.** Comparison between BIAcore response (RU) and ELISA (Absorbance) for anti-CSF114(Glc) IgG detection.

The results indicate that the new immunosensor for BIAcore analysis was able to distinguish between normal blood donors and MS patients (Figure 3.2.3). Furthermore, the biosensor seems to correctly estimate the positive control sample MS31 that on the contrary resulted a false negative in ELISA. Moreover, false positive samples in ELISA, i.e., DS25 and DS27, resulted negative in BIAcore analysis (Figure 3.2.4).

In conclusion, we can assess that in Multiple Sclerosis patients' sera antigen-antibody interaction can be efficiently detected by BIAcore technology compared to ELISA method. Moreover, BIAcore technology was able to improve antibody recognition in sera compared to ELISA. In fact, we were able to distinguish MS patients and normal blood donors by BIAcore using the newly developed immunosensor based on Biotin-CSF114(Glc). In addition, sera samples in ELISA need overnight incubation compared to immunosensor analysis, which can be performed in real-time with antibody detection in less than 20 minutes for each serum with a significant decrease of time analysis.

Moreover, BIAcore analysis using the new Biotin-CSF114(Glc)-based immunosensor could be a promising technology compared to ELISA because it was able to avoid false negative and false positive controls. Further studies on a large number of samples (possibly a statistically significant number of MS and NBDs samples) will be able to confirm these very promising results.





#### 4. *Real-time measurements of antigen-antibody force interactions in Multiple Sclerosis by Optical Tweezers*

Binding and interaction studies between different classes of molecules are generally analysed in bulk solution samples, as it occurs for example in ELISA and SPR. A large number of molecules can be analysed at the same time in this kind of assay, and the system is in thermodynamic equilibrium where the molecules are exposed only to thermal forces. In recent time, however, a number of novel techniques have been developed, which are able to analyze interactions between individual pairs of molecules. Scanning probe microscopy,<sup>57</sup> optical tweezers,<sup>58</sup> biomembrane force probe,<sup>59</sup> and flexible micro needles<sup>60</sup> techniques have been used to investigate biomolecular interactions.

Recently, **Optical Tweezers** (OT) have been particularly successful to investigate a variety of biological systems. This technique is able to directly measure forces on trapped objects. In fact, in OT experiments, a micrometer sized bead with high refractive index is trapped by optical forces in an electric field gradient near a laser focus.<sup>61</sup> Because the optical trap works as a mechanical potential well and displays virtual spring properties, forces can be measured following bead displacement from its equilibrium position in the trap centre. OT are typically compliant (<1 pN/nm) and possess a force resolution in the sub-picoNewton (pN) range. Moreover, the maximal trapping

---

<sup>57</sup> Binnig, G.; Quate, C.F.; Gerber, C. *Physical Review Letters*, **1986**, 56(9), 930-933.

<sup>58</sup> (a) Ashkin, A.; Dziedzic, J.M.; Bjorkholm, J.E.; Chu, S. *Optics Lett*, **1986**, 11(5), 288-290. (b) Gordon, J.P. *Physical Review A*, **1973**, 8(1), 14-21.

<sup>59</sup> Evans, E.; Ritchie, K.; Merkel, R. *Biophys J*, **1995**, 68(6), 2580-2587.

<sup>60</sup> Essevaz-Roulet, B.; Bockelmann, U.; Heslot, F. *Proc Natl Acad Sci USA*, **1997**, 94, 11935-11940.

<sup>61</sup> (a) Ashkin, A. *Proc Natl Acad Sci USA*, **1997**, 94, 4853-4860. (b) Ashkin, A.; Dziedzic, J.M. *Science*, **1987**, 235(4795), 1517-1520. (c) Ashkin, A.; Dziedzic, J.M.; Yamane, T. *Nature*, **1987**, 330, 769-771.

## PART A

force is typically smaller than 200 pN. In fact, it is determined by several factors, i.e., the diameter and refractive index of the bead, the numerical aperture and geometry of the optical system, and the incident optical power.<sup>62</sup> Optical tweezer is a recent technique able to study binding and/or adhesion of biomolecules in real time under biologically relevant conditions.

In order to measure the forces necessary to break antigen-antibody formed bonds, when possible at the single-molecule level, the mechanics and mechano-chemistry of the interaction have been studied by Optical Tweezers. For this purpose, design and synthesis of molecular handles for grabbing purified antibodies from Multiple Sclerosis patients' sera specific for the glycopeptide antigen CSF114(Glc), had to be developed for manipulation in the Optical Tweezers instrument.

### **4.1 Design and synthesis of optically labelled CSF114(Glc)-glycopeptide analogues for Optical Tweezers measurement.**

The glycopeptide CSF114(Glc) and the unglycosylated one have been appropriately modified to be employed in Optical Tweezers technology. To this purpose, glycopeptide antigen required a functional group, possibly far away from the epitope, which could be covalently linked to beads. Therefore, we used a Biotin-PEG-NovaTag™ resin as a solid support for SPPS. This resin incorporated a PEG spacer between Biotin and the peptides and glycopeptides to be synthesized.

Peptides were synthesized following the Fmoc/tBu SPPS strategy, as described in details in the Experimental Part, using commercially available Fmoc-amino acids and HOBt/TBTU/NMM activation. Peptides were targeted at the N-terminus with fluorescein introduced to differentiate, in Optical Tweezers

---

<sup>62</sup> For more details about optical tweezers see chapter concerning description of the techniques in the experimental part.

procedure, beads containing peptides by fluorescence imaging. For this reason, after having synthesized the desired peptide sequences, 5(6)-carboxyfluorescein was manually introduced at the N-terminus of the resin-bound biotinylated peptides using HOBt/DIPCDI as coupling reagents.

**Table 4.1 Analytical data of fluorescent-labelled peptides.**

Peptide	HPLC ( $R_t$ ,min)	ESI-MS [ $M+3H$ ] <sup>3+</sup> Calc (found)
Fluoresceinyl-CSF114(Glc)-Biotin ( <b>III</b> )	12.3 <sup>a</sup>	1187.9 (1188.83)
Fluoresceinyl-CSF114-Biotin ( <b>III'</b> )	14.7 <sup>b</sup>	1078.3 (1078.7)

<sup>a</sup>Analytical HPLC gradients at 1 mL min<sup>-1</sup>, 35-75% B in 30 min, 30-60% B in 30 min, solvent system A: 0.1% TFA in H<sub>2</sub>O, B: 0.1% TFA in CH<sub>3</sub>CN.

After cleavage from the resin and deprotection of the side chains of the peptide sequences using the scavenger cocktail TFA/H<sub>2</sub>O/EDT/phenol/anisol (92:2:2:2:2), final deprotection of the hydroxyl functions of the sugar moiety linked to Asn residue (using MeONa/MeOH) in the case of the glycopeptide **III**, as described in details in the Experimental Part, all the peptides were purified by semi-preparative HPLC and characterized by ESI-MS. Analytical data are reported in Table 4.1.

## 4.2 Functionalization of the microscopic beads

Specific anti-CSF114(Glc) purified antibodies were attached to functionalized anti-human IgG polystyrene (latex) beads. Unbound antibodies were removed after gently washing in D-PBS buffer. Detailed procedure is reported in details in the experimental part.

Subsequently, streptavidin-coated latex beads were coated with biotinylated Fluoresceinyl-CSF114-Biotin and Fluoresceinyl-CSF114(Glc)-Biotin respectively. The PEG spacer introduced between peptide and biotin at the C-terminus reduces steric hindrance between the peptide and the avidin leading to better binding of biotin. Furthermore, if binding of antigen-antibody pairs are close enough, adjacent antigens could form a new bond only when the existing linkage has ruptured. Tethering the peptide to the bead by a spacer can

## PART A

be helpful for interactions because it can reduce these steric hindrance (Figure 4.2).<sup>63</sup>

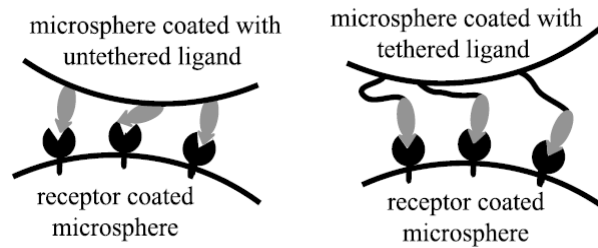


**Figure 4.2.** Schematic representation of adhesion between two microspheres, mediated by receptor-ligand bonds. In one case (left) the ligand was attached directly to the microsphere, which restricted the orientation of the ligands and resulted in strained bonds when multiple bonds were formed. In the other case (right) the ligand was attached to the microsphere by a tether, allowing greater freedom of orientation of the ligands to form multiple unstrained bonds.

### 4.3 Real-time antigen-antibody interaction measurements

In collaboration with Prof. V. Lombardi (Laboratorio di Fisiologia, Dipartimento di Biologia Animale e Genetica, Università degli Studi di Firenze), forces necessary to break bonds formed between the modified mimetic glycopeptide antigen **III** and IgG antibodies have been studied. Considering that the sensibility of the sophisticated instrument control and data acquisition of the optical tweezers should be absolutely necessary for reliable measurements, the apparatus interface had to be previously calibrated (Figure 4.3.1).

---

<sup>63</sup> Kulin, S.; Kishore, R.; Hubbard, J.B.; Helmerson, K. *Biophysical Journal*, **2002**, 83, 1965-1973.

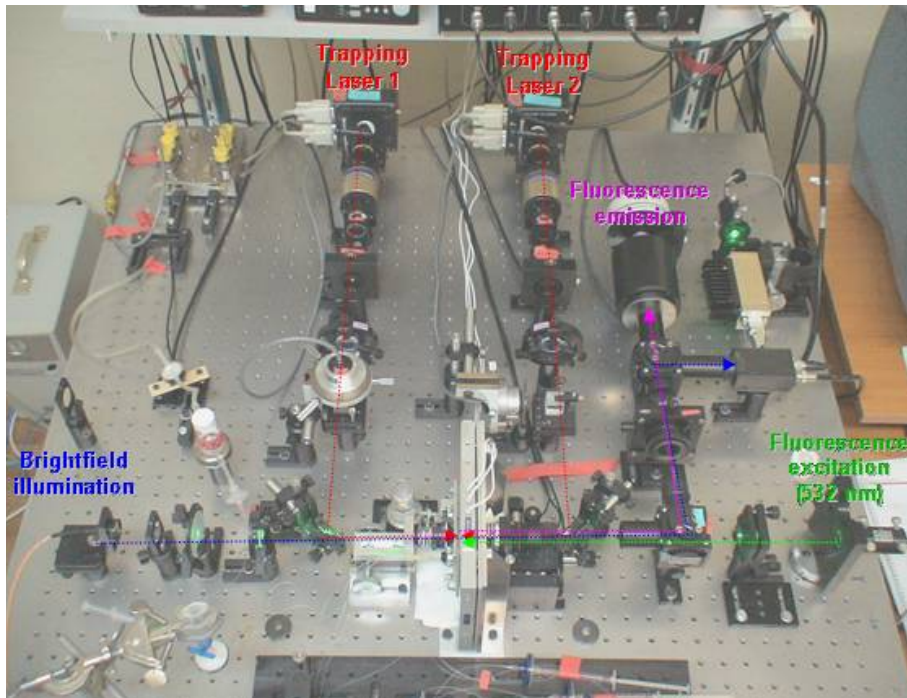


**Figure 4.3.1.** Image of the Optical Tweezers instrument. Colour lines indicate the different optical trajectories (blue: brightfield, red: trapping lasers, green: fluorescence excitation, magenta: fluorescence emission).

All measurements were made inside a home-made microchamber. In order to withstand the fluid pressure, the chamber was sealed by melting the parafilm layers pressed between two coverglasses. A micropipette and 80- $\mu\text{m}$ -diameter glass tubes were placed between the two parafilm layers prior to sealing. The chamber was clamped on a holder with two aluminium brackets with threaded holes to connect tubing to the chamber by means of flangeless fittings. Polystyrene beads of 1-10  $\mu\text{m}$  diameters can be held on the tip of the pipette by suction. A syringe attached to the other end of the micropipette tubing was used to apply suction and pressure in the pipette. Two gravity-controlled containers were attached to the other end of the two tubes to introduce in the flow cell both isolated antibody and antigen molecule covalently attached to different polystyrene beads.

## PART A

CSF114(Glc)-coated beads were flown in the microchamber, and one bead was captured with the glass micropipette controlling by fluorescence that the peptide was really attached (Figure 4.3.2). Furthermore, fluorescence intensity signal registered the peptide density into the bead.

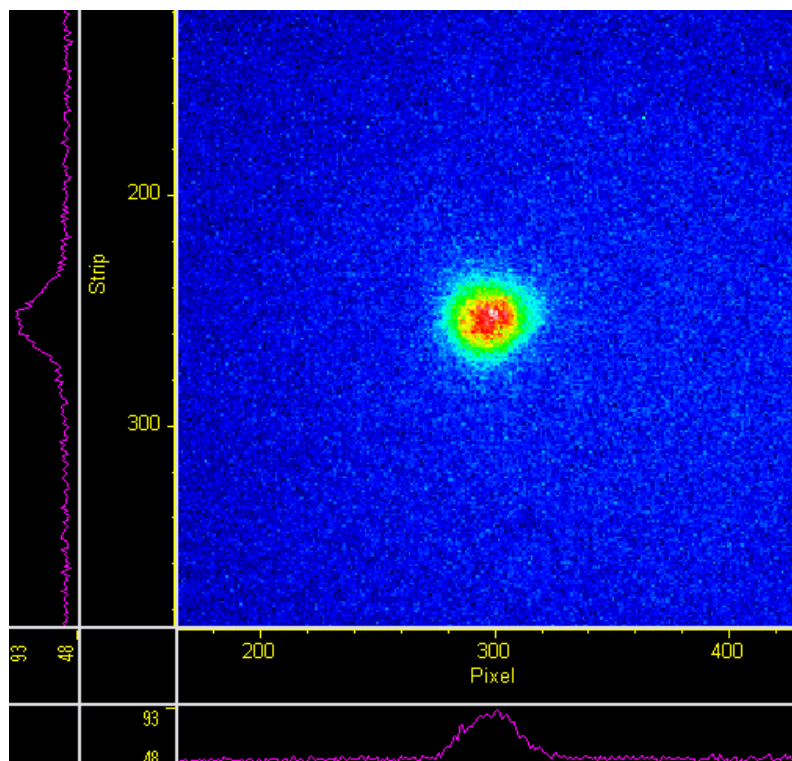


**Figure 4.3.2.** Fluorescence image of CSF114(Glc)-coated microbead..

Antibody-coated beads were entered into the chamber, and one bead was captured in the optical trap. Moving the micropipette towards the trap, the two beads were pressed together (Figure 4.3.3i). The beads were held pressed together for a pre-adjusted period. Subsequently, the micropipette was pulled away from the trap (Figure 4.3.3ii) with a preadjusted velocity. We measured the force at the instant that the connection between the two beads was ruptured (Figure 4.3.3iii).

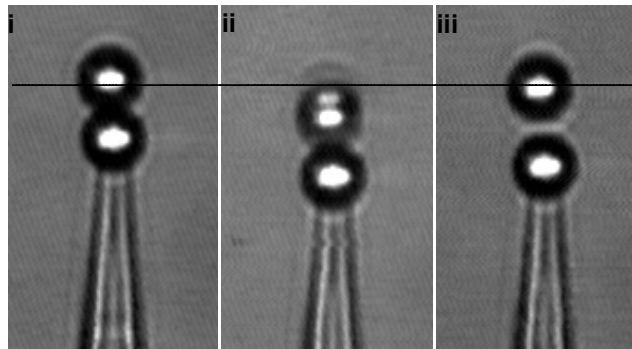


**Figure 4.3.3.** Picture sequence of the experimental procedure for measuring interaction forces. On the top, antibody-coated bead captured in the optical trap. The lower bead is the CSF114(Glc)-coated bead held with a moveable glass micropipette. The beads were first pressed together (i), then pulled apart (ii) until a rupture event occurred followed by the sudden return of the upper bead to its equilibrium position in the trap centre (iii).

Characteristic force versus time traces obtained in antigen-antibody interaction force spectroscopy experiments is shown in Figure 4.3.4. Positive forces correspond to interaction forces, and negative forces to compression forces with which the beads were pressed together.

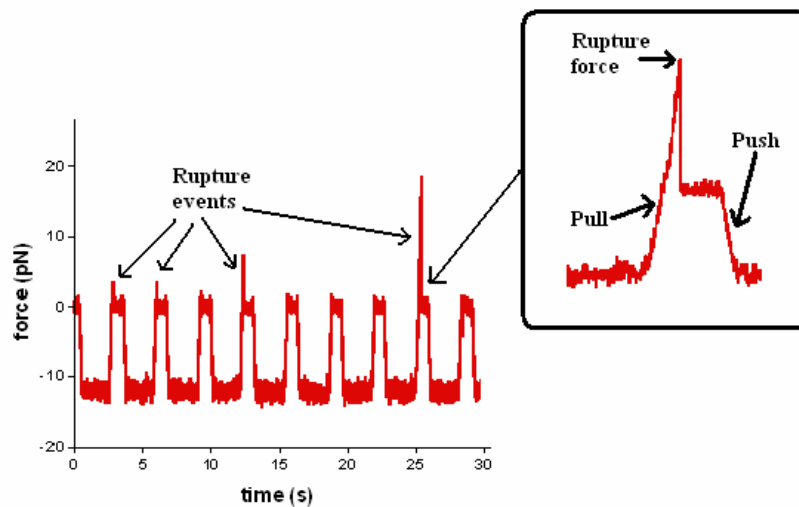


**Figure 4.3.4.** Time-dependent force trace of interaction between a bead coated with CSF114(Glc) and a bead coated with isolated anti-CSF114(Glc) IgG (rigor bond).

## PART A

In the force spectrum reported in Figure 4.3.4 we can observe tooth-shaped peaks consisting of a rising slope, a peak, and a rapid force drop. Force increases during stretch because interactions formed between antigen and antibody during the compression period hold the beads together. The peak corresponds to the force in the instant of the rupture of antigen-antibody interaction. This rupture force, which is an important parameter of the mechanical properties of the antigen-antibody interaction, was measured under various experimental conditions.

To assure that the observed force spectra was certainly because of interaction between the synthetic antigen CSF114(Glc) and purified antibodies, several negative control experiments have been performed. First, the adhesion experiment was carried out using both microspheres processed with IgG antibodies (Figure 4.3.5A). No attachment was observed. In a second series of experiments, we studied possible adhesions between spheres coated with the isolated antibodies and spheres containing the fluoresceinyl derivative of the unglycosylated peptide CSF114 **III'**, used as negative control in ELISA due to its well known lack of activity (Figure 4.3.5B).. Adhesion was observed only in the case of the glucosylated peptide analogue **III** interacting with antibody-coated spheres. Moreover, previous studies guarantee the resistance of streptavidin-biotin bond at forces exceeding 60 pN, which far exceed forces range in which antigen-antibody rupture events were observed in different systems.<sup>64</sup>

---

<sup>64</sup> Bianco, P. Mechanics of titin-actin interaction explored with force-measuring optical tweezers, PhD Thesis, **2006**, Università degli Studi di Firenze.



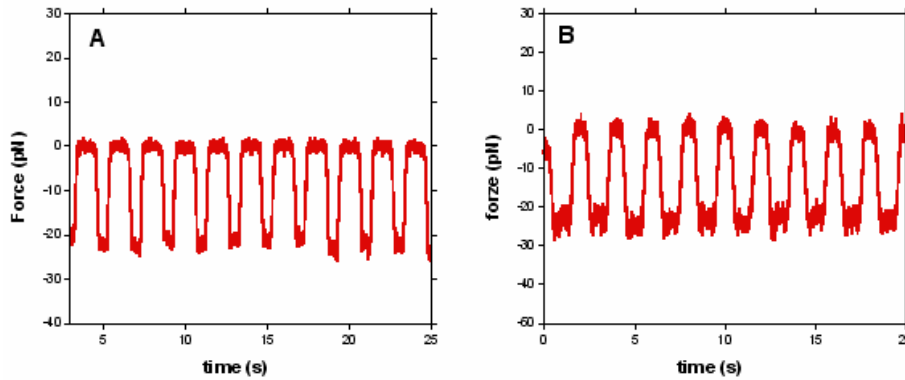


**Figure 4.3.5.** Collection of force traces obtained in control experiments: *A.* Control experiment between beads coated with isolated anti-CSF114(Glc) IgG antibodies, respectively; *B.* Control experiment between beads coated with isolated anti-CSF114(Glc) antibodies and CSF114 (III'), respectively.

#### 4.4 Rupture force statistic study of CSF114(Glc)-anti-CSF114(Glc) IgG antibodies

A hundred series of beads-touching were performed allowing a statistical study of the rupture forces distribution for the synthetic antigen CSF114(Glc) and anti-CSF114(Glc) IgG antibodies at different stretch rates. Figure 4.4.1 reports the probability of the rupture force value.

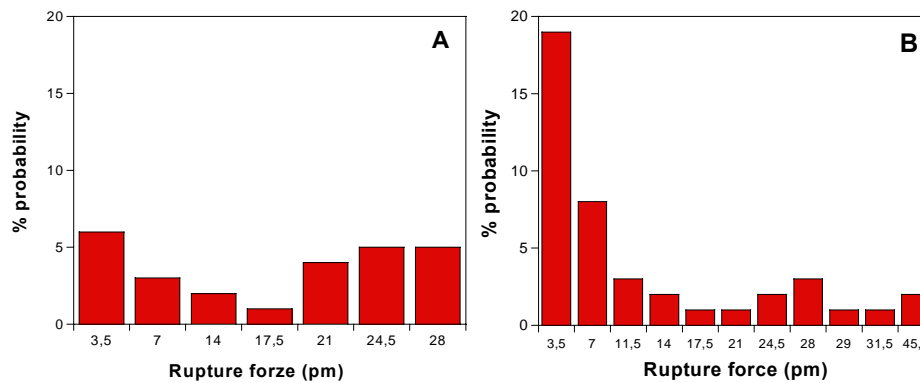


**Figure 4.4.1.** Distribution of rupture forces of CSF114(Glc) – anti-CSF114(Glc) IgG antibodies in the case of 5000 nm/s stretch rates (*A*) and 250 nm/s (*B*). No-interaction probability is 66% (*A*) and 53% (*B*).

## PART A

At a stretch rate of 5000 nm/s a relatively wide distribution is observed, with rupture forces ranging from 3.5 to 28 pN. Zero-rupture force value (no interaction) had the maximum probability value higher than 60% as expected (Figure 4.4.1A).

Decreasing stretch rate to 250 nm/s resulted in widened rupture force range from 3.5 to 48 pm (Figure 4.4.1B). Moreover, rupture force event probability was increased from 40% to 50% probably because contact-time between beads increased.

Intensity peak at ~3.5 pN (Figure 4.4.1B) could be explained at the single molecular level, which might correspond to the single antigen-antibody rupture force. The wide range of forces could be due to the interaction of multiple antibody molecules with different coated-antigens. Supporting previously reported hypotheses, all the experimental rupture force values are approximately multiple of 3.5 pN. Considering the experimental error, it is possible to establish a rupture force value for antigen-antibody interaction at the single molecular level:  **$3.5 \pm 1$  pN**.

In conclusion, a platform to study single-molecule interactions between the glycopeptide antigen CSF114(Glc) and its specific antibodies isolated from MS patients' sera has been set-up. This platform let us to obtain the force value necessary to break antigen-antibody linkage.

## **PART B: Study on molecular mechanisms of autoantibody recognition in Multiple Sclerosis**

In order to characterize the molecular mechanism of autoantibody recognition in Multiple Sclerosis, it is necessary to investigate the structural aspects involved in autoimmune response. In Multiple Sclerosis, possibly native proteins protruding from the surface of myelin membrane are no more recognized as self-antigens and are involved in an autoimmune response. The structure-based designed glycopeptide CSF114(Glc) previously developed in our laboratories, is able to recognize high antibody titre in sera of Multiple Sclerosis patients. These results were validated in a simple immunoenzymatic assay on a statistical significant number of MS patients' sera compared to other immune diseases.<sup>25</sup> Therefore, CSF114(Glc) works like a mimetic molecule of different epitopes produced in native myelin proteins. For this reason, we decided to investigate the behaviour of the glycopeptide antigen CSF114(Glc) in a membrane environment. By electrochemical measurements of the glycopeptide activity in a membrane model system, it could be possible to obtain detailed information about its behaviour in a membrane environment.

### ***5. Bilayers mimicking biological membranes***

#### **5.1 Cells natural barrier**

To stay alive, all living cells need membranes. Membranes typically define enclosed spaces or compartments in which cells could maintain a chemical or biochemical environment that differs from outside. Membranes not only sustain cell, but have an active role in regulating flux of molecules, ions, and signals from one side to the other, preventing undesirable agents from entering cells. Probably the most important feature of a biological membrane (biomembrane) is its selective permeability. This means that the size, charge,

## PART B

and other chemical properties of atoms and molecules attempting to cross it will determine whether they succeed to do so. Selective permeability is essential for effective separation of a cell or organelle from its surroundings.

To understand membrane it is necessary to know its organization. All membranes have a general common structure, in which two-layered sheet of lipids have different molecules (glycoproteins, cholesterol, etc) embedded in them. Membrane formation is a consequence of the amphipathic nature of lipids. In aqueous environment the polar head groups face water, whereas the hydrocarbon tails interact with each other. The lipids, proteins, and other molecules are held together mainly by non-covalent interactions organized as fluid mosaic model.<sup>65</sup> This model describes the cellular membranes as two-dimensional, viscous solutions of lipids and proteins at thermodynamic equilibrium. Recently, this model system has been updated,<sup>66</sup> assuming the non-randomness distribution of lipid and protein components in a membrane, which is characterized by variable patchiness, and thickness, and higher protein occupancy than it was generally considered before (Figure 5.1).

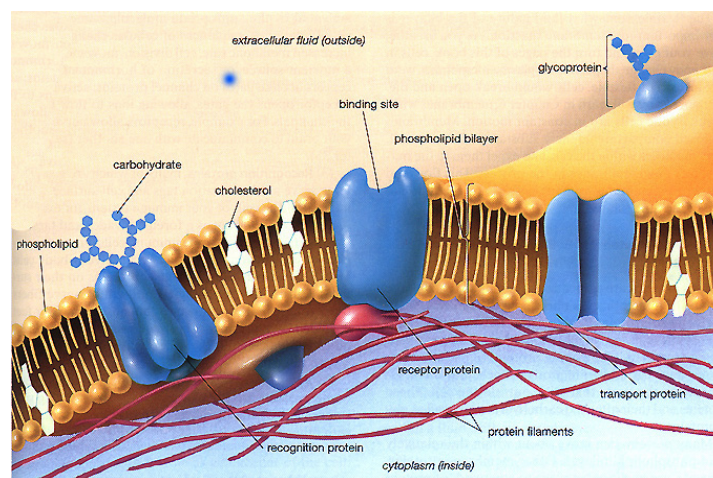


**Figure 5.1** Diagram of various classes of proteins associated with the lipid bilayer

---

<sup>65</sup> Singer, S.J., Nicolson, G.L. *Science*, **1972**, 175, 720-731.

<sup>66</sup> Engelman D.M. *Nature*, **2005**, 438, 578-580.

## 5.2 Why mimicking a biological membrane?

The complexity of the lipid bilayer system has made the biological membrane an extensive and exciting field of study. In particular, many researchers have focused the attention on membrane proteins. In fact, one of the major challenges in biosciences today is mimicking a bilayer lipid membrane to investigate membrane-related processes like cell adhesion, nerve excitation, photosynthesis, respiration etc. Biomimesis has represented a prominent concept in biosciences. As a consequence, biomimetic membranes represent a model that does not just copy biological membranes, but use the fundamental ideas and principles from biology, in a simplified approach. The biological membranes obey the laws of physics and chemistry. To explain a biological system such as a biomembrane in physical, chemical and physiological terms, as well as the behaviour of single proteins, it is necessary to employ a simplified model system.

## 5.3 Biomimetic membranes: model systems

The first membrane models to be studied were the bilayer lipid membranes (BLMs).<sup>67</sup> These planar membranes were obtained by spreading a lipid solution in a small hole (1 mm diameter) of a teflon septum separating two compartments, which contain an aqueous buffer. Evaporation or diffusion of the lipid solvent leads to thinning of the film across the small hole to its final bilayer state. Because of the lack of light reflectance, they are also called black lipid membranes.

Concurrently with the development of the BLMs, other researchers studied the behaviour of free lipids in aqueous solutions. According to electron microscope experiments, they observed that lipids spontaneously formed a

---

<sup>67</sup> Mueller, P., Rudin, D.O., Tien, H.T., Wescott, W.C. *J. Phys. Chem.*, **1963**, 67, 534-535.

## PART B

closed bilayer membrane in aqueous environment.<sup>68</sup> This structure, the so-called liposome, was proven highly useful in a number of studies on membrane structure and function, in which proteins or molecules can be incorporated and investigated by fluorescence,<sup>69</sup> etc. The accessibility to only one side of the membrane limits the use of liposomes in electrochemical studies.

The introduction of Solid-Supported bilayer lipid Membranes (SSMs)<sup>70</sup> (Figure 5.3a) has represented an advancement in stability of membrane models. Thanks to the improved mechanical and long-term stability, combined with a more useful configuration, the SSM can be investigated by a variety of experimental techniques.

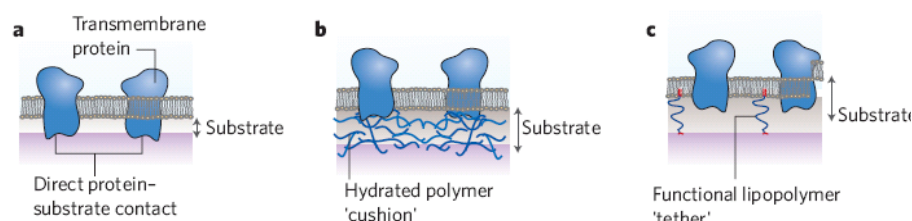


**Figure 5.3.** A schematic illustration of SSM (a), polymer-supported psBLM (b), and tBLMs (c).

An alternative strategy to improve some of the above-mentioned limitation of the original SSMs is represented by the development of hybrid SSMs. The lack of a well-defined ionic reservoir on the solid side of the bilayer represents an important drawback when studying membrane transport through ion carriers and channels.<sup>71</sup> This model system is characterized by a first monolayer (commonly an alkanythiol monolayer) covalently attached to a metal substrate, on which a lipid monolayer is deposited either by transfer from air–water

<sup>68</sup> Bangham, A.D., Standish, M.M., Watkins, J.C. *J. Mol. Biol.* **1965**, 13, 238-252.

<sup>69</sup> Gatto, E.; Mazzuca, C.; Stella, L.; Venanzi, L.; Toniolo, C.; Pispisa, B. *J. Phys. Chem. B*, **2006**, 110 (45), 22813-22818.

<sup>70</sup> Sackmann, E. *Science* **1996**, 271, 43–48

<sup>71</sup> Raguse, B., Braach-Maksvytis, V., Cornell, B.A., King, L.G., Osman, P.D.J., Pace, R.J., Wiczorek, L. *Langmuir* **1998**, 14, 648-659.

interface or through vesicle unrolling. However, stiffness of alkanylthiol/lipid SSMS is much higher than that of fluid biological membranes. In addition, the structure of thiol-based SSMS prevents formation of a water layer between the bilayer and the metal support. Therefore, such mixed SSMS are unsuitable for incorporation of integral proteins and for studies of ion transport through ionophores.

In conclusion, SSMS are more stable in aqueous solution than their unsupported counterparts. Nevertheless, the proximity of the solid support may lead to decreased bilayer fluidity and represents a problem particularly for incorporation of transmembrane proteins.

To avoid this problem it is possible to separate the membrane from the solid substrate using soft polymeric materials that are attached on the substrate and support the membrane. This approach, the so-called polymer-supported Bilayer Lipid Membranes (psBLM) (Figure 5.3b), has significantly reduced the frictional coupling between membrane-incorporated proteins and the solid support, and hence the risk of protein denaturation.<sup>70,72,73</sup>

Another recent significant advance is represented by tethered Bilayers Lipid Membranes (tBLMs) (Figure 5.3c). The tethered system is composed of a first monolayer covalently attached to the solid surface and a second monolayer of free lipids. One of the most interesting properties of tBLMs is their high mechanical stability which provides a long and stable functionality<sup>74</sup>. Moreover metal supported tBLMs are characterized by a hydrophilic region interposed between the bilayer and the metal, which can accumulate small and medium molecules that pass across the membrane mimicking the biological system. These properties are due to a hydrophilic molecule terminating at one end with a disulfide group that anchors this “hydrophilic spacer” to the

---

<sup>72</sup> Sackmann, E., Tanaka, M. *Trends Biotechnol.* **2000**, 18, 58–64.

<sup>73</sup> Knoll, W., Frank, C.W., Heibel, C., Naumann, R., Offenhäuser, A., Rühle, J., Schmidt, E.K., Shen, W.W., Sinner A. *Rev. Mol. Biotechnol.* **2000**, 74, 137–158.

<sup>74</sup> Vockenroth et al. *BBA Biomembranes*, **2007**, 1768, 1114-1120.

## PART B

surface of the metal. The other end of the hydrophilic spacer may be covalently linked to the polar head of a phospholipid molecule, giving rise to a supramolecule termed “thiolipid”. The tethered lipid bilayer is characterized by mechanical stability and fluidity. Moreover, this system allows the incorporation of many different proteins.

In conclusion, different biomimetic models have been so far developed opening new perspectives in the field of medical diagnostics, drug screening, and environmental control. Up to now, biomimetic membranes are not ready to incorporate integral proteins of high molecular weight, but incorporation of small proteins or fragments from epitopes have been widely demonstrated.



## 6. *Role of $\beta$ -turn structures in membrane permeability*

Nowadays, recurrent structural and functional activity in a membrane environment has been evaluated for peptides of diverse composition. Although hundreds of peptides interacting with membranes have now been characterized, these peptides have been classified into few conformational paradigms. In fact, strong relationship between conformation governing peptide structure and membrane activity among peptides have been previously defined.<sup>75</sup>

$\beta$ -Turn and  $\beta$ -sheet peptide conformations represent a highly diverse group of molecules at the level of primary structure. Despite such primary sequence differences, peptides presenting a common  $\beta$ -turn motif and interacting with a membrane share common features, with distinct hydrophilic and hydrophobic surfaces. Less is known about structures adopted by tryptophan-rich peptides. Trp residue possesses some crucial chemical properties. In fact it has a distinct preference for the interfacial region of lipid bilayers. In combination with Arg, participates in cation- $\pi$  interactions, thereby facilitating enhanced peptide-membrane interactions. Trp side-chains are also implicated in peptide and protein folding in aqueous solution, where they contribute by maintaining native and non native hydrophobic contacts. Moreover, they lead to structures for membrane-mimetic bound peptides that go far beyond regular  $\alpha$ -helices and  $\beta$ -sheet structures.<sup>76</sup> Synthetic peptides with defined secondary structure scaffolds, namely hairpins and helices, containing tryptophan residues, have been investigated to probe the influence of a large number of aromatic amino acids on backbone conformations. Several examples of prototypic  $\beta$ -structures conformations have been previously reported and studied. Moreover, it has been reported that membrane interaction could stabilize  $\beta$ -hairpin structures.<sup>77</sup>

---

<sup>75</sup> Yeaman, Y.; Yount, N. *Pharmacological Reviews*, **2008**, 55(1), 27-54.

<sup>76</sup> Chan, D.I.; Prenner, E.J.; Vogel, H.J. *B.B.A. Biomembranes* (**2006**), 1758 (9), 1184-1202

<sup>77</sup> Rotondi, K.; Gierasch, L. *Biopolymers*, **2004**, 71(6), 638-651.

## PART B

### 6.1 CSF114(Glc) a $\beta$ -turn structure-based designed glycopeptide

The glycopeptide CSF114(Glc) is characterized by the same amino acid composition, but in a different primary sequence of the myelin oligodendrocyte glycoprotein (MOG) peptide fragment [Asn<sup>31</sup>(Glc)]hMOG(30-50). CSF114(Glc) was potentially endowed with divergent conformational behavior, intended to optimally expose the glucosyl structure in the solid-phase conditions of and ELISA plate. Such optimal exposition could be obtained positioning the Asn residue at the tip of the specific CSF114(Glc)  $\beta$ -hairpin structure definitely designed with hMOG(30-50) peptide amino acids. In particular, it is well known that the Asn-Gly sequence is the best choice in a type I'  $\beta$ -turn structure. To stabilize the hairpin structure, the two putative turn residues were positioned in an almost central position in the primary sequence of the peptide, and the flanking residues were selected to optimize cross strand tertiary interactions. In particular, Glu-5 and Ser-6 side chains can interact throughout hydrogen bond formations, while Val-4 and Val-11 undergo hydrophobic interaction.

**A: KN(Glc)ATGMEVGWYRPPFSRVVHL**

**B: TPRVERN(Glc)GHSVFLAPYGWMVK**

**Figure 6.1.** Amino acids primary sequence of (A) Asn<sup>31</sup>(Glc)]hMOG(30-50) and (B) CSF114(Glc) .

The conformational properties of CSF114(Glc) in solution were investigated by NMR spectroscopy. Conformational studies based on mono and bi-dimensional NMR experiments in HFA/H<sub>2</sub>O (1:1 v/v) showed that CSF114(Glc) contains a  $\beta$ -hairpin motif between residues 2 and 14 with a type I'  $\beta$ -turn, with Asn<sup>7</sup> and Gly<sup>8</sup> as central residues.<sup>23</sup>

## 7. *Mimetic antigens in a membrane model environment*

The glycopeptide CSF114(Glc), possibly mimicking neoepitopes from myelin proteins, has been studied in a membrane environment. Moreover, a small library of peptide analogues of CSF114(Glc) has been also synthesized and studied in the biomimetic membrane system. To further confirm the importance of the secondary structure of CSF114(Glc) peptide antigen we also synthesized the corresponding peptide characterised by the scrambled sequence Scramble CSF114(Glc) (**VI**) (see Table 7.1). In this random sequence containing the same amino acids of CSF114(Glc) (**I**) only the glucosylated Asn<sup>7</sup> residue was left at its initial position in the sequence. Circular Dichroism studies of the scrambles sequence **VI** indicated a high tendency to the helix formation, and NMR analysis confirmed this indication. Several NMR parameters indicate the presence of a  $\alpha$ -helix along residues 4-15. Calculated structures (Figure 7.1) showed the expected helical segment.

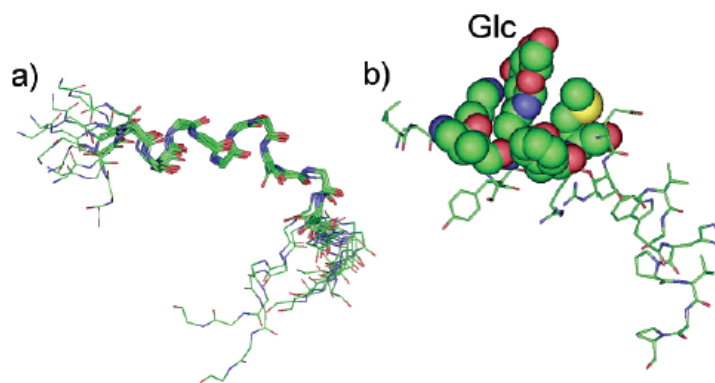


**Figure 7.1.** (a) Superposition of the 10 lowest energy conformers of **6**. Structures were superimposed using the backbone heavy atoms of residues 3-15 (thicker lines). Heavy atoms are shown with different colours (carbon, green; nitrogen, blue; oxygen, red; sulphur, gold). Side chains and hydrogen atoms are not shown for clarity. (b) Lowest energy conformer of **6**. Asn<sup>7</sup>(Glc) and residues Lys<sup>3</sup>, Val<sup>4</sup>, Phe<sup>8</sup>, and Met<sup>10</sup> are shown as Van der Waals surfaces.

**Table 7.1 Peptide and glucopeptide sequences studied in biomimetic membranes**

Peptide	Sequence
CSF114(Glc) ( <b>I</b> )	TPRVERN(Glc)GHSVFLAPYGWMVK
CSF114 ( <b>I'</b> )	TPRVERNGHSVFLAPYGWMVK
Scramble CSF114(Glc) ( <b>VI</b> )	LAKVSYN(Glc)FRMETRVGWHPVGP
Scramble CSF114 ( <b>VI'</b> )	LAKVSYNFRMETRVGWHPVGP

### 7.1 The tethered Bilayer Lipid Membrane (tBLM) system

We used tBLMs supported by a hanging-drop mercury electrode as an experimental model, as well as vesicles to be used in fluorescence experiments. With respect to gold, mercury has the advantage of providing a defect-free and fluid surface to the self-assembling spacer.

The thiolipid used as linker in the tBLM was DPTL, 2,3-di-O-phytanyl-sn-glycerol-1-tetraethylene glycol-D,L- $\alpha$ -lipoic ester (Figure 7.1.1). DPTL is composed of three distinct parts: a lipid head, a hydrophilic spacer, and an anchor group.

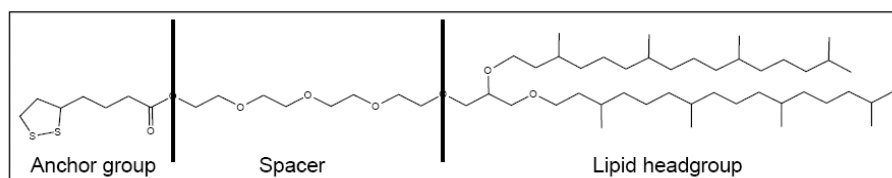


**Figure 7.1.1.** The DPTL structure.

The lipid residue facilitates to form the proximal lipid monolayer according to Van der Waals interactions between the hydrocarbon tails. The ion reservoir is represented by four ethylene glycol units and the anchor group provides stability of the proximal layer of the membrane through the covalent bond of the thiol group with mercury. Lipoic acid fragment provides a disulfide bridge, which is more stable than a simple thiol bond.

Subsequent immersion of the DPTL monolayer covalently linked to the mercury electrode, across a lipid film of DphyPC (Di-phytanoyl Phosphatidyl Choline) previously spread on the surface of the electrolyte solution, let obtain a lipid bilayer interposed between the hydrophilic moiety of the thiolipid and the aqueous solution.

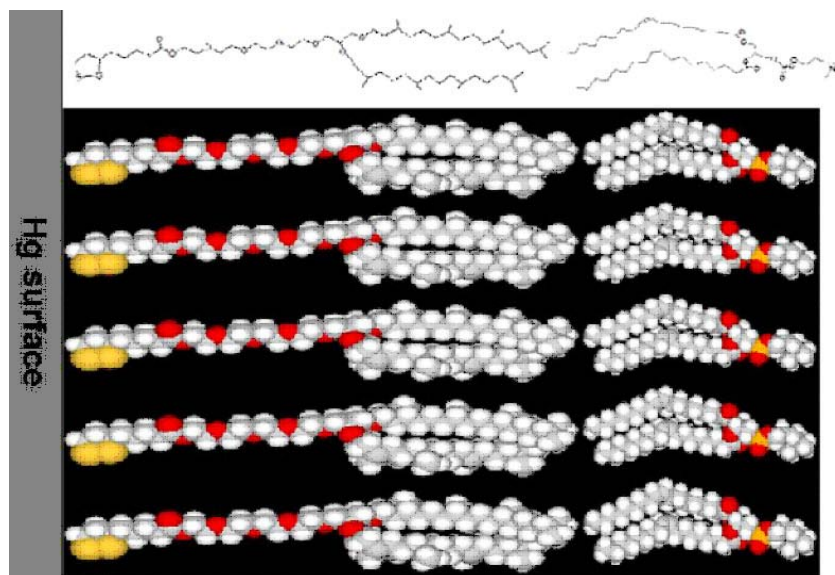


**Figure 7.1.2.** Representation of the different sub-structural elements of the tBLM, an Hg-supported DPTL/DphyPC film bathed by aqueous 0.1 M KCl.

The electrical properties of a tBLM have been analyzed by AC Voltammetry and Electrochemical Impedance Spectroscopy (EIS). Fitting EIS data to a simple equivalent circuit (consisting of a RC mesh, which simulates the whole film, with in series the resistance of the aqueous electrolyte) it was possible to obtain the capacitance and resistance, which were fully compatible with formation of a tBLM starting from a DPTL monolayer.<sup>78</sup> In this way, substrate has been identified as an accurate bilayer formation.

<sup>78</sup> Wiegand, G.; Arribas-Layton, N; Hillebrand, H; Sackman, E; Wagner, P. *J. Phys. Chem. B*, **2002**, 106, 4245.

## 7.2 Behaviour of glycosylated peptides CSF114(Glc) (I) and Scramble CSF114(Glc) (VI) in biomimetic membrane

To further characterise the glycosylated peptide antigen CSF114(Glc) (I) in a membrane environment, we decided to study in parallel the random coil glycosylated peptide structure Scramble CSF114(Glc) (VI).<sup>26</sup>

We incorporated CSF114(Glc) and Scramble CSF114(Glc) into different tBLMs and both glycopeptides were added independently into the electrolyte solution in a cell.

In Figure 7.2 we can observe the in-phase component *versus* the applied potential  $E$ . The applied potential is gradually shifted toward more negative values, and the electric field within the hydrophilic spacer decreases in magnitude giving rise to a bell-shaped curve. The conductance of membrane-containing glycopeptides shows a very steep rise in the proximity of  $-0.900$  V/SCE, followed by a rapid decrease probably due to the saturation of the hydrophilic region by the supporting cation  $K^+$ , thus increasing tBLM permeability.

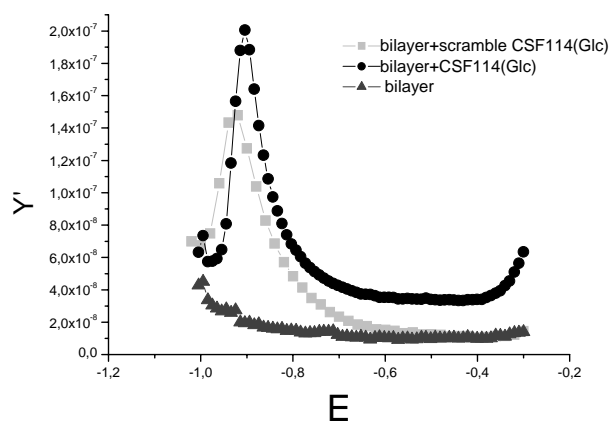


**Figure 7.2.** Plot of the in-phase component,  $Y'$ , of Hg-supported DPTL/DphyPC film bathed by aqueous  $0.1$  M KCl against the applied potential  $E$ , both in the absence ( $\blacktriangle$ ) and in the presence of CSF114(Glc) ( $\bullet$ ) or Scramble CSF114(Glc) ( $\blacksquare$ ). Freq =  $10$  Hz.

Permeability of membranes containing each glucopeptide could be due to the hydroxyl functions of glucose moiety linked to Asn at position 7. The use of elevated negative potentials (-0.900 mV) probably induce variations in the dipole of the hydroxyl groups. These electric changes in the glucosyl moiety could orient glucopeptides near the working electrode disrupting the membrane in the polar heads region.

### 7.3 Behaviour of unglucosylated peptides CSF114 (I') and Scramble CSF114 (VI') in biomimetic membrane

We synthesized the unglucosylated peptide sequences CSF114 (I') and Scramble CSF114 (VI') to be studied in the membrane model tBLM. Figure 7.3.1 shows the conductance of a Hg-supported DPTL/DPhyPC film incorporating CSF114 and Scramble CSF114 against the applied potential  $E$ , as measured by the in-phase component  $Y'$ , of the electrode admittance at 10 Hz.

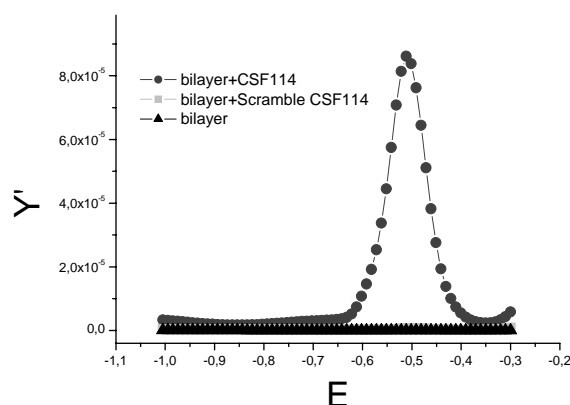


**Figure 7.3.1.** Plot of the in-phase component,  $Y'$ , of Hg-supported DPTL/DPhyPC film bathed by aqueous 0.1 M KCl against the applied potential  $E$ , both in the absence ( $\blacktriangle$ ) and in the presence of CSF114 ( $\bullet$ ) or Scramble CSF114 ( $\blacksquare$ ).

## PART B

The results obtained for the CSF114-containing membrane were similar to those reported for a membrane containing Gramicidin D, a voltage-dependent well-known peptide forming ion channels in a membrane environment.<sup>79</sup> Moreover, the presence of Scramble CSF114 (VI') did not disrupt membrane properties. These results prompted us to perform a more detailed study.

Plotting the real part against the imaginary part of impedance gives a Nyquist plot. The advantage of a Nyquist plot is that it gives a rapid data overview and allows qualitative interpretation. When plotting data in the Nyquist format is performed, the real axis should be equal to the imaginary axis so the shape of the curve should not be distorted. The shape of the curve is important for a qualitative interpretation of the data. The disadvantage of the Nyquist plot is that the frequency dimension of the data cannot be obtained.

Figure 7.3.2 shows a variant of Nyquist plot,  $\omega Z'$  vs  $-\omega Z''$ , where  $Z'$  and  $Z''$  are the in-phase and quadrature components of the impedance and  $\omega$  is the angular frequency.

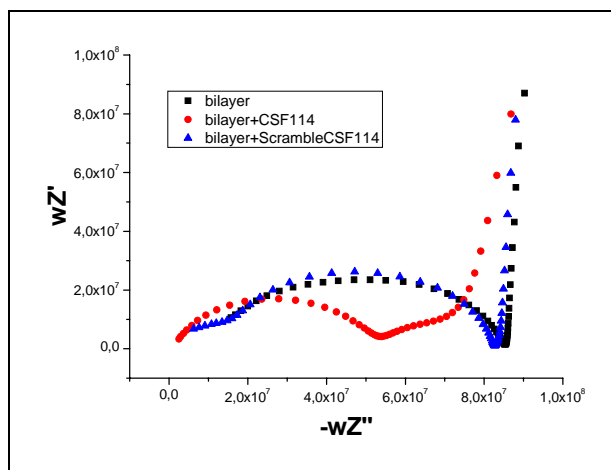


**Figure 7.3.2.** Exchanged axis Nyquist plot of bilayer (black), bilayer+ Scramble CSF114 (blue), and bilayer + CSF114 (red).

---

<sup>79</sup> Moncelli, M.R.; Beccuci, L.; Schiller, S.M. *Bioelectrochemistry*, **2004**, 63, 161– 167.



Impedance data can be interpreted on the basis of equivalent circuit models. These models are built with well-known passive elements i.e., resistors, capacitors, and inductors. These elements can be combined in series and in parallel to obtain complex equivalent circuits. A certain physical meaning is then assigned to the various elements of the equivalent circuit as described in Figure 7.3.3a.

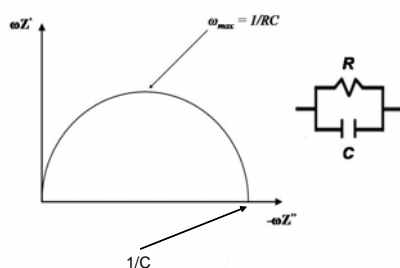


**Figure 7.3.3a.** Graphic representation of various elements of the equivalent circuit.

In the case of a bilayer, an isolated RC mesh, consisting of a resistance  $R$  and a capacity  $C$  in parallel, is represented by a semicircle whose diameter is equal to the reciprocal of the capacity of the mesh and whose maximum lies at an angular frequency equal to the reciprocal of the time constant  $RC$  of the mesh. EIS data were fitted to an equivalent circuit consisting of a low resistance of the aqueous solution in series with a RC mesh (Figure 7.3.3b).

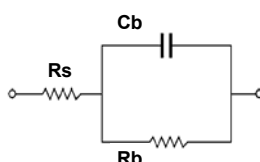


**Figure 7.3.3b.** Schematic plot of the equivalent circuit used as a model for the bilayer.

When the peptides were incorporated into the bilayer, EIS data were fitted to an equivalent circuit consisting of the circuit for the bilayer with an additional semicircle (Figure 7.3.4).

## PART B

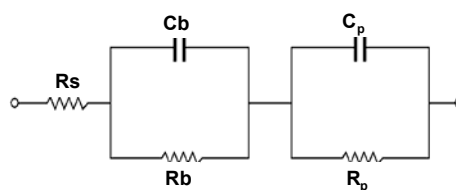


**Figure 7.3.4.** Schematic plot of the equivalent circuit used as a model for the bilayer incorporating peptides.

Fitting values are reported in Table 7.3.1.

**Table 7.3.1.** Fitting values obtained for the bilayer and the bilayer incorporating unglycosylated peptides.

	bilayer	Bilayer+CSF114	Bilayer+Scramble CSF114
<b>Rs</b> ( $\Omega \cdot \text{cm}^2$ )	3.098	3.549	3.005
<b>Cb</b> ( $\mu\text{F}/\text{cm}^2$ )	0.937	1.501	1.222
<b>Rb</b> ( $\text{k}\Omega \cdot \text{cm}^2$ )	247	3.715	202
<b>Cp</b> ( $\mu\text{F}/\text{cm}^2$ )	-	7.535	2.514
<b>Rp</b> ( $\text{k}\Omega \cdot \text{cm}^2$ )	-	785	62.5

We can observe an increase in membrane capacitance and a decrease in membrane resistance in the presence of CSF114 (**I'**). The decrease in membrane resistance of three orders of magnitude, which may be due to ionic currents through possible pores, is therefore much higher in CSF114-incorporating membrane. The increase in membrane capacitance, which is related to the charge separation across the membrane, indicates a much more fluid and less densely packed membrane. The presence of a poorly packed bilayer in the presence of the unglycosylated peptide  $\beta$ -turn structure CSF114 is evident. However, the capacitance remains below  $2.4 \mu\text{F cm}^{-2}$ , indicating the integrity of the membrane. On the other hand, the presence of random coil Scramble CSF114 (**VI'**) did not disrupt the membrane.

These results let us to hypothesize that a  $\beta$ -turn peptide structure is crucial for interaction with the bilayer.

### 7.3.1 Charge through the membrane in the particular case of the $\beta$ -turn structure CSF114 (I')

Charge  $Q$  versus time  $t$  has been recorded on a tBLM incorporating  $4\mu\text{M}$  CSF114 immersed in aqueous  $0.1\text{ M}$  KCl, performing a potential step from  $-0.300\text{ V}$  to  $-1.00\text{ V}$ . After an initial abrupt increase in charge, due to the flow of the capacitive current required charging the tBLM, the curve assumes a sigmoidal shape tending to a constant limiting value (Figure 7.3.5).

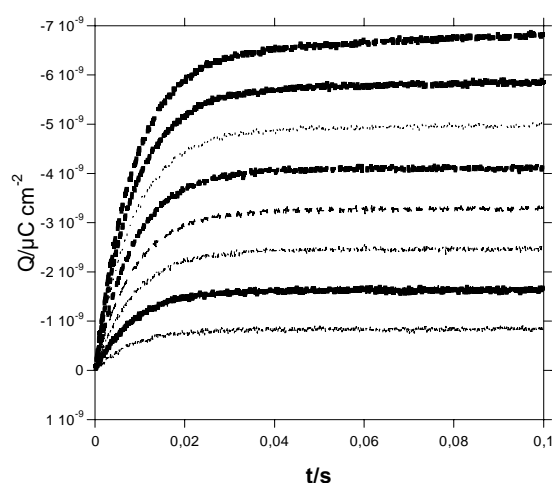


**Figure 7.3.5.** Charge versus time curve of a tBLM in  $0.1\text{ M}$  KCl incorporating CSF114  $4\mu\text{M}$  following a potential step from  $-0.300\text{ V}$  to  $-1.0\text{ V}$  with  $100\text{ mV}$  decrements.

It was previously reported the relationship between the charge through the bilayer and a nucleation-and-growth mechanism of the peptide into the membrane.<sup>80</sup> The absence of changes in the curve of the charge  $Q$  as we proceed toward more negative potentials strongly suggests that the interaction

---

<sup>80</sup> Beccuci, L.; Moncelli, M.R.; Naumann, R.; Guidelli, R. *J. Am. Chem. Soc.* **2005**, *127*, 13316-13323.

## PART B

with the  $\beta$ -turn peptide CSF114 (**I'**) proceeded without a nucleation-and-growth mechanism.

### 7.3.2 Fluorescence studies of the $\beta$ -turn structure CSF114 incorporated in liposomes

Tryptophan fluorescence is widely used as a tool to monitor changes in proteins conformation. Thanks to the presence of Trp in CSF114 sequence, fluorescence studies in liposomes were performed in collaboration with Prof. M. Venanzi at the University of Rome "Tor Vergata" (Dipartimento di Scienze e Tecnologie Chimiche).

To shed further light on results obtained in tBLM environment, membrane-perturbing activity of the  $\beta$ -turn structure CSF114 was investigated by fluorescence studies. The peptide-liposome interaction was measured by incubating 4  $\mu$ M CSF114 (**I'**) with PC/PG liposomes (2:1) at different concentrations (0-300  $\mu$ M). The fluorescence of Trp residue was measured at an excitation wavelength of 280 nm and an emission wavelength between 320 and 420 nm.

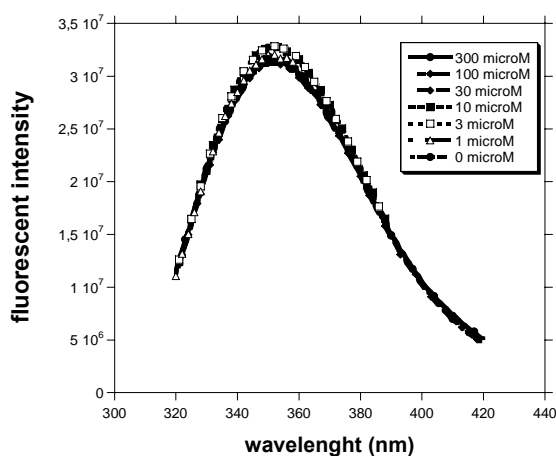


**Figure 7.3.6.** Plot of the fluorescence intensity of the  $\beta$ -turn structure CSF114 (**I'**) incorporated in liposomes at different concentrations.

All Trp-emission spectra recorded at different liposome concentrations were identical (Figure 7.3.6) suggesting that liposomes did not perturb the overall  $\beta$ -turn conformation of the peptide. The extrinsic fluorescence intensity of Trp residue was modified to a minor extent, if any, by the membrane environment. Analogous results were observed at higher peptide concentration (data not shown). If the Trp residue is not involved in the peptide-membrane-interaction, the possibility of fluorescence intensity changes are less likely because its position 18 near the C-terminus in CSF114-peptide sequence.

For this reason, we decided to undertake anisotropy experiments. Anisotropy allows studying changes in the emission dipole during the excited state lifetime, measuring the relative orientation between the absorption and emission dipoles. Molecules are free to rotate and randomly oriented in solution, so the direction of the transition dipoles is randomized. If vesicles-peptide interactions occur, the random disposition of the peptide could change, thus modifying its anisotropy.

Anisotropy of both isolated vesicles and CSF114-containing vesicles were calculated using a polarization mode. The G-factor of the instrument was previously calculated (1,566332). Anisotropy of a solution containing 10  $\mu$ M CSF114 was calculated in the absence and in the presence of liposomes (300  $\mu$ M). Results are reported in Table 7.3.2.

**Table 7.3.2. Anisotropy values obtained for Trp residue.**

	<b>Anisotropy</b>
CSF114	0.0212
CSF114 + liposomes	0.0176

The absence of Trp anisotropy variation suggests that both the position and orientation of Trp residue in the peptide are not involved in the membrane disruption, even though the peptide can be moved to different positions around the liposomes.

## PART B

### 7.3.3 *Electrochemical study of different $\beta$ -turn peptide structure MBH36 and TrpZip*

Different unglycosylated peptide  $\beta$ -turn structures have been selected from the literature to study their behaviour in biomimetic membranes. In particular, starting from observations previously reported by Perez-Paya *et al.*,<sup>81</sup> we selected MBH36 possessing high population of type I'  $\beta$ -hairpin structure in solution (as demonstrated by detailed CD and NMR analysis) and a sequence rich in Trp residues (TrpZip) containing a structural motif, the Tryptophan zipper, greatly stabilizing the  $\beta$ -hairpin conformation, even in short peptides consisting of only 12 amino acid residues. The peptide TrpZip is monomeric and folds cooperatively in water and the NMR structure analysis reveals exceptionally a well-defined  $\beta$ -hairpin conformation stabilized by cross-strand pairs of indole rings.<sup>82</sup>

Peptide sequences reported in Table 7.3 have been studied in the membrane model system tBLM.

**Table 7.3 Peptide sequences studied in biomimetic membranes**

Peptide	Sequence
MBH36 (VII)	RGKYTYNGITYEGR
TrpZip (VIII)	SWTWENGKWTWK

Both  $\beta$ -hairpin peptide structures characterised by different primary sequences, MBH36 (VII) and TrpZip (VIII), were studied in a membrane environment (Figure 7.3.7). Peptide MBH36 did not disrupt the mimetic membrane and TrpZip presented a small interaction (two orders below CSF114 (I') interaction value).

<sup>81</sup> Pastor, M. T.; de la Paz, M. L.; Lacroix, E.; Serrano, L.; Perez-Paya, E. *Proc. Natl. Acad. Sci.* **2002**, 99, 614-619.

<sup>82</sup> Cochran, A.G.; Skelton, N.J.; Starovasnik, M.A. *Proc. Natl. Acad. Sci.* **2001**, 98, 5578-5583.

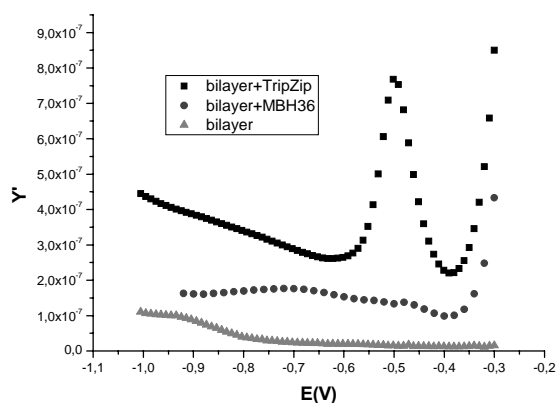


**Figure 7.3.7.** Plot of the in-phase component,  $Y'$ , of a Hg-supported DPTL/DphyPC film bathed by aqueous 0.1 M KCl against the applied potential  $E$ , both in the absence ( $\blacktriangle$ ) and in the presence of MBH36 ( $\bullet$ ) or TrpZip ( $\blacksquare$ )

Several aspects of peptide structures relevant to membrane activity have to be considered. In particular, structural parameters such as conformation, charge, hydrophobicity, amphipathicity, and polar angle could be correlated with the membrane activity (Figure 7.3.8).

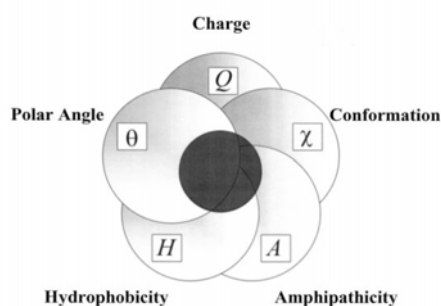


**Figure 7.3.8.** Inter-relationship among structural determinants in peptides: amino acid sequence influences charge ( $Q$ ), amphipathicity ( $A$ ), and/or hydrophobicity ( $H$ ), but also governs polar angles ( $\theta$ ) and/or conformation ( $\chi$ ).

It is important to note that these molecular determinants are interdependent, and therefore, modification of one parameter often leads to compensatory effects in others.

## PART B

Even if CSF114 (**I'**) and Scramble CSF114 (**VI'**) have the same amino acid-composition (but different primary sequence), their membrane activity. In this case, differences in their peptide structure ( $\beta$ -turn *versus* random coil) results in different activity in a membrane environment.

In the particular case of TrpZip, the peptide presents small activity probably due to the Trp rich sequence.<sup>83</sup>

Therefore, changes in composition, sequence, and intramolecular bonds may profoundly affect the structure-activity relationships of peptides in solution, upon binding to target membranes. Moreover, these features may be specific for distinct peptides as they interact with specific pathogens or in specific physiologic microenvironments. Therefore, all the parameters described above can be related to membrane-peptide interactions.

---

<sup>83</sup> Yeaman, M.R.; Yount, N.Y. *Pharmacological Reviews*, **2003**, *55*, 27-55.



## Experimental Part

### 8. *Experimental Part A*

#### 8.1 Materials and methods

The chemicals were purchased from Sigma-Aldrich and used without further purification. Peptide-synthesis grade N,N-dimethylformamide (DMF) was from Scharlau (Barcelona, Spain). HPLC-grade MeCN was purchased from Carlo Erba (Italy). Dry solvent DCM was distilled immediately before use over CaH<sub>2</sub> under nitrogen. Protected amino acids and resins were obtained from Calbiochem-Novabiochem AG (Laufelfingen, Switzerland). HATU, TBTU and HOBt were purchased from Advanced Biotech Italia (Milano, Italy). Activation products that contain triazine were obtained from EspiKem (Firenze).

TLC were carried out on silica gel precoated plates (Merck; 60 Å F<sub>254</sub>) and spots located with: (a) UV light (254 and 366 nm), (b) ninhydrin (solution in acetone), (c) Cl<sub>2</sub>/toluidine, (d) Fluram® (Fluka; fluorescamine, 4-phenyl-spyro[furan-2(3H),1'-isobenzofuran]-3,3'-dione) in acetone, (f) a basic solution of permanganate [KMnO<sub>4</sub> (3 g), K<sub>2</sub>CO<sub>3</sub> (20 g), and NaOH (0.25 g) in water (300 ml)], (g) 10% H<sub>2</sub>SO<sub>4</sub> in EtOH. Flash Column Chromatography (FCC) was performed on Merck silica gel 60 (230-400 mesh) according to Still et al<sup>84</sup>.

<sup>1</sup>H and <sup>13</sup>C NMR spectra were recorded at 400 and 100 MHz, and 200 and 50 MHz respectively, on a Varian spectrometer in deuterated solutions and are reported in parts per million (ppm), with solvent resonance used as reference. Chemical shifts (δ) are reported in ppm relative to TMS and coupling constants (J) are reported in Hz. The multiplicity were marked as s=singlet, d

---

<sup>84</sup> W.C. Still, M. Khan, A. Mitra, *J. Org. Chem.*, **1985**, 50, 2394-2395.

## EXPERIMENTAL PART

= doublet, t = triplet, q = quartet, m = multiplet. Intensities of signals were estimated as vs = very strong, s = strong, m = medium, w = weak, b = broad.

Semi-preparative purification via HPLC were performed by a Phenomenex Jupiter C18 (250 × 4.6 mm) column at 28 °C using using an Waters instrument (Separation Module 2695, detector diode array 2996) or using a Beckman System Gold Nouveau apparatus equipped with a diode array detector. Analytical HPLC were performed by a Waters instrument (2996 Alliance) using a Phenomenex Jupiter column 5m C18 300Å (250 × 4.6 mm). The solvent systems used were: A (0.1% TFA in H<sub>2</sub>O) and B (0.1 % TFA in CH<sub>3</sub>CN). The flow rates were 1 mL/min for analytical HPLC and 4 mL/min for semi-preparative HPLC, with the indicated linear gradients. Products were characterized by ACQUITY UPLC (Waters Corporation, Milford, Massachusetts) coupled to a single quadrupole ESI-MS (Micromass ZQ) using a 2.1 x 50 mm 1.7 μm ACQUITY BEH C18 at 30 °C, with a flow rate of 0.45mL/min. The products were lyophilized with an Edwards apparatus, model Modulyo.

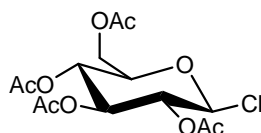
Cyanogen-bromide activated resin (CNBr-sepharose) used for the affinity column and bovine serum albumin (BSA) used for the quantification of the isolated antibody fractions were purchased from Sigma-Aldrich (Milan, Italy). The solutions used for the affinity chromatography were: Hydrochloric acid (1 mM), coupling buffer (0.1 M, NaHCO<sub>3</sub>, NaCl, 0.5 M), glycine solution (0.2 M, pH 8.0), acetate buffer (0.1 M, pH 4.3, 0.5 M NaCl), phosphate buffer saline (PBS) (0.1 M, pH 7.0), glycine solution (0.1 M pH 2.6). NaHCO<sub>3</sub> buffer (0.1 M, pH 8.3). All reagents were obtained from Merck (Darmstadt, Germany).

## 8.2 Synthesis of glucosyl amino acid derivatives.

### 8.2.1 2,3,4,6-tetra-O-acetyl-β-D-glucopyranosyl chloride (1)

The commercially available 1,2,3,4,6-pentaacetate α-D-glucopyranose (12 mmol) was dissolved in DCM (25 mL), then SOCl<sub>2</sub> (10 eq.) and AcOH (3 mL)

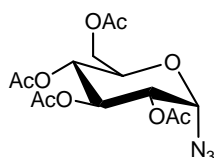
were added under nitrogen atmosphere. The mixture was allowed to react at 0 °C for 1 h and then left for 16 h at r.t. under stirring. The reaction was monitored by TLC [AcOEt/hexane (1:1), developed by vanilline]. After evaporation of the solvent under vacuum, coevaporation with toluene the crude was purified by cristallisation from petroleum ether/ diethyl ether.



(1) Yield 91%.  $R_f = 0.63$  [AcOEt/hexane (1:1), vanilline].  $^1\text{H NMR}$  (400 MHz,  $\text{CDCl}_3$ ):  $\delta = 5.28$  (d, 1H,  $J_{1,2}=8.2$  Hz, H-1), 5.20–5.12 (m, 3H,  $J_{4,5}=9.7$  Hz, H-2, H-3, H-4), 4.24 (dd, 1H,  $J_{6a,6b}=12.5$  Hz, H-6a), 4.15 (dd, 1H, H-6b), 3.80 (ddd, 1H,  $J_{5,6a}=4.7$  Hz,  $J_{5,6b}=2.3$  Hz, H-5), 2.08, 2.06, 2.01, 1.99 (4s,  $4 \times 3\text{H}$ ,  $4 \times \text{Ac}$ );  $^{13}\text{C NMR}$  (125 MHz,  $\text{CDCl}_3$ ):  $\delta = 170.5$ , 170.0, 169.2, 169.0 ( $4 \times \text{CO-Ac}$ ), 87.5 (C-1), 75.5 (C-5), 73.3 (C-3), 72.7 (C-2), 67.5 (C-4), 61.5 (C-6), 20.6, 20.5, 20.4 ( $4 \times \text{CH}_3\text{-Ac}$ ). Results are consistent with data previously reported.<sup>85</sup>

### 8.2.2 2,3,4,6-Tetra-O-acetyl- $\alpha$ -D-glucopyranosyl azide (2 $\alpha$ )

To a solution of 2,3,4,6-tetra-O-acetyl- $\beta$ -D-glucopyranosyl chloride (1) (11.5 mmol) in THF, TBAT (1.35 eq.) and  $\text{TMS-N}_3$  (1.35 eq.) were added. After 36 h under reflux the reaction mixture was quenched. Crude was cristallized from EtOH obtaining the anomeric mixture 9:1 ( $\alpha/\beta$ ). The two anomers were successfully purified independently by FCC (AcOEt/Hexane, 1:1) and recrystallized from EtOH.



(2) Yield = 56%,  $R_f = 0.3$  [DCM, vanilline],  $^1\text{H NMR}$  (200MHz,  $\text{CDCl}_3$ )  $\delta = 5.59$  (d,  $J_{1,2}=4.4$  Hz, 1H, H-1), 5.33 (t,  $J=10$  Hz, 1H, H-2), 5.05 (d,  $J=9.4$  Hz, 1H, H-3), 4.90–5.00 (m, 2H, H-4 H-5), 4.29–4.10 (m, 2H, H-6 H-6'), 2.09–2.01 (m, 12H,  $4 \times \text{OAc}$ ). Results are in agreement with data previously reported.<sup>86</sup>

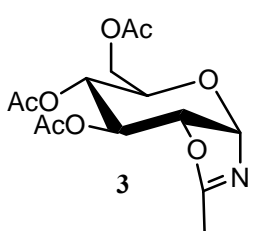
<sup>85</sup> Ibatullin, F.M.; Stanislav, I.S. *Tetrahedron letters*, **2002**, 43, 9577-9580.

<sup>86</sup> Ogawa, T.; Nakabayashi, S.; Shibata, S *Can J Chem.* **1980**, 47, 281-285.

## EXPERIMENTAL PART

### 8.2.3 3,4,6-Tri-*O*-acetyl- $\alpha$ -D-glucopyranosyl isoxazoline (3)

2,3,4,6-Tetra-*O*-acetyl- $\beta$ -D-glucopyranosyl azide (**2**) (300 mg, 0.804 mmol) and Ph<sub>3</sub>P (210 mg, 0.804 mmol) were dissolved in 1,2-dichloroethane (8 mL) in the presence of 4Å molecular sieves under Argon in a sealed vessel. The resulting solution was heated at 130°C under microwave conditions at 100W for 10 minutes. Then the reaction mixture was cooled to room temperature and concentrated under *vacuum*. Compound **3** was purified by FCC (hexane/AcOEt/Et<sub>3</sub>N, 1:3:1%) obtaining pure isoxazoline **3** (137 mg, 52%) as a colourless oil. R<sub>f</sub> = 0.23 (hexane/AcOEt, 1:3, vanilline);



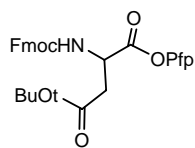
<sup>1</sup>H NMR (400 MHz, CDCl<sub>3</sub>)  $\delta$  = 2.01 (s, 3H, OAc), 2.04 (s, 3H, OAc), 2.07 (s, 3H, OAc), 2.09 (s, 3H, OAc), 3.62 (ddd,  $J$  = 8.8, 5.2, 2.4, 1H, H-5), 4.11 (dd,  $J$  = 12.6, 2.8, 1H, H-6), 4.23 (dd,  $J$  = 12.4, 5.2, 1H, H-6'), 4.37 (dd,  $J$  = 7.0, 4.0, 1H, H-2), 4.88 (dd,  $J$  = 8.6, 4.2, 1H, H-4), 5.13 (t,  $J$  = 4.2, 1H, H-3), 5.81 (d,  $J$  = 7.4, 1H, H-1) ppm; <sup>13</sup>C NMR (100 MHz, CDCl<sub>3</sub>)  $\delta$  = 14.3, 20.7, 20.8, 20.8, 63.2, 67.3, 67.7, 70.7, 75.9, 92.7, 168.4, 169.2, 169.5, 170.3 ppm; ESI-MS:  $m/z$  calcd for C<sub>14</sub>H<sub>20</sub>O<sub>8</sub>N (M + H)<sup>+</sup> = 330.12, found 330.12. Results are consistent with previously reported data.<sup>87</sup>

### 8.2.4 Fmoc-Asp(OtBu)-Opfp (4a)

Pentafluorophenol (4 mmol) was added dropwise to a solution of Fmoc-L-Asp(OtBu)-OH (1 equiv) in dioxane (12 mL) and then DCC (1 equiv) was added at 0 °C. The mixture was stirred 2 h at r.t. and checked by TLC R<sub>f</sub> = 0.53 [DCM/MeOH, 13:1; KMnO<sub>4</sub>]. After filtration, the solution was concentrated. Crude oil was re-crystallized from hexane obtaining the desired product as a white powder.

<sup>87</sup> Damkaci, F.; DeShong, P. *J. Am. Chem. Soc.* **2003**, 125, 4408-4409.

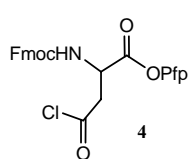
## EXPERIMENTAL PART



Yield = 97%,  $^1\text{H}$  MNR (200 MHz, DMSO)  $\delta$  = 7.74 (d, 2H, 4-H 5-H Fmoc), 7.57 (d, 2H 1-H 8-H Fmoc), 7.32 (m, 4H, Fmoc), 5.96 (d, 1H,  $J=9.2$  Hz, NH), 5.10-4.95 (m, 1H,  $H_\alpha$ ), 4.23-4.54 (m, 3H,  $\text{CH}_2$  CH Fmoc), 3.03 (2H, ABMX system,  $J_{AB}=17.6$  Hz,  $J_{AM}=4.9$  Hz,  $J_{BM}=4.7$  Hz), 1.46 (s, 9H, *t*Bu).  $^{13}\text{C}$ -NMR (DMSO)  $\delta$ (ppm): 169.76 (COOPfp), 166.7 (COO*t*Bu), 155.94 (OCONH), 82.70 (OCCH3 *t*Bu), 67.49 ( $\text{CH}_2$  Fmoc), 50.24 ( $\alpha$ -CH), 47.02 (CH Fmoc), 37.56 ( $\beta$ - $\text{CH}_2$ ), 27.91 (3  $\text{CH}_3$  *t*Bu). IR (KBr)  $\nu(\text{cm}^{-1})$ : 3367 (NH), 3080 (CH aromatic), 2980-2855 (CH alifatic), 1798 (C=O pentafluorophenylester); 1725 (C=O ester Asp), 1706 (C=O uretane Fmoc), 1515 (C=C aromatico).

### 8.2.5 Fmoc-Asp(Cl)-OPfp (4)

Fmoc-Asp(O*t*Bu)-OPfp **4a** (3.8 mmol) was treated with TFA (3 ml). After 30 min  $\text{SOCl}_2$  was added to the reaction mixture (100 eq.), which was left under stirring by one day at r.t. Reaction was monitored by  $^1\text{H}$  NMR. Solvent was co-evaporated with THF to obtain compound **4** as a white solid.



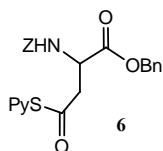
$^1\text{H}$ -NMR ( $\text{CDCl}_3$ )  $\delta$ (ppm): 7.75 (2 H, d, 4-H and 5-H Fmoc), 7.56 (2 H, d, 1-H e 8-H Fmoc), 7.31 (4 H, m, 2-H, 7-H, 3-H and 6-H Fmoc), 5.70 (1 H, d, N-H,  $J=8.4$  Hz), 4.98 (1H, m, 2-H), 4.50 (2 H, d,  $\text{CH}_2$  Fmoc,  $J=6.6$  Hz), 4.25(1H, t, CH Fmoc,  $J=6.6$  Hz), 3.69 (2 H, ABMX system, 3-H2,  $J_{AB}=19$  Hz,  $J_{AM}=5.1$  Hz,  $J_{BM}=4.8$  Hz).  $^{13}\text{C}$ -NMR ( $\text{CDCl}_3$ )  $\delta$ (ppm): 172.27 (COCl), 143.36 (COOPfp), 141.35 (OCONH), 67.64 ( $\text{CH}_2$  Fmoc), 50.36 ( $\alpha$ -CH), 48.62 ( $\beta$ - $\text{CH}_2$ ), 47.03 (CH Fmoc). IR (KBr)  $\nu(\text{cm}^{-1})$ : 3322 (NH), 3072 (CH aromatic), 2951 (CH aliphatic), 1788 (C=O pentafluorophenylester), 1740 (C=O Asp-Cl); 1699 (C=O uretane Fmoc); 1519 (C=C aromatico), 739 (C-Cl).

## EXPERIMENTAL PART

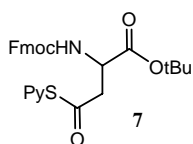
### 8.2.6 *Modification on the side chain of the aspartic acid with a thiopyridine moiety*

*General procedure:* Oxalyl chloride (1.1 eq.) was added dropwise to a stirred solution of commercially available Fmoc-Asp(OH)-OtBu (2.43 mmol) or Z-Asp(OH)-OtBu (0.55 mmol) at 0°C under N<sub>2</sub>. The reaction mixture was stirred at 0 °C for 1 h and then warmed to r. t. over 2 h. The crude chloride compound was taken up in DCM and then added to a solution of thiopyridine (1 eq.) and triethylamine (1 eq.) in DCM at 0 °C. After stirring for 30 min, the mixture was poured into ice-cold water. The organic phase was separated and washed with ice-chilled KOH solution (5%), and water. The organic phase was separated, dried over Na<sub>2</sub>SO<sub>4</sub>, filtered, and concentrated under reduced pressure, to give the desired compound in quantitative yield. This material was used immediately without further purification.

**Z-Asp(Spy)-OBzl (6):** <sup>1</sup>H NMR (200 MHz, CDCl<sub>3</sub>) δ = 3.32- 3.39 (m, 2H, CH<sub>2</sub> Asp), (m, 1H, CH Asp), 5.05-5.16 (m, 4H, CH<sub>2</sub> Z, CH<sub>2</sub> Bzl), 5.79 (d, 1H, J=7.4 Hz, NH), 7.29 (m, 14H, Ar Bzl, Ar Z, Ar Py).



**Fmoc-Asp(SPy)-OtBu (7):** <sup>1</sup>H NMR (200 MHz, CDCl<sub>3</sub>) δ = 1.45 (s, 9H, tBu), 2.68-2.96 (m, 2H, CH<sub>2</sub> Asp), 4.23-4.52 (m, 5H, CH<sub>2</sub> Fmoc, CH Fmoc, CH Asp), 5.8 (d, 1H, J=8.4 Hz, NH), 7.28-7.78 (m, 12H, Fmoc, Py). ESI-MS: *m/z* calculated (M + H)<sup>+</sup>=505.60.12, found 505.30.

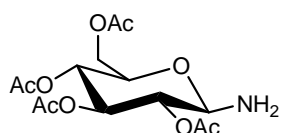


### 8.2.7 *2,3,4,6-Tetra-O-acetyl-β-D-glucopyranosylamine (8)*

To a solution of commercially available 2,3,4,6-tetra-O-acetyl-β-D-glucopyranosyl azide (10 mmol) in MeOH, we added 20% Pd(OH)<sub>2</sub>/C. The mixture was stirred for 24 h at r.t. under H<sub>2</sub>, checked by TLC [AcOEt/hexane, 3:1; UV, fluorescamine, and vanilline], filtered over *celite*, washed with

MeOH and concentrated. The desired compound **1** was re-crystallized from THF/hexane.

2,3,4,6-tetra-*O*-acetyl- $\beta$ -D-glucopyranosylamine (**8**), yield 98%. *R*<sub>f</sub> = 0.37. <sup>1</sup>H



NMR (200 MHz, CDCl<sub>3</sub>)  $\delta$  = 2.03 (s, 3H, OAc), 2.04 (s, 6H, 2×OAc), 2.07 (s, 3H, OAc), 3.67-3.75 (m, 1H, H-5), 4.03 (d, *J* = 12.2 Hz, 1H, H-6), 4.28 (pd, *J* = 12.8 Hz, 1H, H-6'), 4.96 (t, *J* = 9.6 Hz, 1H, H-2), 5.12 (t, *J* = 10 Hz, 1H, H-4), 5.27-5.36 (m, 2H, H-1 and H-3) ppm.

### 8.2.8 Coupling reactions between modified aspartic acid and glucose

*General procedure via 3,4,6-tri-O-acetyl- $\alpha$ -D-glucopyranosyl isoxazoline intermediate:*

2,3,4,6-Tetra-*O*-acetyl- $\alpha$  or  $\beta$ -D-glucopyranosyl azide (0.72 mmol) and Ph<sub>3</sub>P (1 eq.) was dissolved in 1,2-dichloroethane (6 mL) in the presence of 4Å molecular sieves. The resulting solution was heated at 130 °C under microwave conditions at 100W for 10 minutes. Then the reaction mixture was cooled to r.t. and concentrated under *vacuum*. The activated amino acid and CuCl<sub>2</sub>·2H<sub>2</sub>O, were added to the reaction mixture, which was heated at 30 °C for 24 h. The reaction mixture was diluted with 100 mL Et<sub>2</sub>O and washed with 2x100 mL H<sub>2</sub>O. The organic layer was dried over Na<sub>2</sub>SO<sub>4</sub> and concentrated under *vacuum* to give the crude product, which was purified by FCC (hexane:EtOAc, 1:1).

*General procedure for microwave-assisted synthesis:*

Fmoc-L-Asp-OtBu (60 mg, 0.144 mmol), 2,3,4,6-tetra-*O*-acetyl- $\beta$ -D-glucopyranosyl amine (**3**) (1 equiv), NMM (1 equiv), and DMT-NMM/BF<sub>4</sub><sup>88,89</sup>

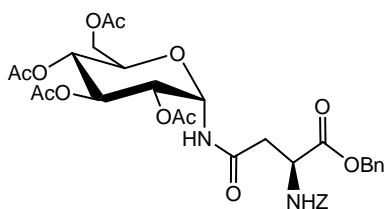
<sup>88</sup> [4-(4,6-dimethoxy-1,3,5-triazin-2-yl)-4-methylmorpholinium tetrafluoroborate], "Process for the preparation of *N*-triazinylammonium salts". Filing date 07/11/2005. Applicant: Italvelluti S.p.a. Inventors: Z. Kaminski, A. M. Papini, B. Kolesinska, J. Kolesinska, K. Jastrzabek, G. Sabatino, R. Bianchini. PCT/EP2005/055793 (2005).

<sup>89</sup> Z. J. Kamiński, B. Kolesińska, J. Kolesińska, G. Sabatino, M. Chelli, P. Rovero, M. Błaszczyk, M. L. Główska, A. M. Papini, *J. Am. Chem. Soc.*, **2005**, *127*, 16912-16920.

## EXPERIMENTAL PART

(1 equiv) as coupling reagent were dissolved in acetonitrile (2 ml). The vessel was charged with the reaction mixture, sealed, and placed into the microwave synthesizer CEM EXPLORER 48® applying the reaction conditions reported in Table 1.1.3. The reaction tube was taken off after performing the coupling reaction. Then the mixture was transferred into a round bottom flask. The solvent was evaporated under reduced pressure, the residue was dissolved in  $\text{CHCl}_3$  and then washed with water, 0.5 M aqueous  $\text{KHSO}_4$ , water, 0.5 M aqueous  $\text{NaHCO}_3$ , and water again. Organic layer was dried over anhydrous  $\text{Na}_2\text{SO}_4$ , filtered off and concentrated to dryness. The two anomers were successfully separated by FCC (AcOEt/Hexane, 1:1). The two independent pure anomers were dried under *vacuum* over  $\text{P}_2\text{O}_5$  and KOH till constant weight

**Z-L-Asn( $\alpha\text{GlcAc}_4$ )-OBn (9a)** The Asparagine derivative was prepared following the general coupling procedure via isoxazoline intermediate employing  $\alpha$ -azide (300 mg, 0.85 mmol),  $\text{Ph}_3\text{P}$  (1 equiv), Z-Asp(SPy)-OBn (1.5 equiv) as acylating reagent, and  $\text{CuCl}_2 \cdot 2\text{H}_2\text{O}$  (1.5 equiv).. After purification of the crude via FCC (hexane/AcOEt, 1:1) we obtained compound 9a as a white solid ( $R_f = 0.30$ , hexane/AcOEt, 1:1).



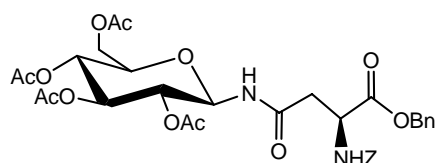
$^1\text{H NMR}$  (400 MHz,  $\text{CDCl}_3$ )  $\delta = 1.96$  (s, 3H), 2.00 (s, 3H), 2.02 (s, 3H), 2.04 (s, 3H), 2.87 (dm,  $J = 16$ , 1H), 2.95 (dm,  $J = 16$ , 1H), 3.84 (m, 1H), 3.97 (dd,  $J = 2, 8$ , 1H), 4.24 (dd,  $J = 4, 8$ , 1H), 4.67 (m, 1H), 5.00-5.20 (m, 6H), 5.25-2.30 (m, 1H), 5.80 (t,  $J = 6$ , 1H), 5.92 (s, 1H), 6.57 (m, 1H), 7.30-7.35 (m, 10H); ESI-MS  $m/z$  calcd 686.2323, found 687.2305.  $^1\text{H NMR}$  Results were consistent with data previously reported by Zhang *et al*<sup>90</sup>.

<sup>90</sup> Zhang, H.; Wang, Y.; Thürmer, R.; Parvez, K.; Atta-ur-Rahman, I. C.; Voelter, W. Z. *Naturforsch., B: Chem. Sci.* **1999**, *54*, 692-698.



## EXPERIMENTAL PART

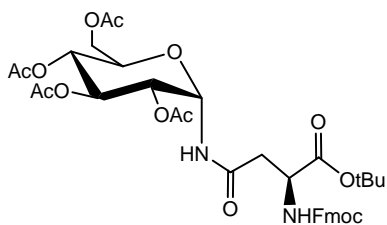
**Z-L-Asn( $\beta$ GlcAc<sub>4</sub>)-OBn (9 $\beta$ )** The Asparagine derivative was prepared following the general coupling procedure via isoxazoline intermediate employing  $\beta$ -azide (300 mg, 0.85 mmol), Ph<sub>3</sub>P (1 equiv), Z-Asp(SPy)-OBn (1.5 equiv) as acylating reagent, and CuCl<sub>2</sub> · 2H<sub>2</sub>O (1.5 eq.) additive. After purification of the residue by FCC (hexane/AcOEt, 1:1) we obtained compound 9 $\beta$  as a white solid (R<sub>f</sub> = 0.2, hexane/AcOEt, 1:1).



<sup>1</sup>H NMR (200MHz, CDCl<sub>3</sub>)  $\delta$ = 7.29-7.21 (m, 10H, 2Ph), 6.61 (d, 1H, J=9.1 Hz, H-1), 5.96 (d, 1H, J=8.6 Hz, NHCOBn), 5.25-4.79 (m, 8H, H-1,2,3,4

2 CH<sub>2</sub>Ph), 4.59-4.55 (m, 1H, CH), 4.24-3.91 (m, 2H, H-6,6'), 3.74-3.66 (m, 1H, H-5), 2.85-2.59 (dd, 2H, J=16.3, J=4.3 Hz, COCH<sub>2</sub>CH), 1.98, 1.97, 1.95,1.93 (4s, 12H, Ac). Results were consistent with data previously reported.<sup>90</sup>

**Fmoc-L-Asn( $\alpha$ GlcAc<sub>4</sub>)-OtBu (10 $\alpha$ ):** The Asparagine derivative was prepared following the procedure for microwave-assisted synthesis. After purification of the crude by FCC (hexane/AcOEt, 1:1) we obtained compound 10 $\alpha$  as a white solid. (R<sub>f</sub> = 0.52, AcOEt/Hexane, 1:1, fluorescamine, vanilline); [ $\alpha$ ]<sub>D</sub> = +13.21; ESI-MS: *m/z* calcd for C<sub>37</sub>H<sub>44</sub>O<sub>14</sub>N<sub>2</sub> = 740.28, found (M+H)<sup>+</sup> = 741,45.



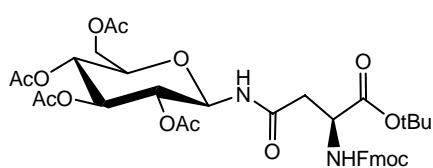
<sup>1</sup>H NMR (400 MHz, CDCl<sub>3</sub>)  $\delta$  = 1.46 (s, 9H, tBu), 2.01, 2.03 (2 s, 12H, 4×OAc), 2.87 (system ABMX, J<sub>AB</sub> = 17.2 Hz, J<sub>AM</sub> = 4.8 Hz, J<sub>BM</sub> = 4.4 Hz, 2 H, Asn- $\beta$ -CH<sub>2</sub>), 3.80 (dq, J = 4.0 Hz, J = 2 Hz, 1H, H-5), 4.06 (pd,

J = 11.6 Hz, 1H, H-6), 4.19 (t, J = 7.2 Hz, 1H, Fmoc-CH), 4.26 (dd, J = 12.8 Hz, 4.4 Hz, 1H, H-6'), 4.32-4.44 (m, 2H, Fmoc-CH<sub>2</sub>), 4.51-4.55 (m, 1H, Asn- $\alpha$ -CH), 5.09-5.15 (m, 2H, H-2 and H-4), 5.23 (t, J=9.6 Hz, 1H, H-3), 5.72 (m, 2H, H-1 and Asn- $\alpha$ -NH) 7.28 (app-dt, 5H, 1-NH and Fmoc-Ar), 7.58 (app-d, 2H, Fmoc-Ar), 7.74 (d, J = 7.2 Hz, 2H, Fmoc-Ar) ppm. <sup>13</sup>C NMR (100 MHz, CDCl<sub>3</sub>)  $\delta$  = 20.5, 20.5, 20.6 (C(O)CH<sub>3</sub>), 27.8 (C(CH<sub>3</sub>)), 36.7 (C $\beta$ ), 47.1(Fmoc

## EXPERIMENTAL PART

CH), 50.5 ( $C_\alpha$ ), 61.3 (C-6), 67.1 (Fmoc-CH<sub>2</sub>), 67.6, 70.1, 72.6, 72.7 (C-2,C-3,C-4,C-5), 82.9 (C(CH<sub>3</sub>)<sub>3</sub>), 91.9 (C-1), 119.9, 125.0, 125.1, 127.0, 127.7, 141.2, 143.7, 143.7 (Ar-C), 155.5, 169.0, 169.0, 169.3, 169.3, 170.0, 170.4 (C=O).

**Fmoc-L-Asn( $\beta$ GlcAc<sub>4</sub>)-OtBu (10 $\beta$ ):** The Asparagine derivative was prepared following the general procedure for microwave-assisted synthesis. After purification of the residue by FCC (hexane/AcOEt, 1:1) we obtained **10 $\beta$**  as a white solid. ( $R_f$  = 0.30 [AcOEt:Hexane, 1:1,(fluorescamine, vanilline)];  $[\alpha]_D=22.94$ ; ESI-MS:  $m/z$  calcd for C<sub>37</sub>H<sub>44</sub>O<sub>14</sub>N<sub>2</sub> =740.28, found (M+H)<sup>+</sup>=741,73;



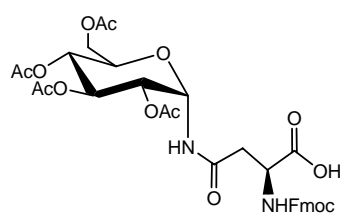
<sup>1</sup>H NMR (400 MHz, CDCl<sub>3</sub>)  $\delta$ = 1.46 (s, 9H, *t*Bu), 1.99, 2.01 (2 s, 12H, 4 $\times$ OAc), 2.84 (system ABMX,  $J_{AB}$  = 16.4 Hz,  $J_{AM}$  = 4.4 Hz,  $J_{BM}$  = 4.0 Hz, 2H, Asn- $\beta$ -CH<sub>2</sub>), 3.70 (*pt*,  $J$  = 4.8 Hz, 1H, H-5), 4.04 (d,  $J$  = 12.4 Hz, 1H, H-6), 4.19 (t,  $J$  = 7.2 Hz, 1H, Fmoc-CH), 4.23 (dd,  $J$  = 12.8 Hz,  $J$  = 4.4 Hz, 1H, H-6'), 4.31-4.42 (m, 2H, Fmoc-CH<sub>2</sub>), 4.69-4.72 (m, 1H, Asn- $\alpha$ -CH), 4.98 (t,  $J$  = 9.6 Hz, 1H, H-2), 5.10 (t,  $J$  = 10 Hz, 1H, H-4), 5.29-5.37 (m, 2H, H-1 and H-3), 6.09 (d,  $J$  = 8.0 Hz, 1H, Asn- $\alpha$ -NH), 6.87 (d,  $J$  = 9.2 Hz, 1H, NH-1), 7.28 (app-t, 2H, Fmoc-Ar), 7.37 (app-t, 2H, Fmoc-Ar), 7.57 (d,  $J$  = 7.2 Hz, 2H, Fmoc-Ar), 7.73 (d,  $J$  = 7.2 Hz, 2H, Fmoc-Ar) ppm. <sup>13</sup>C NMR (100 MHz, CDCl<sub>3</sub>)  $\delta$  = 20.5, 20.5, 20.6 (C(O)CH<sub>3</sub>), 27.8 (C(CH<sub>3</sub>)<sub>3</sub>), 37.9 (C $_\beta$ ), 47.1(Fmoc CH), 50.9 ( $C_\alpha$ ), 61.5 (C-6), 67.1 (Fmoc-CH<sub>2</sub>), 68.0, 70.5, 72.6, 73.6 (C-2,C-3,C-4,C-5), 78.0 (C-1), 82.4 (C(CH<sub>3</sub>)<sub>3</sub>), 119.9, 125.1, 125.1, 127.0, 127.6, 141.2, 143.7, 143.8 (Ar-C), 156.1, 169.5, 169.7, 169.8, 170.5, 170.7, 171.0 (C=O). Results were consistent with the data previously reported<sup>91</sup>

<sup>91</sup> Van Ameijde, J.; Albada, H.B.; Liskamp, R.; *J. Chem. Soc. Perkin Trans. 1*, **2002**, 1042-1049.

### 8.2.9 *tert*-Butyl deprotection of Fmoc-protected amino acids

The pure *t*-Bu esters **10 $\alpha$**  and **10 $\beta$**  were dissolved in TFA in DCM (1:1). The reaction mixture was stirred for 3 hours at r.t. The solvents were evaporated and after dissolution in water and freeze drying, Fmoc-protected glycosyl amino acids **11 $\alpha$**  and **11 $\beta$**  were obtained.

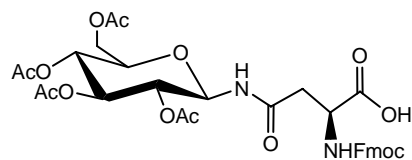
**Fmoc-L-Asn( $\alpha$ GlcAc<sub>4</sub>)-OH (11 $\alpha$ )** yield 97%. Rf = 0.24 (AcOEt/Hexane, 2:1,



UV and vanilline). <sup>1</sup>H NMR (400 MHz, CDCl<sub>3</sub>)  $\delta$  = 2.01, 2.03 (2 s, 12H, 4 $\times$ OAc), 2.87 (system ABMX,  $J_{AB}$  = 17.2 Hz,  $J_{AM}$  = 4.8 Hz,  $J_{BM}$  = 4.4 Hz, 2 H, Asn- $\beta$ -CH<sub>2</sub>), 3.80 (dq,  $J$  = 4.0 Hz,  $J$  = 2 Hz, 1H, H-5), 4.06 (*pd*,  $J$  = 11.6 Hz, 1H, H-6),

4.19 (t,  $J$  = 7.2 Hz, 1H, Fmoc-CH), 4.26 (dd,  $J$  = 12.8 Hz, 4.4 Hz, 1H, H-6'), 4.32-4.44 (m, 2H, Fmoc-CH<sub>2</sub>), 4.51-4.55 (m, 1H, Asn- $\alpha$ -CH), 5.09-5.15 (m, 2H, H-2 and H-4), 5.23 (t,  $J$  = 9.6 Hz, 1H, H-3), 5.72 (m, 2H, H-1 and Asn- $\alpha$ -NH) 7.28 (app-dt, 5H, 1-NH and Fmoc-Ar), 7.58 (app-d, 2H, Fmoc-Ar), 7.74 (d,  $J$  = 7.2 Hz, 2H, Fmoc-Ar) ppm. <sup>13</sup>C NMR (100 MHz, CDCl<sub>3</sub>)  $\delta$  = 20.5, 20.5, 20.6 (C(O)CH<sub>3</sub>), 36.7 (C $_{\beta}$ ), 47.1(Fmoc CH), 50.5 (C $_{\alpha}$ ), 61.3 (C-6), 67.1 (Fmoc-CH<sub>2</sub>), 67.6, 70.1, 72.6, 72.7 (C-2,C-3,C-4,C-5), 91.9 (C-1), 119.9, 125.0, 125.1, 127.0, 127.7, 141.2, 143.7, 143.7 (Ar-C), 155.5, 169.0, 169.0, 169.3, 169.3, 170.0, 170.4 (C=O).

**Fmoc-L-Asn( $\beta$ GlcAc<sub>4</sub>)-OH (11 $\beta$ )**, yield 95%. Rf = 0.19 (AcOEt/Hexane, 2:1,



UV and vanilline). <sup>1</sup>H NMR (400 MHz, CDCl<sub>3</sub>)  $\delta$  = 2.00, 2.02 (2 s, 12H, 4 $\times$ OAc), 2.85 (system ABMX,  $J_{AB}$  = 16.4 Hz,  $J_{AM}$  = 4.4 Hz,  $J_{BM}$  = 4.0 Hz, 2H, Asn- $\beta$ -CH<sub>2</sub>),

3.74 (*pt*,  $J$  = 4.8 Hz, 1H, H-5), 4.05 (d,  $J$  = 12.4 Hz, 1H, H-6), 4.19 (t,  $J$  = 7.2 Hz, 1H, Fmoc-CH), 4.27 (dd,  $J$  = 12.8 Hz,  $J$  = 4.4 Hz, 1H, H-6'), 4.31-4.40 (m, 2H, Fmoc-CH<sub>2</sub>), 4.59-4.61 (m, 1H, Asn- $\alpha$ -CH), 4.94 (t,  $J$  = 9.6 Hz, 1H, H-2), 5.07 (t,  $J$  = 10 Hz, 1H, H-4), 5.27-5.35 (m, 2H, H-1 and H-3), 5.59 (broad s, 1H, COOH), 6.25 (d,  $J$  = 8.0 Hz, 1H, Asn- $\alpha$ -NH), 7.06 (d,  $J$  = 9.2 Hz, 1H, NH-

## EXPERIMENTAL PART

1), 7.28 (app-t, 2H, Fmoc-Ar), 7.37 (app-t, 2H, Fmoc-Ar), 7.57 (d,  $J = 7.2$  Hz, 2H, Fmoc-Ar), 7.73 (d,  $J = 7.2$  Hz, 2H, Fmoc-Ar) ppm.

### 8.3 Solid Phase Peptide Synthesis

#### 8.3.1 General procedure for batch SPPS on the manual PLS 4x4 synthesizer

Peptides are synthesized on a manual batch synthesizer (PLS 4x4, Advanced ChemTech) using a Teflon reactor (20 mL), following the Fmoc/tBu SPPS procedure. The resin is placed in the 20 mL Teflon reactor, equipped with a filter. Mixing is provided by vortex, while filtration is performed connecting the reactor to a *vacuum* pump. The resin is swelled for 40 min with DMF (1 mL/100 mg of resin) before use. Each amino-acid cycle is characterized by the following four steps:

*Fmoc-deprotection*: Resin is washed twice ( $1 \times 5$  min +  $1 \times 15$  min) with 20% piperidine in DMF (1 mL/100 mg of resin).

*Washings*: DMF ( $3 \times 5$  min),

*Coupling reaction*: Fmoc protected amino acids (2.5 equiv) in DMF (1 mL/100 mg resin), TBTU/HOBt/NMM (2.5 equiv, 2.5 equiv, 3.5 equiv) as coupling system for 45 min.

*Washings*: DMF ( $3 \times 5$  min) and DCM ( $2 \times 5$  min).

Deprotection of the second residue should be performed by a fast protocol to avoid DKP formation ( $3 \times 5$  min). For the coupling step a solution of the Fmoc-amino acid (4 equiv), TBTU (4 equiv), HOBt (4 equiv), and NMM (8 equiv) in DMF (1 mL  $\times$  100 mg resin) is added to the resin. After DCM washings each coupling reaction is checked by a Kaiser test. After the last Fmoc-removal the resin is washed with DCM and dried under vacuum.

### 8.3.2 *General procedure for in batch SPPS on an automatic peptide synthesizer*

All the reactions are performed in a Prelude™ parallel peptide synthesizer, in sealed reaction vessel under N<sub>2</sub>, where mixing and filtration is provided by a N<sub>2</sub> flow. The resin is then swollen for 40 min. Each amino-acid cycle is characterised by the following four steps:

- Fmoc-deprotection (1×5 min + 1×15 min),
- Washings with DMF (5×2 min),
- Coupling (2 x 20 min),
- Washings with DMF (3×2 min).

For the coupling reaction a 0.5 M solution of the Fmoc-protected amino acid and HOBT in DMF (4 equiv), 0.5 M solution of TBTU in DMF (4 equiv), and 4 M solution of NMM in DMF (8 equiv) are used. DMF is eventually added to reach the good swelling volume of the resin (1 mL×100 mg). After removal of the last Fmoc-residue, the resin is washed with DCM and dried under N<sub>2</sub> flow for 30 min.

### 8.3.3 *General procedure for Microwave-assisted SPPS*

The microwave-assisted solid phase peptide synthesis is performed on a Liberty™ Microwave Peptide Synthesizer (CEM Corporation, Matthews, NC), an additional module of Discover™ (CEM Corporation, Matthews, NC) that combines microwave energy at 2450 MHz to SPPS following the Fmoc/*t*Bu strategy.

Each deprotection and coupling reaction is performed using microwave energy and N<sub>2</sub> bubbling. Microwave cycle is characterized by two deprotection steps, the first one for 30 seconds, the second one for 180 seconds. All coupling reactions are performed for 300 seconds (Table 8.3.3).

## EXPERIMENTAL PART

**Table 8.3.3 Microwave cycles for automatic MW-SPPS.**

Step	Temp. (°C)	MW Power (W)	Time (sec)
1 <sup>st</sup> deprotection	70-75	25	30
2 <sup>nd</sup> deprotection	70-75	25	180
coupling	70-75	25	300

Peptides are synthesized on pre-loaded Wang Resin, using a scale of 0.1 or 0.25 mmol. Deprotections are performed with 20% piperidine in DMF solution. All coupling reactions are performed with 2.5 equiv of 0.25 M solution of TBTU in DMF, 2.5 equiv of 0.1 M solution of amino acids in DMF and 3.5 equiv of 0.7 M solution of DIPEA in NMP solution. Washing steps are performed with DMF and DCM. A complete amino acid coupling cycle is completed in 30 min.

### **8.3.4 General procedure for cleavage**

Peptides and glycopeptides are cleaved from the resin using as cleavage mixture TFA/ethanedithiole/thioanisole/H<sub>2</sub>O/phenol (82.5:5:2.5:5:5) (reagent K). The peptide-resins are treated for 2.5 h with reagent K (1 mL × 100 mg of resin) at r.t.. The resin is filtered off and the solution is concentrated flushing with N<sub>2</sub>. The peptide is precipitated from cold Et<sub>2</sub>O or isoprophylethere as indicated for each reaction, centrifuged and lyophilized.

### **8.3.5 General procedure for glycopeptide deacetylation**

Deacetylation of the sugar linked to the peptide is accomplished by adding 0.1 M MeONa in MeOH to a solution of the raw material in dry MeOH (12 ml) until pH 12. After 1 h under stirring the reaction is quenched by adding dry CO<sub>2</sub> to neutrality, the solvent is evaporated under vacuum and the residue lyophilized.

### 8.3.6 *General procedure for pre-purification by solid-phase extraction (SPE)*

SPE is performed on RP-C18 LiChroprep columns. Main steps are reported here: Column washings with MeOH (3 column volumes) and CH<sub>3</sub>CN (3 column volumes); column conditioning with H<sub>2</sub>O (3 column volumes); dissolving the peptide in H<sub>2</sub>O (1 column volume), checking the pH that should be neutral. Peptides are absorbed on silica by passing their solution for 3 times; eluting with H<sub>2</sub>O (3 column volumes) and after with 5%, 10%, 15%, 20% H<sub>2</sub>O/CH<sub>3</sub>CN (column volume for each concentration), and 100% CH<sub>3</sub>CN. Fractions are checked by analytical UPLC-ESIMS, and then lyophilized.

*Purification:* All Peptides are further purified by semipreparative RP-HPLC using methods and solvent system reported in tables. Fractions are checked by UPLC-ESIMS to homogeneous ones

### 8.3.7 *Synthesis of CSF114( $\alpha$ -Glc) (I $\alpha$ ) and CSF114( $\beta$ -Glc) (I $\beta$ )*

Glycopeptides **I $\alpha$**  and **I $\beta$**  were synthesized on an automatic Prelude™ peptide synthesizer, as described in the general procedure, starting from Fmoc-Lys(Boc)-Wang resin (100 mg, 0.55 mmol/g). Fmoc-L-Asn( $\alpha$ -GlcAc<sub>4</sub>)-OH (**11 $\alpha$** ) and Fmoc-L-Asn( $\beta$ -GlcAc<sub>4</sub>)-OH (**11 $\beta$** ) (1.5 equiv) were manually coupled using HOBt (1.5 equiv), TBTU (1.5 equiv) and NMM (3 equiv) in DMF for 1 h. Glycopeptides were cleaved from the resin and side chains were deprotected as described in the general procedure. Deprotection of the hydroxyl functions of sugars was performed as described in the general procedure and the glycopeptides were pre-purified by SPE and further purified by semipreparative RP-HPLC. Characterization of the peptides was performed using analytical HPLC and ESI-MS spectrometry. The analytical data are reported in Table 1.2.2.

## EXPERIMENTAL PART

### 8.3.8 *Synthesis of Biotin-CSF114(Glc) (II) and Biotin-CSF114 (II')*

Biotinylated peptides **II** and **II'** were synthesized on an automatic Prelude™ peptide synthesizer, as described in the general procedure, starting from Fmoc-Lys-Wang resin (100 mg, 0.55 mmol/g). Fmoc-L-Asn(GlcAc4)-OH (**11**) (1.5 equiv) was coupled in a manual batch synthesizer using HOBt (1.5 equiv), TBTU (1.5 equiv), and NMM (3 equiv) in DMF for 1 h. Peptide sequences were then completed in the automatic peptide synthesizer. N-biotinyl-6-aminohexanoic acid was manually introduced at the N-terminus of the resin-bound peptides using HOBt/TBTU (2.5 equiv) as activators for 1 h.

Peptide cleavage from the resin and deprotection of the amino-acid side chains were carried out using reagent K. The resin was stirred for 3 h at room temperature. The resin was washed with TFA and the filtrate partially evaporated. Each crude product was then precipitated with diethyl ether, collected by centrifugation, dissolved in H<sub>2</sub>O and lyophilized. Deacetylation of the sugar moiety of peptide **II** was performed using 0.1 M MeONa in MeOH until pH = 12 added to a solution of the lyophilized peptide in dry MeOH (1 mL/100 mg of resin). After 3 h the reaction was quenched by adding conc. HCl until pH = 7, the solvent was evaporated under vacuum and the residue lyophilized. Analytical data of the peptides are reported in Table 3.1.

### 8.3.9 *Synthesis of fluoresceinyl-CSF114(Glc)-PEG-Biotin (III) and fluoresceinyl-CSF114-PEG-Biotin (III')*

Peptides **III** and **III'** were synthesized on an automatic Prelude™ peptide synthesizer, as described in the general procedure, starting from biotin-PEG-NovaTag™ resin (100 mg, 0.48 mmol/g). Fmoc-LAsn(GlcAc4)-OH (**11**) (1.5 equiv) was manually coupled using HOBt (1.5 equiv), TBTU (1.5 equiv), and NMM (3 equiv) in DMF for 1 h. Peptide sequences were then completed in the automatic peptide synthesizer. 5(6)-Carboxyfluorescein was manually introduced at the N-terminus of the resin-bound biotinylated peptides using HOBt/DIPCDI (2.5 equiv) as activators for 2 h.



Peptides were cleaved and side chains were deprotected as described in the general procedure. Deprotection of the hydroxyl functions of the glycopeptide **III** was performed as described in the general procedure and the sequences were pre-purified by SPE and further purified by semipreparative RP-HPLC. Characterization of the peptides was performed using analytical HPLC and ESI-MS spectrometry. Analytical data of the peptides are reported in Table 4.1.

### 8.3.10 *Synthesis of ferrocenyl-labelled peptides and glycopeptides*

SPPS was performed by Liberty<sup>TM</sup> Microwave Peptide Synthesizer (CEM Corporation, Matthews, NC), an additional module of Discover<sup>TM</sup> (CEM Corporation, Matthews, NC) that combines microwave energy at 2450 MHz following the Fmoc/tBu SPPS strategy as described in the general procedure for microwave-assisted synthesis. CSF114 and CSF114(Glc) were prepared starting from Fmoc-Lys(Boc)-Wang resin (0.67 mmol/g). The glucosyl moiety of glycosylated peptides was introduced by the building-block Fmoc-L-Asn(GlcOAc4)-OH (2.5 equiv) which was synthesized as previously reported in section 1.1.

Ferrocenyl carboxylic acid (Fc-COOH) (2.0 equiv) was coupled with TBTU (2 equiv), HOBt (2 equiv), and NMM (3 equiv) at the N-terminus of CSF114(Glc) and CSF114 sequences respectively for 1.5 h on a manual batch synthesizer (PLS 4×4, Advanced ChemTech) using Teflon reactors (10 mL) obtaining peptides **IV** and **IV'**. (Sp,S)-(+)-2-(tert-butoxycarbonylamino)-4-(ferrocenylphenylthiophosphino)butanoic acid was coupled with TBTU (2 equiv), HOBt (2 equiv), and NMM (3 equiv) at the N-terminus of the CSF114(Glc) and CSF114 sequences respectively for 1.5 h on a manual batch synthesizer obtaining peptides **V** and **V'**.

Peptide cleavage from the resin and deprotection of the amino-acid side chains were carried out with 1 mL/100 mg resin of TFA/anisole/1,2-ethanedithiol/phenol/H<sub>2</sub>O solution (96:1:1:1:1 v/v/v/v/v). Cleavage reaction mixture was maintained for 3 h at room temperature under stirring. The resin

## EXPERIMENTAL PART

was washed with TFA and the filtrate partially evaporated. Each crude product was precipitated with diethyl ether, collected by centrifugation, dissolved in H<sub>2</sub>O and lyophilized. Deacetylation of the sugar moiety linked to the peptide **I-IV** and **V** was performed adding 0.1 M methanolic MeONa solution until pH = 12 to a solution of the lyophilized peptide in dry MeOH (1 mL/100 mg resin). After 3 h the reaction was quenched by adding conc. HCl until pH = 7. The solvent was evaporated under *vacuum* and the residue lyophilized. All peptides were purified by semipreparative RP-HPLC and the purity of the peptides was checked using methods reported in Table 2.2.

### 8.4 Immunoassays

#### 8.4.1 *Solid-phase not competitive indirect ELISA (SP-ELISA)*

Serum was obtained for diagnostic purposes from patients and healthy blood donors who had given their informed consent, and stored at -20 °C until use. Antibody responses were determined in SP-ELISA. Ninety-six wells activated polystyrene ELISA plates (NUNC Maxisorb SIGMA) were coated with 1 µg per 100 µl of peptides per well or glycopeptides in pure carbonate buffer 0.05 M (pH 9.6) and incubated at 4 °C overnight. After five washes with saline containing 0.05% Tween 20, non specific binding sites were blocked by fetal calf serum (FCS), 10% in saline Tween 20 (100 µl per well) at room temperature for 60 min. Sera diluted from 1:100 to 1:100.000 were applied at 4 °C overnight in saline/Tween 20/10% FCS. After five washes, it was added 100 µl of alkaline phosphatase conjugated anti-human IgM (diluted 1:200 in saline/Tween 20/FCS) or IgG (diluted 1:8000 in saline/ Tween 20/FCS) (Sigma) to each well. After 3 h at room temperature incubation and five washes, 100 µl of substrate solution consisting of 1 mg/ml p-nitrophenyl phosphate (Sigma) in 10% diethanolamine buffer was applied. After 30 min, the reaction was stopped with 1M NaOH (50 µl), and the absorbance was read in a multichannel ELISA reader (Tecan Sunrise) at 405 nm. ELISA plates,

coating conditions, reagent dilutions, buffers, and incubation times were tested in preliminary experiments.<sup>24</sup> The antibody levels are expressed as absorbance in arbitrary units at 405 nm (sample dilution 1:100).

#### **8.4.2 Measurement of antibody affinity by competitive ELISA**

Antibody affinity was measured following the methods previously reported.<sup>92</sup> The semi-saturating sera dilution (1:600) was calculated from the preliminary titration curves (absorbance, 0.7). At this dilution, Abs were preincubated with increasing synthetic peptide antigen concentration (0;  $7.68 \times 10^{-11}$ ;  $7.68 \times 10^{-10}$ ;  $7.68 \times 10^{-9}$ ;  $7.68 \times 10^{-8}$ ;  $7.68 \times 10^{-7}$ ;  $7.68 \times 10^{-6}$ ;  $3.84 \times 10^{-5}$ ) for 1 h at room temperature. Unblocked Abs were revealed by ELISA, and the antigenic probe concentration-absorbance relationship was presented graphically.

#### **8.4.3 Antibodies purification by affinity chromatography**

Cyanogen-bromide activated resin (CNBr-Sepharose) was placed in a solid phase extraction tube (Supelco, Milan, Italy) and the resin was washed with 12 ml of ice cold HCl (1 mM). This washing step facilitated the removal of lactose, used for stabilisation of the resin using freeze-drying. The resin was hence washed with Milli-Q water (12 ml) and a coupling buffer composed of  $\text{NaHCO}_3$  (0.1 M) and NaCl (0.5 M) pH = 8.3 (1 ml). The glycopeptide, CSF114(Glc), 1 mg, was dissolved in 1 ml coupling buffer ( $\text{NaHCO}_3$ , 0.1 M, NaCl 0.5 M, pH = 8.3). The glycopeptide solution was thereafter added to the column and shaken overnight at room temperature. The functionalised resin was hence transferred to a solid phase extraction column closed at one end with a frit. The resin was allowed to settle and was subsequently washed with the coupling buffer. Unreacted groups were blocked using a glycine solution (0.2 M, pH = 8.0). In order to remove the washing solution, the functionalised resin was washed with the alkaline coupling buffer (10 ml), followed by washing with an acetate buffer (0.1 M, pH 4.3, 0.5 M NaCl) (10 ml).

---

<sup>92</sup> Rath, S.; Stanley, C. M.; Steward, M. W. *J Immunol Methods*, **1988**, 106, 245–249.

## EXPERIMENTAL PART

The serum from which the antibodies would be isolated was diluted 1:10 in PBS buffer and filtered through a 0.22  $\mu\text{m}$  filter (Millex®-GS). Thereafter, the serum was loaded on the functionalised affinity column. The diluted serum was recirculated three times on the column. Anti-CSF114(Glc) antibodies were eluted by washing with: (a) 10 ml coupling buffer (pH = 8.3), (b) 10 ml PBS (pH = 7.0). Finally, the antibodies bound to the antigen (peptide) anchored to the resin, were eluted using a 0.2 M glycine solution (pH = 2.6). Washing and elution solutions were collected in Eppendorf tubes. Immediately after elution, fractions containing glycine buffer were immediately neutralised with 0.5 M  $\text{NaHCO}_3$  buffer. In order to determine the immunoreactivity the fractions were characterised using UV spectroscopy and Enzyme-linked immunosorbent assay (ELISA).

### **8.4.4 BIAcore measurements procedure**

Direct amino coupling was carried out by directly linking the peptide antigens to the CM5 dextran coated chip. The immobilisation was achieved by firstly activating the sensor surface with N-hydroxysuccinimide (50 mM) and N-(3-dimethylaminopropyl)-N'-ethylcarbodiimide (200 mM) in water. 1 mM solution of peptide CSF114 was flowed through FC1 and a solution 1 mM of peptide CSF114(Glc) was flowed in the FC2 using 12 minutes interaction time with the sensor surface at a flow rate of 10  $\mu\text{l}/\text{min}$ . Remaining activated sites were blocked using ethanolamine.

Biotin/streptavidin coupling was performed by sensor chip activation using a solution of N-hydroxysuccinimide (50 mM) and N-(3-dimethylaminopropyl)-N'-ethylcarbodiimide (200 mM) in water. Thereafter, streptavidin (100  $\mu\text{g}/\text{ml}$ ) in acetate buffer (10 mM, pH = 5.0) was passed over the chip for 10 minutes at a flow rate of 10  $\mu\text{l}/\text{min}$ . Finally, a solution of ethanolamine-HCl (1 M, pH = 8.5) was used to block any remaining activated sites. The peptide antigens, biotin-CSF114, as negative control and biotin-CSF114(Glc) were dissolved in Milli-Q water to a concentration of 1 mM and were hence diluted in HBS-EP

buffer to obtain final peptide concentration of 1  $\mu$ M. Flow cell 3 (FC3) was saturated with biotin-CSF114 and flow cell 4 (FC4) was saturated with biotin-CSF114(Glc) using 12 minutes interaction time with the sensor surface at a flow rate of 10  $\mu$ l/min.

Specific anti-CSF114(Glc) antibodies and serums were injected and flowed at 30  $\mu$ l/min in the designed flow cells for 120 sec. Anti-human IgG substrate was injected at dilution 1:100 for 120 sec at flow rate 30  $\mu$ l/min. Regeneration solution was injected at 30  $\mu$ l/min for 30 sec.

### 8.5 Ferrocenyl electrochemical studies

In a cyclic voltammetry (CV) experiment, the potentiostat applied a potential ramp to the working electrode to gradually change the potential and then reversed the scan, returning to the initial potential at a constant scan rate. The electrochemical instrumentation includes an EG&G 283 potentiostat connected to a PC and the collected data were analyzed using a Princeton Applied Research Software, Power Suite. A special electrochemical cell was used to handle only few microliters. The auxiliary electrode is a platinum wire and the reference is an Ag|AgCl electrode separated from the solution by a vycor tip. The active working electrode is a 1.6 mm diameter gold electrode (BAS) protected by 11-mercaptoundecanoic acid SAM for the ferrocenyl glycopeptide **IV**. In the case of **V** and **V'**, a mixture of 11-mercaptoundecanoic acid and decanethiol was used after immobilization of the ferrocenyl glycopeptides.

The electrochemical measurements have been realized in a 0.05% Tween 20 solution containing LiClO<sub>4</sub> 0.1M and potassium ferrocyanide (K<sub>4</sub>Fe(CN)<sub>6</sub>, Aldrich),  $9 \times 10^{-4}$  M at room temperature. The concentration of Fc-CSF114(Glc) is  $1.77 \times 10^{-4}$  M. Specific autoantibodies were diluted at 1:1000. All solutions were deoxygenated prior to experiments

## EXPERIMENTAL PART

### 8.6 Optical Tweezers procedures

#### 8.6.1 Preparation of functionalized microscopic beads

Both antigens and antibodies were coated to different functionalized polystyrene (latex) microparticles.

Specific anti-CSF114(Glc) antibodies, purified as described in section 8.4.3, were attached to goat anti-human IgG (H&L) polystyrene latex microparticles ( $\varnothing$  3,0-3,9  $\mu\text{m}$ , KISKER) by mixing in a vortex for 2 h. To remove unbound antibodies the bead suspension was allowed to sediment for 1 hour on ice. Subsequently the supernatant was decanted and the pellet gently resuspended in D-PBS buffer supplemented with 0.5 mg/ml BSA and subsequently centrifuged. This procedure was repeated three times. Finally beads were suspended in 2 ml D-PBS buffer.

A solution containing 50  $\mu\text{g}$  of fluoresceinyl biotinylated peptides **III** and **III'** were attached to polystyrene (latex) beads functionalized with streptavidin (KISKER) by stirring for 30 min. Bead suspension was then centrifuged and washed with D-PBS buffer repeating for 3 times. The attachment of peptides to the beads was checked with fluorescence microscopy.

#### 8.6.2 Optical Tweezers measurements

Interaction forces between the antigen CSF114(Glc) and specific IgG antibodies were measured with a double-beam counter-propagating optical tweezers apparatus.<sup>93</sup> Further customized set-up has been previously reported.<sup>64</sup> Data acquisition were carried out by using custom-written LabView algorithms. The assay was carried out at room temperature in D-PBS buffer and 0.5 mg/ml BSA to block non-specific interactions. Microscopic beads were diluted.

---

<sup>93</sup> (a) Kellermayer, M.S.Z., S.B. Smith, H.L. Granzier, and C. Bustamante, *Science*, **1997**, 276(5315), 1112-6. (b) Kellermayer, M.S., S.B. Smith, C. Bustamante, and H.L. Granzier, *Biophys J*, **2001**, 80(2), 852-63. (c) Smith, S.B., Y. Cui, and C. Bustamante, *Science*, **1996**, 271(5250), 795-9.

## 9. *Experimental Part B*

### 9.1 **Materials and methods**

The water used was obtained from demineralized water by distilling it once and then distilling the water so obtained from alkaline permanganate. Merck suprapur® KCl was baked at 500 °C before use to remove any organic impurities. Dioleoylphosphatidylcholine (DOPC) was obtained from Lipid Products (South Nutfield, Surrey, England), while diphytanoylphosphatidylcholine (DphyPC), PG (L- $\alpha$ -phosphatidyl-DL-glycerol), PC (egg yolk L- $\alpha$ -phosphatidylcholine), PS (phosphatidylserine) and 2,3-di-Ophytanyl-sn-glycerol-1-tetraethylene-glycol-D,L- $\alpha$  lipoic acid ester lipid (DPTL) were obtained from Avanti Polar Lipids (Alabaster, AL). DOPC and DphyPC solutions were prepared by diluting a proper amount of stock solutions of these phospholipids with pentane. Solution of 0.2 mg/ml DPTL in ethanol was prepared from a 2 mg/ml solution of DPTL in ethanol. Stock solutions of these products were stored at -18 °C. Stock solutions of peptides were prepared  $5 \times 10^{-3}$  M in methanol and were stored at +4 °C. The other chemicals and solvents were commercially available and used as received.

A Pyrex® glass sheltered beaker of 100 ml is used as electrochemical cell. Electrodes, as well as the bubbling scrubber used for induce gas deoxygenation, are supported in five holes in the cell tip. The whole cell is enclosed in a water-jacketed box thermostatically controlled at  $25.5 \pm 0.1$  °C. Moreover, the cell is put on a magnetic stirrer enabling to stir the solution. All the equipment is placed in a Faraday cage to decrease the background noise and supported by an antivibrating desk, to reduce vibrations interfering measures at low frequencies (Figure 9.1).

## EXPERIMENTAL PART

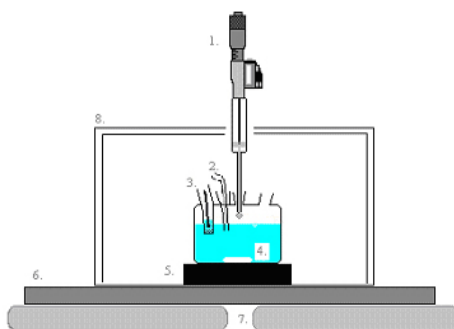


**Figure 9.1.** The scheme shows the equipment: 1, working electrode; 2, scrubber with auxiliary electrode; 3, reference electrode; 4, magnetic bar; 5, magnetic stirrer; 6, antivibrating desk; 7, air cushion; 8, water-jacketed box thermostatically controlled.

All measurements were performed using a three-electrodes potentiostatic system, consisting of a Ag/AgCl (0.1M) as reference electrode, platinum wire wrapped around the scrubber as auxiliary electrode, and a home-made hanging mercury drop electrode (HMDE) as working electrode<sup>94</sup>. It allows accurate changes in drop area of as little as 0.04 mm<sup>2</sup>. Use was made of a home-made glass capillary (Metrohm, n°6.1209.010) with a finely tapered tip, about 1 mm in outer diameter. Capillary was silanized as described in the following section. Periodically, calibration and a test for reproducibility of the HMDE are performed. The HMDE and the support were moved vertically and horizontally, respectively, by means of two oleodynamic systems that ensured the complete absence of vibrations. Using the oleodynamic system, mercury drop of the HMDE could be completely immersed into the electrolyte solution passing through the interface solution.

All glassware is treated with chromic acid solution, useful to remove organic deposits; sometimes the cleaning procedure is performed under heating, to remove lipidic residues. Then, so-treated glassware is washed with abundant

---

<sup>94</sup> Moncelli, M.R.; Becucci, L, *Journal of Electroanalytical Chemistry*, **1997**, 433, 91-96.



bi-distillate water and, finally, is covered with a tinfoil and dried at 150°C in the oven.

AC voltammetry and impedance spectroscopy measurements were carried out with an Autolab instrument (EchoChemie) supplied with FRA2 module for impedance measurements, SCAN-GEN scan generator and GPES3 software. Potentials were measured versus one Ag/AgCl (0.1 M KCl) reference electrode. The applied potential was then measured over a potential range, while continuously monitoring the curve of the differential capacity,  $C$ , vs. the applied potential,  $E$ .

### **9.1.1 Capillary silanization**

The silanization procedure is described as follow: the capillary was put in a NaOH 1M alcoholic solution for 12h, to remove the old silanization. After that, it was washed with a HCl 0.1M solution, bi-distillate water and finally ethanol. Then, it was dried in oven at 140-150°C for 2h and successively cooled to room temperature. When the previous silanization is completely removed, it is possible to make a new one, putting the head of capillaries in 2-3 cm of a 5% dimethylchlorosilane (DMS) in toluene solution. In this condition, the silanizing solution will climb up inside the wall of the capillary. This step require a great attention to keep out water from DMS solution, otherwise there will be an occlusion of capillaries due to the polimerization of silane. The excess of DMS is washed with abundant toluene, dry in oven at 140-150°C for 2 h and cooled to room temperature.

### **9.1.2 Electrochemical Analysis**

The stand-by potential to conserve membrane integrity was -0.4V. Electrochemical analyses were performed using the next parameters *AC Voltammetry* scans were recorder for potentials between -0.2V and -1.2V using 0.00705V as step potential.

## EXPERIMENTAL PART

*Cyclic Voltammetry* scans were performed from -0.9V as first vertex potential to -0.3V as second vertex potential with a scan rate of 0.5 V/s and a step potential of 0.00244V.

*Electrochemical impedance spectroscopy (EIS)* spectra were recorded for frequencies between 0.01/0.1 Hz and  $10^5$  Hz starting from -0.3 V potential to -1 V.

### 9.2 Peptide and glycopeptide synthesis

Glycopeptides CSF114(Glc) **I** and Scramble CSF114(Glc) **VI** were synthesized on an automatic Prelude synthesizer, as described in the general procedure, starting from Fmoc-Lys-Wang resin (100 mg, 0.6 mmol/g) and Fmoc-Pro-Wang resin respectively. Fmoc-L-Asn(GlcAc4)-OH (1.5 equiv) was manually coupled using HOBt (1.5 equiv), TBTU (1.5 equiv), and NMM (3 equiv) in DMF for 1.5 h in a manual PLS 4x4 synthesizer.

Peptides CSF114 (**I'**), Scramble CSF114 (**VI'**), MBH36 (**VII**), and TripZip (**VIII**) were synthesized in an automatic Prelude synthesizer, as described in the general procedure, starting from the corresponding Fmoc-Xaa(Pg)-Wang resin (100 mg, 0.6 mmol/g).

Peptides and glycopeptides were cleaved and side chains were deprotected as described in the general procedure. Deprotection of the hydroxyl functions of glucose was performed as described in the general procedure and the peptides were pre-purified by SPE and further purified by semi-preparative HPLC. Characterization of the peptides was performed using analytical HPLC and ESI-MS spectrometry. Analytical data of all peptides are reported in Table 9.2.

**Table 9.2. Peptides in biomimetic membrane**

peptide	HPLC ( $R_t$ , min)	ESI-MS [ $M+2H$ ] <sup>2+</sup> Calc (found)
CSF114(Glc) (I)	14.8 <sup>a</sup>	1303.6 (1303.8)
CSF114 (I')	14.1 <sup>a</sup>	1223.3 (1223.9)
Scramble CSF114(Glc) (VI)	17.0 <sup>b</sup>	1303.6 (1304.1)
Scramble CSF114 (VI')	15.1 <sup>c</sup>	1223.3 (1223.9)
MBH36 (VII)	15.4 <sup>d</sup>	839.4 (839.9)
TripZip (VIII)	7.4 <sup>e</sup>	804.8 (805.4)

<sup>a</sup>Analytical HPLC gradients at 1 mL min<sup>-1</sup>, 20-60% B in 20 min, <sup>b</sup>25-35% B in 25 min, <sup>c</sup> 25-40% B in 30 min, <sup>d</sup> 05-40% B in 20 min, <sup>e</sup> 30-70% B in 20 min; solvent system A: 0.1% TFA in H<sub>2</sub>O, B: 0.1% TFA in CH<sub>3</sub>CN;

### 9.3 Bilayer preparation

The preparation of a tethered bilayer lipid membrane (tBLM) consists in two steps:

- 1) preparation of a self-assembled monolayer of a thiolipid,
- 2) formation of a phospholipids monolayer on top of the thiolipid monolayer.

DPTL was self-assembled on the HMDE by keeping the mercury drop immersed in the small vessel containing the spacer solution (0.2 mg/ml) for 20 min (Figure 9.3.1) A solution of DOPC or DphyPC in pentane was spread on the surface of the 0.1 M KCl aqueous solution contained in the electrochemical cell. The amount of phospholipids spread corresponds to five or six monolayers at the air/solution interphase.

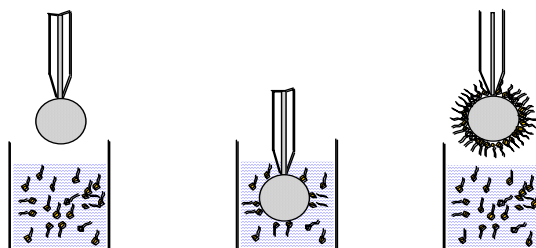


*Figure 9.3.1. DPTL monolayer formation steps.*

## EXPERIMENTAL PART

Using the oleodynamic system, the spacer-coated HMDE was then extracted from the vessel, washed with the organic solvent to remove the excess of adsorbed spacer, and kept in an Ar atmosphere for the time necessary to allow the solvent to evaporate. Immediately afterwards, the electrochemical cell containing the aqueous solution, on whose surface the phospholipid had been previously spread, was placed just below the HMDE and the electrode was then immersed into the electrolyte solution across the phospholipid film (figure 9.3.2).

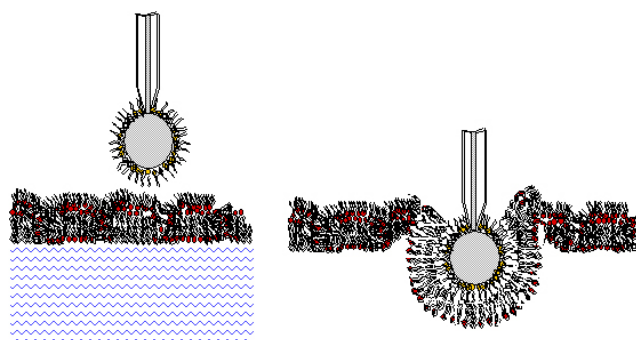


*Figure 9.3.2. Second step: bilayer formation immersing DPTL-coated Hg drop through a DphyPC film spreaded at air-water interface.*

The integrity of self-assembled bilayer was characterized using AC voltammetry and electrochemical impedance spectroscopy (EIS) techniques. Peptides and glycopeptides were directly added to the electrolyte solution.

### 9.4 Liposomes-peptide incubation

Peptides-liposomes interactions were assayed by measuring fluorescence. A film of lipid was prepared on the inside wall of a round-bottom flask by evaporation of  $\text{CHCl}_3$  solutions containing the proper amount of PC/PG (2:1). The suspension was freeze-thawed in liquid nitrogen for nine cycles and extruded 30 times through polycarbonate filters (two stacked 0.2- $\mu\text{m}$  pore size filters) using an Avanti Mini-Extruder (Avanti Polar Lipids inc., Alabaster, AL). Vesicles in suspensions containing 100  $\mu\text{M}$  lipids were incubated with various concentrations of the peptide CSF114 (0.6–20  $\mu\text{M}$ ), or the fixed

## EXPERIMENTAL PART

concentration of CSF114 (1  $\mu\text{M}$ ) was incubated with vesicles (4-300  $\mu\text{M}$ ). The fluorescence of the Trp residue was assessed with a spectrofluorometer (Perkin-Elmer LS55) at an excitation wavelength of 280 nm and an emission wavelength between 320 and 420 nm. The experiments were conducted at 25°C.

### **9.4.1 Anisotropy measurements**

Anisotropy of vesicles and vesicles containing peptide CSF114 was calculated using a polarization mode. The fluorescence of the Trp residue was assessed with a spectrofluorometer (Perkin-Elmer LS55) at an excitation wavelength of 280 nm and an emission wavelength 350 nm. G-factor of the instrument was previously calculated (1,566332). Anisotropy of a solution containing 10  $\mu\text{M}$  of CSF114 was calculated in absence and in presence of liposomes (300  $\mu\text{M}$ )



## 10. Description of the techniques

### 10.1 Surface plasmon resonance

The physical principles of SPR are complex, but fortunately, an adequate working knowledge of the technique does not require a detailed theoretical understanding. It suffices to know that SPR-based instruments use an optical method to measure the refractive index near (within ~300 nm) a sensor surface. In the BIAcore this surface forms the floor of a small flow cell, through which an aqueous solution (henceforth called the running buffer) passes under continuous flow (1-100  $\mu\text{l min}^{-1}$ ). In order to detect an interaction one molecule (the ligand) is immobilised onto the sensor surface.

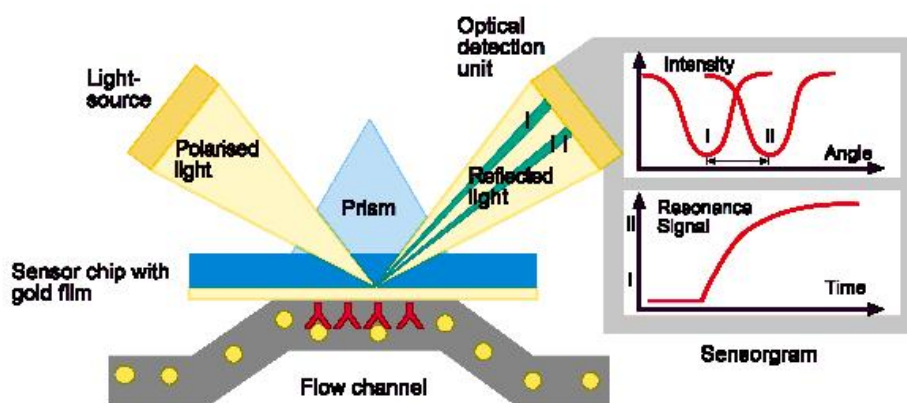


Figure 10.1 Schematic diagram of Surface Plasmon Resonance.

Its binding partner (the analyte) is injected in aqueous solution (sample buffer) through the flow cell, also under continuous flow. As the analyte binds to the ligand, the accumulation of protein on the surface results in an increase in the refractive index. This change in refractive index is measured in real time, and the result plotted as response or resonance units (RUs) versus time (a sensorgram). Importantly, a response (background response) will also be generated if there is a difference in the refractive indices of the running and sample buffers. This background response must be subtracted from the

## DESCRIPTION OF THE TECHNIQUES

sensorgram to obtain the actual binding response. The background response is recorded by injecting the analyte through a control or reference flow cell, which has no ligand or an irrelevant ligand immobilized to the sensor surface. By effectively adding a third dimension to the surface, much higher levels of ligand immobilisation are possible.

### 10.2 Optical Tweezers

Optical Tweezers use light to manipulate microscopic objects as small as a single atom. The radiation pressure from a focused laser beam is able to trap small particles. The optical forces exerted on a particle originate from the momentum change of the photons impinging on the particle. These forces have traditionally been decomposed into two components: gradient force and scattering force.<sup>95</sup> The scattering force acts, for a symmetric beam, in the propagation direction of the beam. The gradient force, in case of a particle with a refractive index greater than that of the surrounding medium, is directed towards the region of highest light intensity.

For a spherical particle with refractive index  $n_p$  greater than that of the surrounding medium ( $n_m$ ), the action of two parallel beams ( $K$  and  $L$ ) with different intensities ( $K > L$ ), both of which becoming refracted and therefore giving rise to a force ( $F$ ), will result in the generation of an asymmetric net force (Figure 10.2.1A). As a result, the particle is propelled toward regions of greater light intensity. In the case of converging light rays ( $M$  and  $N$ ), as near a focal point of a microscopy objective lens (Figure 10.2.1B), the net force points in a direction parallel with the optical axis. Depending on the position of the bead relative to the focal point, however, the net force may point down or up (Figure 10.2.1B) the optical axis. In the balance of gradient and scattering forces the particle may become stably trapped. Stable trapping will occur if the potential well defined by the optical trap is deep enough compared

---

<sup>95</sup> Ashkin, A.; Dziedzic, J.M.; Bjorkholm, J.E.; Chu, S. *Optics Lett*, **1986**, 11(5), 288-290.



## DESCRIPTION OF THE TECHNIQUES

with the thermal energy of the particle. The geometry depicted in Figure 10.2.1B forms the basis of the most commonly used single-beam optical tweezers.

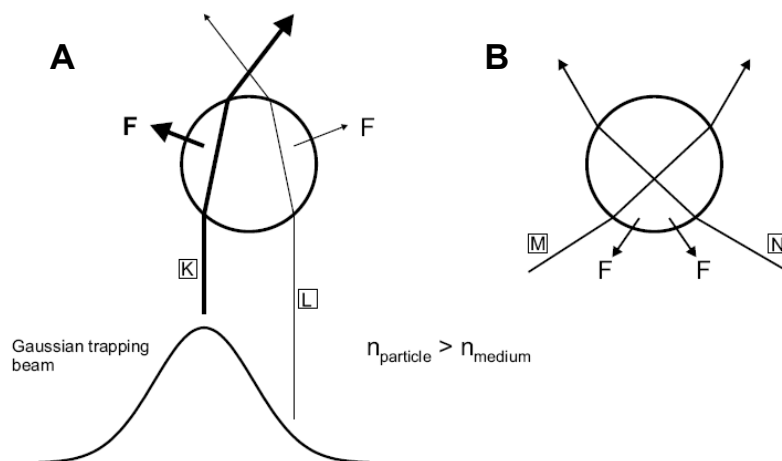


**Figure 10.2.1.** Schematics of the geometrical optics description of gradient force for a particle with an index of refraction greater than that of the medium. (A) For a lateral intensity gradient, the resulting force, due to the refraction of the light at the interface, has a component toward the greater intensity. (B) In a focused laser beam, the axial force propels the particle toward the focal point.

The potential well defined by the optical trap can be thought of as a spatially-defined virtual spring with a stiffness (spring constant) of  $\kappa$ . The force acting on the particle can then be written as

$$\vec{F} = -\kappa\Delta\vec{x},$$

where  $\Delta x$  is the displacement of the particle from the trap center. Thus, if we know the trap stiffness, measuring bead position allows the determination of the force acting on the bead. With a  $\sim 10$  nm position measurement accuracy of microscope image processing techniques and  $\sim 0.1$  pN/nm stiffness of common optical tweezers,  $\sim 1$  pN force resolution may be reached. By using more sophisticated position sensing methods, the force resolution may be increased further. Bead position may be measured with high precision by using quadrant

## DESCRIPTION OF THE TECHNIQUES

photodetectors.<sup>96</sup> Another simple method is projecting the position – in the condenser back focal plane – of the trapping laser, after it has left the optical trap, onto a position-sensing photodiode.<sup>97</sup> These approaches yield sub-piconewton force resolution. Considering that the changes in the laser-beam trajectory evoked by interaction with the trapped bead reflect the changes in light momentum, by measuring the position of the laser beam after it has left the trap allows, in principle for a direct measurement of force (Figure 10.2.2).<sup>98</sup>

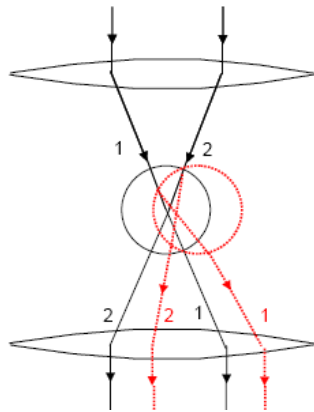


**Figure 10.2.2.** *Measuring the force on a trapped bead. When a bead is moved from the trap centre due to an external force, the trapping laser beam is deflected. If the input aperture of the objective is underfilled in a dual-beam optical tweezers instrument, this deflection can be directly measured using a position-sensitive photodiode detector.*

In this arrangement all the photons entering the trap must be collected after they have left the trap and deviated from the optical axis, the objective lens back aperture needs to be underfilled with the laser beam. On the other hand, a major advantage of this arrangement is that the often tedious trap stiffness procedures can be avoided. In this thesis such a dual-beam counter-

---

<sup>96</sup> Finer, J.; Simmons, R.; Spudich, J. *Nature*, **1994**, 368, 113-119.

<sup>97</sup> Ghislain, L.P.; Switz, N.A.; Webb, W.W. *Rev Int Instrum*, **1994**, 65(9), 2762-2768.

<sup>98</sup> (a) Smith, S.B.; Cui, Y.; Bustamante, C. *Methods Enzymol*, **2003**, 361, 134-62. (b) Smith, S.B.; Cui, Y.; Bustamante, C. *Science*, **1996**, 271(5250), 795-799.

propagating optical tweezers instrument that functions as a light-momentum sensor was used.

### 10.3 AC Voltammetry

Alternating current (AC) voltammetry is a frequency-domain technique that involves the superimposition of a small-amplitude AC voltage on a linear ramp (Figure 10.3). The alternating potential, usually, has a frequency of 50-100 Hz and an amplitude of 10-20 mV. The AC signal thus causes a perturbation in the surface concentration, around the concentration maintained by the DC potential ramp. The resulting AC current is displayed versus the potential. The detection of AC component allows to separate the contributions of the faradaic and charging currents. The former is phase shifted  $45^\circ$  relative to the applied sinusoidal potential, while the background component is  $90^\circ$  out of phase. The current is recorded as a function of time. Since the potential also varies with time, the results are usually reported as the potential dependence of current, or plots of  $I$  vs.  $E$ , hence the name voltammetry.

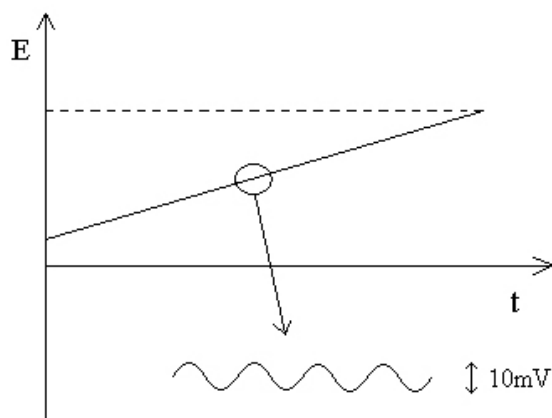


*Figure 10.3. Potential-time waveform used in AC voltammetry.*

## DESCRIPTION OF THE TECHNIQUES

### 10.4 Cyclic Voltammetry

Cyclic voltammetry is the most widely used technique for acquiring qualitative information about electrochemical reactions. The efficacy of cyclic voltammetry results from its ability to rapidly provide considerable information on the thermodynamics of redox processes, on kinetics of heterogeneous electron-transfer reactions, and on coupled chemical reactions or adsorption processes. Cyclic voltammetry consists of scanning linearly the potential of a stationary working electrode, starting from an initial potential  $E_i$  to a final potential  $E_f$ , using a triangular potential waveform (Figure 6.12). Depending on the information sought, single or multiple cycles can be used. During the potential sweep, the potentiostat measures the current resulting from the applied potential.

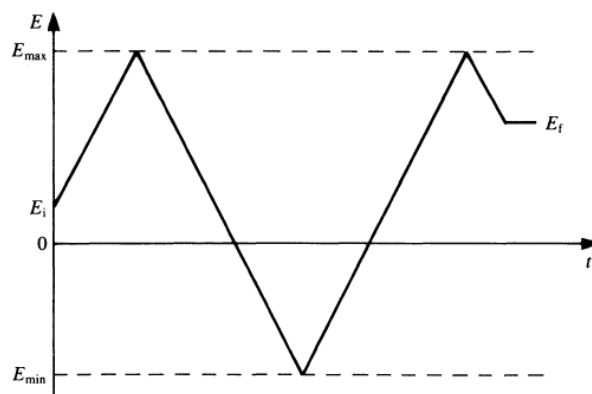


**Figure 10.4.** Potential-time signal in cyclic voltammetry.

The characteristic peaks in the cyclic voltammogram are caused by the formation of the diffusion layer near the electrode surface, generating different process (reversible, irreversible or quasi-reversible).

The electron transfer reaction  $O + ne^- \rightarrow R$  can be considered with only O initially present in solution. Therefore the initial sweep direction must be negative.

A faradaic current,  $I_f$ , depends on the kinetics and transport by diffusion of the electroactive species, is registered in the relevant zone of applied potential

## DESCRIPTION OF THE TECHNIQUES

where electrode reaction occurs. There is also a capacitive contribution: on sweeping the potential the double layer charge changes; this contribution increases with increasing sweep rate. The total current is:

$$I = I_c + I_f = C \, dE/dt + I_f$$

In absence of faradaic process, such as the case of lipidic monolayers on mercury, the current is purely capacitive; therefore:

$$I = \frac{dQ}{dt} = C \frac{dE}{dt}$$

Because of  $dE/dt$  represents the scan velocity, it has obtained

$$I = C \cdot v$$

As a consequence, cyclic voltammogram has a diagram reflecting trend of differential capacity. Moreover, based on Ohm's Law  $V = i \cdot R$ , it is possible to calculate the inclination of cyclic voltammogram, that is  $1/R$ .

### 10.5 Electrochemical impedance spectroscopy

Electrochemical Impedance Spectroscopy (EIS) represents a powerful technique for the characterization of biological systems. Although, in recent years, EIS has found widespread applications in the field of characterization of materials, it results a suitable technique for the investigation of diffusion of ions across membranes.

In a typical impedance spectral measurement, a small amplitude sinusoidal voltage is applied between two electrodes at successive frequencies and the current response is measured. A low amplitude sine wave ( $\Delta E \sin \omega t$ ), of a particular frequency, is superimposed on the dc polarization voltage  $E_0$ . This results in a current response of a sine wave  $\Delta I \sin(\omega t + \Phi)$  superimposed on the dc current  $I_0$ . The current response is shifted with respect to the applied potential.

The frequency-dependent impedance  $Z$  is usually described by complex numbers, whose real and imaginary parts are derived from the currents in

## DESCRIPTION OF THE TECHNIQUES

phase and  $90^\circ$  out of phase with the applied ac voltage, respectively. An impedance spectrum can often be fitted by an equivalent electrical circuit composed of resistors and capacitors.

The relationship between the applied potential and the current flow is known as the impedance, which is analogous to the resistance-current-potential relationship of a dc circuit. The impedance ( $Z$ ) has a magnitude ( $\Delta E/\Delta i$ ) and phase ( $\varphi$ ) and is thus a vector quantity.

If a sinusoidal potential is applied across a pure resistance of magnitude  $R$ , then the magnitude of the impedance  $Z = R$  and the phase  $\varphi = 0$  for all frequencies. This is shown on a plot of the real and imaginary components as a point on the real axis overleaf.

## Abbreviations

Ab: antibody;

Ac: Acetyl;

Ag: Antigen;

APC: Antigen presenting cell;

BLM: bilayer lipid membrane;

Bn: Benzyl;

Boc: tert-butoxycarbonyl;

CNS: Central Nervous System

DCM: dichloromethane;

DIPEA: diisopropylethylamine;

DMF: N,Ndimethylformamide;

DMS: dimethylchlorosilane;

DOPC: dioleoyl phosphatidylcholine;

DPhyPC: diPhytanyl phosphatidyl coline;

DPTL: 2,3-di-O-phytanyl-sn-glycerol-tetraethyleneglycol-lipoic acid ester lipid;

EIS: electrochemical impedance spectroscopy;

ELISA: enzyme-linked immunosorbent assay;

FCC: flash column chromatography;

FCS: fetal calf serum;

FIA: fluorescence immunoassay;

Fmoc: 9-H-fluoren-9-ylmethoxycarbonyl;

GBS: Guillian Barré syndrome;

HMDE: hanging drop mercury electrode;

HOBt: 1-hydroxybenzotriazole;

HPLC: high performance liquid chromatography;

Ig: immunoglobulin (IgE, IgG, etc.);

MHC: major histocompatibility complex;

## ABBREVIATIONS

MOG: myelin oligodendrocyte glycoprotein;  
MRI: Magnetic Resonance Imaging;  
MS: Multiple Sclerosis;  
MW: microwaves;  
NBD's: Normal Blood Donors;  
NMM: N-methyl morpholine;  
NMR: nuclear magnetic resonance;  
OT: Optical tweezers;  
PBS: phosphate buffered saline;  
PEG: polyethylene glycol;  
Pfp: pentafluorophenyl;  
Ph: phenyl;  
psBLM: polymer-supported bilayer lipid membranes;  
RA: Rheumatoid Arthritis;  
RIA: radioimmunoassay;  
SPE: solid phase extraction;  
SPPS: solid phase peptide synthesis;  
SPR: Surface plasmon resonance;  
ssBLM: solid supported bilayer lipid membranes;  
SSM: solid supported membrane;  
TBAT: Tetrabutylammonium Triphenyldifluorosilicate;  
tBLM: tethered bilayer lipid membranes;  
TBTU: 2 - (1H-benzotriazole-1-yl) - 1,1,3,3 - tetramethyluronium tetrafluoroborate;  
tBu: tert-butyl;  
TCR: T-cell receptor;  
TFA: trifluoroacetic acid;  
THF: tetrahydrofuran;  
TLC: Thin layer chromatography.  
TMS-N<sub>3</sub>: trimethylsilyl azide.



*Understanding Biology Using Peptides*  
Sylvie E. Blondelle (Editor)  
American Peptide Society, 2005

## **Does an Aberrant Glucosylation Trigger Autoimmunity in Multiple Sclerosis?**

**Francesca Nuti, Ilaria Paolini, Elisa Peroni, Feliciano Real-Fernández, Marta Pazzagli, Maria C. Pozo-Carrero, Francesco Lolli, Mario Chelli, Paolo Rovero and Anna M. Papini**

*Laboratory of Peptide & Protein Chemistry & Biology, Polo Scientifico, University of Florence, I-50019 Sesto Fiorentino (FI), Italy*

### **Introduction**

Glycoproteins are ubiquitous in all forms of life from bacteria to humans and are involved in immune response. In fact the presence of carbohydrates in proteins provides unique epitopes for molecular recognition.

In the literature there are many examples demonstrating that a loss or change in glycosylation of proteins and/or glycolipids (glycosylation defects) are often associated with a large number of autoimmune disorders [1], such as Multiple Sclerosis (MS) [2-4].

Very recently, we reported that auto-antibodies in MS can be recognized as biomarkers only using the glucosylated antigenic probe CSF114(Glc) [4]. The corresponding native antigen has not been yet characterized.

### **Results and Discussion**

It is well known that natural *N*-glycoproteins are heterogeneous, but share the typical core formed by a  $\beta$ -*N*-acetylglucosamine linked to an Asn side chain ( $\beta$ -GlcNA<sub>sn</sub>), that is the putative first glycosylated moiety. Up to now, only one example of novel forms of *N*-glycoproteins have been recognized. In particular a  $\beta$ -D-glucose was unequivocally demonstrated to be linked to the Asn side chain in *Halobacterium halobium* cross-reacting with the laminin glycoprotein [5-6]. Moreover, in our laboratory we demonstrated that Asn(Glc) in the glycopeptide CSF114(Glc) is fundamental for auto-antibody recognition in MS [4,7].

In *N*-glycoproteins, the Asn glycosylation site is always located in the specific amino acid sequence Asn-Xaa-Ser/Thr (sequon). With the aim of identifying the native glycoprotein myelin auto-antigen recognized by CSF114(Glc), and possibly related to the pathogenesis of MS, we undertook a deductive approach to rule out sequons.

As a proof of concept, among the 19 x 2 tripeptides, we started synthesizing the ones containing Xaa = Gly or Lys. In particular, N(Glc)GS (**1**), N(Glc)GT (**2**), N(Glc)KS (**3**), and N(Glc)KT (**4**), as well as N(Glc)GH (**5**), N(Glc)KH (**6**), derived from the original glucosylated core of CSF114(Glc), and N(Glc)AT (**7**), present in [Asn<sup>31</sup>(Glc)]hMOG(30-50) [8]. All tripeptides were acetylated and synthesized as amides, to mimic auto-Ab binding sites (Table 1).

The anti-CSF114(Glc) antibody titer to the glycopeptides was evaluated by inhibition ELISA. Most of the glucosylated sequons inhibit anti-CSF114(Glc) antibodies independently from the Xaa-amino acid. These results let us to formulate a hypothesis on the molecular mechanism of the recently characterized auto-antibody mediated MS pattern: an aberrant glucosylation on Asn residues of myelin proteins creates neoantigens triggering the autoimmune response. Thus, randomly

## SUPPLEMENTARY MATERIAL

Table 1. Glucosylated tripeptides

Glucosylated core peptide	Sequence
Glycoprotein consensus sequence	Ac-N(Glc)GS-NH <sub>2</sub> (1); Ac-N(Glc)GT-NH <sub>2</sub> (2); Ac-N(Glc)KS-NH <sub>2</sub> (3); Ac-N(Glc)KT-NH <sub>2</sub> (4).
CSF114(Glc)	Ac-N(Glc)GH-NH <sub>2</sub> (5) Ac-N(Glc)KH-NH <sub>2</sub> (6)
[Asn <sup>31</sup> (Glc)]hMOG(30-50)	Ac-N(Glc)AT-NH <sub>2</sub> (7)

glucosylated myelin proteins will be recognized as non-self antigens, and CSF114(Glc) may be a mimetic of all aberrantly glucosylated myelin proteins.

### Acknowledgments

We thank Fondazione Ente Cassa di Risparmio di Firenze and the Travel Award Committee for the financial support to the participation of F. Nuti at 19th APS.

### References

1. Saso, L., *et al. Inflammation* **17**, 465-479 (1993).
2. Orlacchio, A., *et al. J. Neurological Sci.* **151**, 177-182 (1997).
3. Demetriou, M., *et al. Nature* **409**, 733-739 (2001).
4. Lolli, F., *et al. Proc. Natl. Acad. Sci. USA* **102**, 10273-10278 (2005).
5. Schreiner, R., *et al. J. Cell. Biol.* **124**, , 1071-1074 (1994).
6. Wieland, F., *et al. Proc. Natl. Acad. Sci. USA* **80**, 5470-5473 (1983).
7. Papini, A. M., *et al. Nat. Med.* **11**, 13 (2005).
8. Mazzucco, S., *et al. Bioorg. Med. Chem. Lett.* **9**, 167-172 (1999).

*Peptides for Youth*  
Emanuel Escher, William D. Lubell, Susan Del Valle (Editors)  
American Peptide Society, 2007

## **Synthesis Of Organometallic Glycopeptides And Electrochemical Studies To Detect Autoantibodies In Multiple Sclerosis Patients' Sera.**

**Feliciana Real-Fernández<sup>1</sup>, Amélie Chamois-Colson<sup>2</sup>, Jérôme Bayardon<sup>2</sup>, Francesca Nuti<sup>1</sup>, Elisa Peroni<sup>1</sup>, Maria R. Moncelli, Rita Meunier-Prest<sup>2</sup>, Sylvain Jugè<sup>2</sup> and Anna Maria Papini<sup>1</sup>**

<sup>1</sup>Laboratory of Peptide & Protein Chemistry & Biology, Polo Scientifico, University of Florence, I-50019 Sesto Fiorentino (FI), Italy; <sup>2</sup>Laboratoire de Synthèse et d'Electrosynthese Organometalliques (LSEO), Université de Bourgogne, 21068, Dijon, France

### **Introduction**

Measurement of disease specific biomarkers, such as antibodies, is an important tool for diagnosis, follow-up, and prevention of autoimmune diseases. Identification of autoantibodies is achieved up to now using native protein antigens in immunoenzymatic assays. Unfortunately, in autoimmune diseases only very low specific antibodies are detected in serum, possibly because protein antigens used in the assays contain more than one epitope, of which only few are involved in the disease. Moreover, the use of recombinant protein antigens doesn't allow reproduction of aberrant post-translational modifications (PTMs) involved in triggering autoantibodies. These observations prompted us to set up an innovative "chemical reverse approach" to select specific synthetic peptide antigens containing the minimal epitope with the correct PTM to fishing out specific biomarkers in biological fluids [1].

As a proof-of-concept, we have recently developed CSF114(Glc), a structure-based designed glycosylated peptide as the first Multiple Sclerosis Antigenic Probe (MSAP) [2], accurately measuring high affinity autoantibodies in sera of a statistically significant patients' population [3]. The ELISA diagnostic/prognostic test MSPepKit [4], based on CSF114(Glc), has been developed to recognize specific autoantibodies in MS patients' sera and follow up disease activity [5].

The aim of our study is to evaluate the specificity and sensitivity of Cyclic Voltammetry (CV) measurements in the analysis of antibody profiles in MS patients' sera, possibly improving detection of a panel of antibodies as specific biomarkers for different forms of the disease. Development of sensitive, quantitative, and specific electrochemical devices, based on a simple, rapid, and reproducible protocol, can dramatically improve the sensitivity of the traditional immunoassays (e.g. ELISA).

### **Results and Discussion**

In this context, our MSAP CSF114(Glc) has been properly modified in N-terminus with new organometallic amino acids as "Electrochemical Probes" to perform CV measurements in solution and/or grafting peptides on a gold electrode. A small library of organometallic glycopeptides was synthesized modifying CSF114(Glc) and the corresponding unglucosylated sequence with a series of specifically designed organometallic amino acids (Fig. 1).

We tested MS patients' sera and Normal Blood Donors' sera (NBDs) in ELISA and competitive ELISA versus the modified peptides. CSF114(Glc) modified with organometallic amino acid **1**, **2**, or **3** is always able to detect and inhibit autoantibodies in MS patients' sera. Therefore, the autoantibody recognition is not

## SUPPLEMENTARY MATERIAL

affected by these modifications. On the other hand, all the peptides are not able to detect any antibody titre in NBDs' sera.

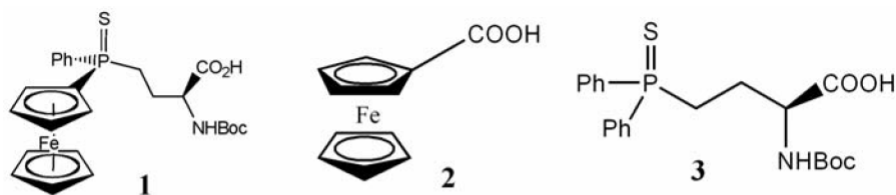


Fig. 1. Organometallic amino acids.

The glycopeptides were used on gold electrodes covered with a proper polymer monolayer of mercaptoundecanoic acid, to perform CV measurements in the presence of antibodies. An increase in intensity of the current (faradic and capacitive) and a shift to more positive potentials have been observed after addition of purified anti-CSF114(Glc) antibodies in a saline solution of the glycopeptide modified with the amino acid **2**.

The same behaviour was observed in the case of the glycopeptide modified with the amino acid **1** (including characteristics of both amino acids **2** and **3**). Moreover, the presence of thiophosphine function in the N-terminus allows glycopeptide immobilization on the gold electrode. CV measurements grafting the glycopeptide antigen directly on the gold electrode showed similar electrochemical response both in solution and on the electrode surface.

The new peptides containing unnatural amino acid **1** or **2** were able to detect specific anti-CSF114(Glc) antibodies in CV. Moreover, thanks to the presence of thiophosphine, CSF114(Glc) modified with **1** was able to build simple monolayers on gold surfaces. The possibility of grafting synthetic probes directly on the electrode surface will enable to obtain innovative strategies to develop new and more reliable techniques for antibody detection and quantitative determination.

### Acknowledgments

PAI Galilée N°11686QA (2006), FIRB Internalization 2005-2008 RBIN04TWKN, MIUR (Italy), Ente Cassa Risparmio di Firenze and 20th APS travel grant committee are gratefully acknowledged

### References

- 1 Lolli F, Rovero P, Chelli M, Papini AM, *Expert Rev. Neurotherapeutics*, **6** (5), 781-794, 2006
- 2 Lolli F, Mulinacci B, Carotenuto A, Bonetti B, Sabatino G, Mazzanti B, D'Ursi AM, Novellino E, Pazzagli M, Lovato L, Alcaro MC, Peroni E, Pozo-Carrero MC, Nuti F, Battistini L, Borsellino G, Chelli M, Rovero P, Papini AM. *Proc Natl Acad Sci U S A.*, **102** (29) 10273-8, 2005.
- 3 Carotenuto A., D'Ursi A. M., Mulinacci B., Paolini I., Lolli F., Papini, A. M., Novellino E., Rovero P., *A. J. Med. Chem.*, **49**, 5072-5079, 2006.
- 4 Papini, A.M. et al. *Nat. Med.*, **11**, 13, 2005.
- 5 Papini, A.M., Rovero P. Chelli M.; Lolli F., Granted U.S.A. Patent & PCT Application WO 03/000733 A2.

## Ferrocenyl Glycopeptides as Electrochemical Probes to Detect Autoantibodies in Multiple Sclerosis Patients' Sera

Feliciana Real-Fernández,<sup>1,2</sup> Amélie Colson,<sup>3</sup> Jérôme Bayardon,<sup>3</sup> Francesca Nuti,<sup>1,2</sup>  
Elisa Peroni,<sup>1,2</sup> Rita Meunier-Prest,<sup>3</sup> Francesco Lolli,<sup>1,4</sup> Mario Chelli,<sup>1,2</sup>  
Christophe Darcel,<sup>3</sup> Sylvain Jugé,<sup>3</sup> Anna Maria Papini<sup>1,2</sup>

<sup>1</sup>Laboratory of Peptide and Protein Chemistry and Biology, Polo Scientifico e Tecnologico, University of Florence, Italy

<sup>2</sup>Department of Organic Chemistry "Ugo Schiff" and CNR ICCOM, Via della Lastruccia 13, University of Florence, Sesto Fiorentino (FI) I-50019, Italy

<sup>3</sup>Institut de Chimie Moléculaire (ICMUB, UMR CNRS 5260), University of Burgundy, Dijon 21078, France

<sup>4</sup>Department of Neurological Sciences and Azienda Ospedaliera Careggi, Viale Morgagni 34, University of Florence, Firenze I-50134, Italy

Received 5 December 2007; revised 24 January 2008; accepted 31 January 2008

Published online 13 February 2008 in Wiley InterScience (www.interscience.wiley.com). DOI 10.1002/bip.20955

### ABSTRACT:

Glycopeptide analogues of CSF114(Glc), modified at *N*-terminus with new ferrocenyl carboxylic acid and a new ferrocenyl- $\beta$ -thiophosphino amino acid, were used to implement a new electrochemical biosensor for autoantibody detection in multiple sclerosis. The ferrocenyl moiety of these "electrochemical probes" did not affect autoantibody recognition both in SP-ELISA and in inhibition experiments. By electrochemical monitoring the interactions of the modified peptides Fc-CSF114(Glc) and 4-FcPhP(S)Abu-CSF114(Glc) with the autoantibodies, we demonstrated that autoantibodies could be detected with a sensitivity comparable to ELISA method. The new electrochemical probes can be proposed to characterize autoantibodies as biomarkers of multiple sclerosis by a simple, rapid, and reproducible cyclic voltammetry-based

diagnostic methodology. © 2008 Wiley Periodicals, Inc.

*Biopolymers (Pept Sci)* 90: 488–495, 2008.

**Keywords:** glycopeptides; ferrocenyl amino acids; biomarkers; diagnostics; electroanalytical methods

This article was originally published online as an accepted preprint. The "Published Online" date corresponds to the preprint version. You can request a copy of the preprint by emailing the *Biopolymers* editorial office at [biopolymers@wiley.com](mailto:biopolymers@wiley.com)

### INTRODUCTION

Autoimmune disorders have a high social impact, affecting mainly young adults and in particular women. Clinical evaluation of autoimmune diseases can require several years before it can be definitively ascertained. Both genetic predisposition and environmental factors could play a synergistic role in the autoimmune diseases. Most of them are characterized by relapsing-remitting forms and adequate therapies should be used early in the disease course and during flares, to prevent chronic damages. Thus, reliable assays are necessary not only for an early diagnosis but also for monitoring the disease activity by evaluating the antibodies, as specific biomarkers, for diagnosis, follow-up, and prevention of the autoimmune disease.<sup>1,2</sup> The autoantibody fluctuation with disease exacerbations or remissions, makes their detection extremely valuable in the follow up of patients.<sup>3</sup> Therefore, quantitative and qualitative measurements of autoantibodies are crucial in the

Correspondence to: Anna Maria Papini, Laboratory of Peptide and Protein Chemistry and Biology, Department of Organic Chemistry "Ugo Schiff" University of Florence, Via della Lastruccia, 13, Sesto Fiorentino (FI) I-50019, Italy; e-mail: [annamaria.papini@unifi.it](mailto:annamaria.papini@unifi.it); or S. Jugé and R. Meunier-Prest, Institut de Chimie Moléculaire de Bourgogne (ICMUB), UMR CNRS 5260, University of Burgundy 9 av. A. Savary, BP 47870, Dijon 21078, France; e-mail: [sylvain.juge@u-bourgogne.fr](mailto:sylvain.juge@u-bourgogne.fr), [rita.meunier-prest@u-bourgogne.fr](mailto:rita.meunier-prest@u-bourgogne.fr)  
© 2008 Wiley Periodicals, Inc.

management of autoimmune disorders, particularly in the development and clinical evaluation of personalized therapeutic treatments.

To help clinicians to follow up patients by a simple blood test detecting autoantibodies two different problems have to be solved, such as: (1) selection of the antigen recognizing specific autoantibodies in a statistically significant number of patients (sensitivity) as compared to other autoimmune diseases and normal controls; (2) selection of the diagnostic technique to detect autoantibodies ["enzyme-linked immunosorbent assay" (ELISA), radioimmunoassay, immunofluorescence, SPR, etc.].

Till now, identification of autoantibodies is achieved using native protein antigens in ELISA. Unfortunately, in autoimmune diseases only very low specific antibodies were detected in serum, possibly because native protein antigens used in the assays contain more specific epitopes for different autoantibodies. Moreover, the use of recombinant protein antigens does not allow replication of possible aberrant modifications (sugars, lipids, citrullines, etc.), involved in triggering an autoantibody response. In fact, it is generally accepted that these modifications can alter the function and immunogenicity of protein/peptide antigens and growing evidences indicate that post-translational modifications, either native or aberrant, may play a fundamental role for specific autoantibody recognition in autoimmune diseases.<sup>4</sup> These observations account, at least in part, for the limited success get in the discovery of biomarkers for autoimmune disorders using proteomic analysis and/or protein microarrays. For that reason we have decided to develop and optimize new synthetic peptides as antigenic probes for fishing out autoantibodies from biological fluids as biomarkers using an innovative "chemical reverse approach." "Reverse" because the screening of the synthetic antigenic probe is guided by autoantibodies circulating in blood and "chemical" because autoantibody recognition drives selection and optimization of the "chemical" structure by defined peptide libraries.

The screening of focused libraries of modified peptides has to lead to the optimized peptide antigen containing the minimal epitope with the correct modification to detect at the best autoantibodies specific of the autoimmune disease under investigation.<sup>5</sup> As a proof-of-concept, in the case of rheumatoid arthritis (RA) several aberrant modifications of proteins (such as Arg deimination and/or methylation) have been associated with pathogenesis and lead to different modified autoantigens used in simple ELISA.<sup>4</sup> A key step in setting up the commercially available ELISA for RA was represented by identification of deiminated sequences of filaggrin that are recognized by a high percentage of RA sera.<sup>6,7</sup> Sensitivity of the assay was increased modifying the peptide structure to optimally expose the citrulline moiety. In fact, a

cyclic citrullinated peptide allows detection of antibodies in up to 70% of RA patients.<sup>8,9</sup> This ELISA is now considered a gold standard for RA diagnosis and follow up.

In the case of multiple sclerosis (MS), one of the most known inflammatory neurological diseases of the central nervous system (CNS), patients accumulate myelin lesions, but also axonal loss, which lead to permanent neurological dysfunctions. Magnetic resonance imaging (MRI) is up to now the most reliable technique to help clinicians not only in diagnosis, but also in prognosis because no standard simple immunoassays are available. However, it is evident that MRI cannot be considered a routine technique and that efficient autoantibodies detection is a useful signal of disease progression when the clinical symptoms are not still visible to guide a targeted MRI checkup.<sup>10</sup>

In previous studies, we developed for the first time the glycopeptide CSF114(Glc), a structure-based designed glucosylated peptide as the first MS Antigenic Probe (MSAP),<sup>11,12</sup> accurately measuring high affinity autoantibodies in sera of a statistically significant patients' population.<sup>13</sup> The glycopeptide is characterized by a  $\beta$ -hairpin structure bearing the minimal epitope (a  $\beta$ -D-glucopyranosyl moiety linked to an Asn residue on the tip of the turn probably reproducing an aberrant N-glycosylation of myelin) fundamental for autoantibody recognition.<sup>14-16</sup>

ELISA diagnostic/prognostic test MSPepKit,<sup>17</sup> based on CSF114(Glc), has been developed to recognize specific autoantibodies in MS patients' sera and follow up disease activity.<sup>18</sup> ELISA offers advantages, such as allowing simultaneous analyses of a large number of samples. To avoid nonreproducible or noninterpretable results due to operator-dependent procedures, industry requires not only a fast, but also a sensitive and more consistent technique, in particular for quantitative determination of autoantibodies.

Electrochemistry, as detection technique of biological and clinical assays, can shorten the time of the analyses and increase the reliability of the assays.

## RESULTS AND DISCUSSION

To implement a new electrochemical technique for autoantibody recognition in MS, we used CSF114(Glc) analogues properly modified at N-terminus with new ferrocenyl derivatives (see Figure 1) as "electrochemical probes" to be used in cyclic voltammetry measurements in solution and/or grafting peptides on a gold electrode.

Availability of a large variety of ferrocenyl derivatives and their favorable electrochemical properties (undergoing a reversible oxidation in aqueous solution) have made ferrocene and its derivatives very trendy molecules for biological applications and for conjugation with biomolecules.<sup>19</sup> Therefore, ferrocenyl derivatives are a new class of linkers useful for

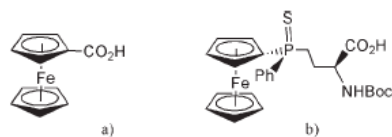


**FIGURE 1** Structure of ferrocenyl derivatives used for SPPS. a) Ferrocenyl carboxylic acid [Fc-COOH] and b) (S,S)-(+)-2-(tert-butoxycarbonylamino)-4-(ferrocenylphenylthiophosphino)butanoic acid [4-FcPhP(S)Abu].

electrochemical and optical biodetections. In this context, we selected ferrocenyl carboxylic acid and a new ferrocenyl-thiophosphine derivative of  $\alpha$ -aminobutyric acid (see Figure 1) as biosensors.

The electrochemical properties of ferrocene, coupled to thiophosphine ability to build simple monolayers on gold surfaces, allow peptides anchoring on the working electrode used for detection. The possibility of grafting the synthetic probe directly on the electrode surface will enable to obtain an innovative strategy to develop new techniques for antibody detection opening strategies in the analysis of antibody profiles in MS patients' sera, possibly improving detection of a panel of antibodies as specific biomarkers for different forms of the disease.

### Labeled Peptide Synthesis

A collection of labeled peptides was prepared by solid phase peptide synthesis (SPPS) using the Fmoc/tBu strategy (Table I). The novel ferrocenyl peptides were synthesized modifying CSF114(Glc) sequence TPRVERN(Glc)GHSVFLAPYGWMVK and the corresponding unglucosylated one TPRVERNHSVFLAPYGWMVK, at the N-terminus with the designed ferrocenyl derivatives (see Figure 1). The amino group of 4-FcPhP(S)Abu was Boc protected and the carboxylic acid of both derivatives was free to be used directly in SPPS.

Only few studies are reported on the solid-phase synthesis of organometallic derivatives of peptides. In fact, decomposi-

tion of organometallic peptides and secondary products of SPPS usually affects final yields.<sup>20</sup> Because microwave technology is proposed as a valid support for enhancement of efficiency of coupling reactions in SPPS, we applied this strategy to synthesize the peptide sequences using a microwave assisted automatic solid-phase peptide synthesizer. Microwave technology decreases chain aggregation during the syntheses, improves the coupling rates, and prevents side reactions in difficult peptide sequences.<sup>21</sup>

Ferrocenyl carboxylic acid and the Boc-protected organometallic amino acid 4-FcPhP(S)Abu (see Figure 1) were introduced at the N-terminus of the resin-bound glycopeptide I and peptide I' to obtain the peptide collection reported in Table I.

The metallocene moieties were demonstrated to be stable during Fmoc-deprotection, cleavage, and in the deacetylation conditions (pH 12) requested for deprotection of the hydroxyl groups of the sugar. However, the final ferrocenyl peptides could be safely obtained when phenol rather than water was used as scavenger in the final cleavage mixture for resin and amino acid side chains deprotection.<sup>20</sup>

All the compounds were analyzed by UPLC-ESIMS and HPLC-ESIMS and purified by RP-HPLC (>95%) to be used for autoantibody detection.

### Immunoenzymatic Assays

The glycopeptide CSF114(Glc) (I), designed as a type I'  $\beta$ -tumor around the minimal epitope Asn(Glc), guarantees an optimal exposure of the epitope for antibody recognition in the solid-phase conditions of the ELISA plate on sera of MS patients. In fact, the CSF114(Glc)-based ELISA allows to recognize both IgM and IgG in sera of 30% of MS patients.<sup>13</sup>

We evaluated, by ELISA, serum antibodies (IgM and IgG class) to the new organometallic peptides and glycopeptides (Table I) in a group of MS patients and compared the results with normal blood donors' sera (NBDs). IgM and IgG

**Table I** Analytical Data from Ultra Performance Liquid Chromatography (UPLC)

Peptide Name	R <sub>t</sub> (min)	RP-HPLC Preparative Gradients of B	Calculated Mass	Observed Mass [M+2H] <sup>2+</sup>
CSF114(Glc) (I)	2.07 <sup>a</sup>	28–30% in 30 min	2606.3	1303.6
Fc-CSF114(Glc) (II)	1.872 <sup>b</sup>	35–70% in 20 min	2820.2	1411.2
4-FcPhP(S)Abu-CSF114(Glc) (III)	1.833 <sup>b</sup>	25–50% in 20 min	3015.5	1508.3
CSF114 (I')	1.96 <sup>a</sup>	28–30% in 30 min	2444.2	1222.6
Fc-CSF114 (II')	1.813 <sup>b</sup>	25–50% in 20 min	2655.3	1329.8
4-FcPhP(S)Abu-CSF114 (III')	1.863 <sup>b</sup>	35–70% in 20 min	2853.5	1427.4

Gradients at 0.45 ml min<sup>-1</sup>. (Solvent system, A: 0.1% TFA in H<sub>2</sub>O, B: 0.1% TFA in CH<sub>3</sub>CN).

<sup>a</sup> 10–60% B in 3.5 min.

<sup>b</sup> 20–70% B in 3.5 min.

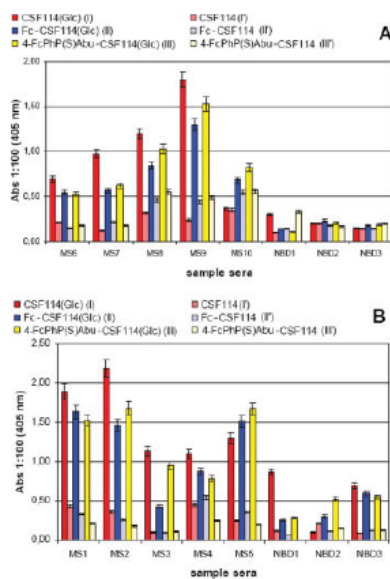


**FIGURE 2** Autoantibody recognition in MS patients' sera and NBDs sera. IgM (A) and IgG (B) classes versus the ferrocenyl glycopeptides (II–III) and the corresponding unglycosylated ones (I'–III') compared to the glycopeptide CSF114(Glc) (I). Data are reported as absorbance at 405 nm of sera diluted 1:100.

responses were detected using as secondary antibodies anti-human IgMs and anti-human IgGs conjugated to alkaline phosphatase.

We compared the antibody recognition to CSF114(Glc) versus the ferrocenyl glycopeptides II and III and the corresponding unglycosylated sequences I'–III' in a first group of patients' sera affected by clinically definite MS using SP-ELISA. It is accepted that the glycopeptide I detects specific antibodies in MS patients' sera.<sup>11</sup> In fact, as we observe in Figure 2, the glycopeptide I presents the highest antibody recognition, but the new ferrocenyl glycopeptides II–III are always able to detect antibodies showing only a relative lower biological recognition. As expected unglycosylated peptides I'–III' are always inactive.

Considering that SP-ELISA reflects essentially the relative affinity, which depends on the exposure of the minimal epitope in the solid phase conditions of the assay, we also investigated the absolute antibody affinity in a competitive ELISA based on inhibition of autoantibodies in solution. In a set of MS positive sera, ferrocenyl glycopeptides II–III inhibited

binding of autoantibodies to I, giving rise to similar inhibition curves. The data of a representative serum (see Figure 3) show that the two modified glycopeptides II and III exhibited equivalent affinity in competitive ELISA, despite the differences of apparent affinity detected in SP-ELISA (see Figure 2). These findings indicated that the new ferrocenyl glycopeptides share an epitope similar to the one presented by I, and the presence of ferrocenyl and/or thiophosphine moiety at the N-terminus does not influence antibody recognition.

Therefore the glycopeptide CSF114(Glc), modified with the ferrocenyl derivatives, is still able to detect and inhibit autoantibodies in MS patients' sera and it cannot detect any antibody titer in NBDs' sera.

**Electrochemical Measurements**

**Grafted Antigen on Gold.** The glucosylated ferrocenyl peptides 4-FcPhP(S)Abu-CSF114(Glc) (III) and the unglycosylated one 4-FcPhP(S)Abu-CSF114 (III') were adsorbed on gold surface to form a self-assembled monolayer (SAM) via

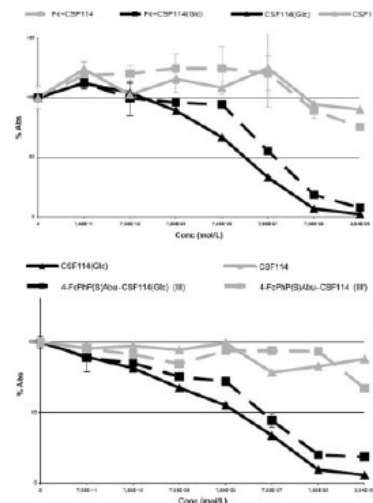


**FIGURE 3** Inhibition curves of anti-CSF114(Glc) IgG Abs with ferrocenyl glycopeptides II–III and with unglycosylated peptides I'–III', in comparison with I in a competitive ELISA. The results are expressed as the percentage of absorbance of a representative MS serum (ordinate axis).



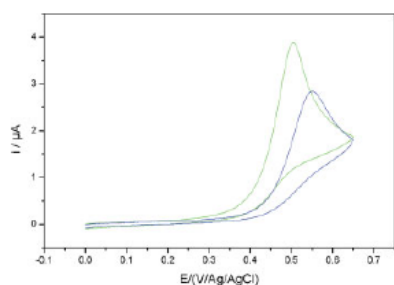


**FIGURE 4** Cyclic voltammetry of Au-III in a tween solution containing  $\text{LiClO}_4$  0.1M and  $\text{Fe}(\text{CN})_6^{4-}$   $9 \times 10^{-4}$  M (green curve) without antibodies and with a solution of purified anti-CSF114(Glc) antibodies at a final dilution of 1:1000 (blue curve). Scan rate 50  $\text{mV s}^{-1}$ .

the sulfur atom. A mixture of 11-mercaptoundecanoic acid and decanethiol was used to block the uncovered surface. The modified electrodes are denoted Au-III for the electrode grafted with III and Au-III' for the electrode grafted with III'. The electrochemical response of the ferrocenyl group was performed by cyclic voltammetry.  $\text{Fe}(\text{CN})_6^{4-}$  was used as catalyst to increase the electrochemical current.<sup>22</sup> Figure 4 shows the electrochemical response of Au-III in a tween solution of  $\text{Fe}(\text{CN})_6^{4-}$ . When a solution of purified anti-CSF114(Glc) antibodies was added, the electrochemical response was shifted towards more positive potentials. The peak potential appeared 46 mV more positive than that of the same solution without antibodies.

When the same experiment was repeated with Au-III', i.e. with the electrode modified by the unglucosylated peptide III', which is not able to recognize autoantibodies in ELISA, the results were completely different (see Figure 5). The electrochemical response of Au-III' did not change significantly after the addition of a solution of purified anti-CSF114(Glc) antibodies. The peak potential was even shifted by few millivolts toward more negative potentials.

**Antigen in Solution.** The detection of interactions between autoantibodies and the ferrocenyl peptides, Fc-CSF114(Glc) (II), i.e. without P=S anchor, was realized in solution. The gold electrode, properly modified with 11-mercaptoundecanoic acid to avoid nonspecific interactions with the biological medium, was introduced in a 0.05% tween 20 solution containing both 0.1 M  $\text{LiClO}_4$  and  $9 \times 10^{-4}$  M  $\text{Fe}(\text{CN})_6^{4-}$  and the ferrocenyl glycopeptide II. Figure 6 shows the cyclic voltammograms before and after addition of anti-CSF114(Glc) antibodies.

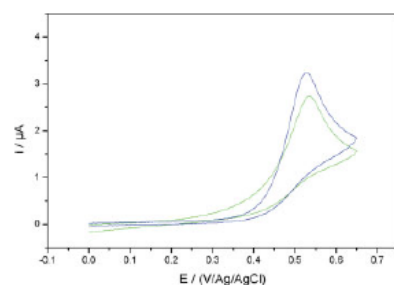


**FIGURE 5** Cyclic voltammetry of Au-III' in a tween solution containing  $\text{LiClO}_4$  0.1M and  $\text{Fe}(\text{CN})_6^{4-}$   $9 \times 10^{-4}$  M (green curve) without antibodies and with a solution of purified anti-CSF114(Glc) antibodies at a final dilution of 1:1000 (blue curve). Scan rate: 50  $\text{mV s}^{-1}$ .

In the case of the glucosylated ferrocenyl peptide II, the peak potential was shifted of 34 mV towards positive values by addition of anti-CSF114(Glc) antibodies. However, in this case, a study of the nature of the protective monolayer should be investigated to confirm the interest of the glycopeptide II for autoantibody detection.

The results are summarized in Figure 7. The glucosylated biosensor Au-III and the glucosylated ferrocenyl peptide II in solution shift of more than 30 mV towards positive values by addition of anti-CSF114(Glc) antibodies. This is indicative of detection of antigen–antibody interaction, and therefore of the presence of autoantibodies in the tested MS patients' sera. The negative control experiments performed with the unglucosylated biosensors showed a very small potential

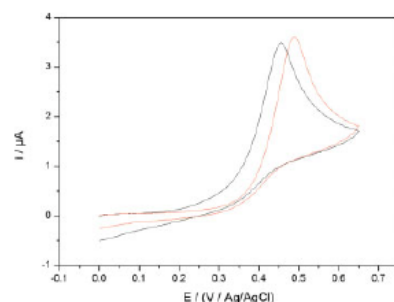


**FIGURE 6** Cyclic voltammetry of II,  $1.77 \times 10^{-4}$  M in a tween solution containing  $\text{LiClO}_4$  0.1M and  $\text{Fe}(\text{CN})_6^{4-}$   $9 \times 10^{-4}$  M (black curve) without antibodies and (red curve) with a solution of purified anti-CSF114(Glc) antibodies at a final dilution of 1:1000. Scan rate: 50  $\text{mV s}^{-1}$ .

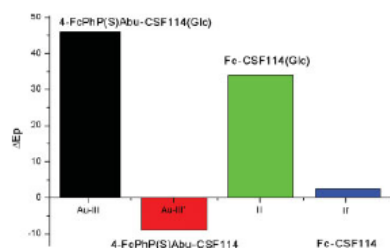


**FIGURE 7** Electrochemical immunoassay: potential difference between the electrochemical response with and without purified anti-CSF114(Glc) antibodies at a final dilution of 1:1000 for (black) the biosensor Au-III, (red) its negative control Au-III', (green) the ferrocenyl glycopeptide II in solution and (blue) its negative control II' in solution.

shift, positive in the case of the ferrocenyl peptide II' and in the opposite direction for Au-III'.

## CONCLUSIONS

In conclusion, the new ferrocenyl peptides containing the unnatural amino acid 4-FcPhP(S)Abu are able to detect specific anti-CSF114(Glc) antibodies by electrochemical technique. Moreover, thanks to the presence of thiophosphine, the modified glycopeptide 4-FcPhP(S)Abu-CSF114(Glc) (III) is able to build simple monolayers on gold surfaces and it can be useful for antibody detection and quantitative determinations. The possibility of grafting these new ferrocenyl glycopeptides, as synthetic antigenic probes, directly on the electrode surface (as a valid alternative analytical method to detect autoantibodies in sera of MS patients) is currently under investigation in our laboratories.

In this article, we demonstrated the possibility of detecting isolated antibodies by Cyclic Voltammetry in samples containing 1:1000 diluted antibodies. This detection limit is in any case lower compared to the one set up in our validated ELISA on sera.<sup>11,12</sup> Therefore, we are confident that this new voltammetry-based technique could be useful in detecting antibodies in sera of multiple sclerosis patients.

## EXPERIMENTAL PROCEDURES

### Materials

Fmoc-protected amino acids and Fmoc-Lys(Boc)-Wang resin were obtained from Novabiochem AG (Laufelfingen, Switzerland). 2-(1*H*-Benzotriazol-1-yl)-1,1,3,3-tetramethyluronium tetrafluoroborate (TBTU) was from Iris-Biotech. Peptide-synthesis grade *N,N*-dimethylformamide (DMF) was from Scharlau (Barcelona, Spain).

Trifluoroacetic acid (TFA), dichloromethane (DCM), piperidine, *N*-methylmorpholine (NMM), *N,N*-diisopropylethylamine (DIPEA), 11-mercaptoundecanoic acid, decanethiol, and ferrocene carboxylic acid (FcCOOH) were purchased from Aldrich. 1-Hydroxy-7-azabenzotriazole (HOAt) was from PerSeptive Biosystems. HPLC-grade acetonitrile (MeCN) was purchased from Carlo Erba (Italy).

### Synthesis of (S<sub>p</sub>S)-(+)-2-(*tert*-butoxycarbonylamino)-4-(ferrocenylphenylthiophosphino)butanoic acid

The ferrocenyl thiophosphine amino acid [4-FcPhP(S)Abu] was synthesized in 48% yield,<sup>23</sup> by reaction of (S)-ferrocenylphenylphosphine borane with the benzyl (S)-(-)-2-[bis(*tert*-butoxycarbonyl)amino]-4-iodobutanoate, (previously prepared according a modified procedure),<sup>24</sup> then subsequent sulfuration and deprotection to afford the free carboxylic acid group.

(S<sub>p</sub>S)-(+)-2-(*tert*-butoxycarbonylamino)-4-(ferrocenylphenylthiophosphino)butanoic acid:<sup>19</sup> orange powder;  $\alpha_D = +49$  ( $c = 0.6$ , CHCl<sub>3</sub>); <sup>1</sup>H NMR (CDCl<sub>3</sub>)  $\delta$  1.35 (s, 9H, t-Bu), 1.79 (m, 1H, CHH), 2.26–2.28 (m, 3H, CH<sub>2</sub>, CHH), 4.12 (s, 5H, Cp), 4.27–4.55 (m, 5H, Cp, CHN), 5.15 (sl, 0.5H, NH), 6.67 (sl, 0.5H, NH), 7.41 (m, 3H, Ph), 7.82 (m, 2H, Ph); <sup>31</sup>P NMR (CDCl<sub>3</sub>)  $\delta$  +42.6; HRMS (ESI, m/z) Calcd for C<sub>25</sub>H<sub>30</sub>FeNO<sub>4</sub>PS: 527.0977 (M<sup>-</sup>); observed: 527.0931. Anal. Calcd for C<sub>25</sub>H<sub>30</sub>FeNO<sub>4</sub>PS: C, 56.94; H 5.73; N 2.66. Found: C, 56.26; H 5.94, N, 2.52.

### Peptide Synthesis

Solid-phase peptide synthesis (SPPS) was performed by microwave assisted automatic peptide synthesizer Liberty<sup>TM</sup> Microwave Peptide Synthesizer (CEM Corporation, Matthews, NC), an additional module of Discover<sup>TM</sup> (CEM Corporation, Matthews, NC) that combines microwave energy at 2450 MHz following the fluorenylmethoxycarbonyl (Fmoc)/*tert*-butyl (tBu) strategy. CSF114 and CSF114(Glc) were prepared starting from a Fmoc-Lys(Boc)-Wang resin (0.67 mmol/g). Fmoc deprotections were performed with a 20% piperidine in DMF solution. Fmoc amino acids were stored as 0.3M DMF solutions. Coupling reagent was predissolved in DMF (0.3M solution). Coupling reactions were performed with 2.5 equiv. of TBTU in DMF (0.25M), 2.5 equiv. of amino acids in DMF (0.1M), and 3.5 equiv. of DIPEA in NMP solution (0.7M). Glucosyl moiety of glycosylated peptide I was introduced as the building-block Fmoc-L-Asn[GlcOAc4]-OH (2.5 equiv.) which was synthesized as previously reported.<sup>16</sup> Deprotection and coupling reactions were performed with microwave energy and nitrogen mixing. Microwave cycle was characterized by two deprotection steps (30 s, 180 s). All microwave coupling reactions were of 300 s at 75°C.

Ferrocenyl carboxylic acid (Fc-COOH) (2.0 equiv.) was coupled with TBTU (2 equiv.), HOBT (2 equiv.), and NMM (3 equiv.) in the N-terminus of CSF114(Glc) and CSF114 sequences, respectively, for 1.5 h on a manual batch synthesizer (PLS 4 × 4, Advanced ChemTech) using Teflon reactors (10 ml) obtaining peptides II and II'. (S<sub>p</sub>S)-(+)-2-(*tert*-butoxycarbonylamino)-4-(ferrocenylphenylthiophosphino)butanoic acid was coupled with TBTU (2 equiv.), HOBT (2 equiv.), and NMM (3 equiv.) in the CSF114(Glc) and CSF114 sequences respectively for 1.5 h on a manual batch synthesizer obtaining peptides III and III'.

Peptide cleavages from the resin and deprotection of the amino acids side chains were carried out with 1 ml/100 mg of resin of TFA/

aniso1,2-ethanedithiol/phenol/H<sub>2</sub>O solution (96:1:1:1 v/v/v/v). The cleavage was maintained for 3 h at room temperature. The resins were washed with TFA and the filtrates partially evaporated. The crude products were precipitated with diethyl ether, collected by centrifugation, dissolved in H<sub>2</sub>O and lyophilized with an Edwards apparatus, model Modulyo.

Deacetylation of sugar moieties linked to the peptides I–III was performed with a 0.1 M methanolic NaOMe solution until pH 12 to a solution of the lyophilized peptides in dry MeOH (1 ml/100 mg of resin). After 3 h the reaction was quenched by adding concentrated HCl until pH 7, the solvent was evaporated under vacuum and the residue lyophilized.

All peptides were purified by semipreparative RP-HPLC Waters mod. 600 with Jupiter C18 (10 μm, 250 mm × 10 mm), at 4 ml min<sup>-1</sup> using methods described in Table I and the purity of the peptides was analyzed using a Waters Alliance (model 2695) with Jupiter Phenomenex column (5 μm, C18, 200 Å, 250 mm × 4.6 mm of diameter) at 1 ml min<sup>-1</sup> of a mixture of eluents: (A) 0.1% TFA in H<sub>2</sub>O (MilliQ) and (B) 0.1% TFA in CH<sub>3</sub>CN, λ = 254 nm.

Characterization of the products were performed by Ultra Performance Liquid Chromatography using an ACQUITY UPLC (Waters Corporation, Milford, Massachusetts) coupled to a single quadrupole ESI-MS (Micromass ZQ) using a 2.1 mm × 50 mm 1.7 μm ACQUITY BEH C18 at 30°C, with a flow rate of 0.45 ml min<sup>-1</sup>.

### Immunological Assays

Serum was obtained for diagnostic purposes from patients and healthy blood donors who had given their informed consent, and stored at -20°C until use.

Antibody responses were determined in SP-ELISA. Ninety-six-well activated polystyrene ELISA plates (NUNC Maxisorb SIGMA) were coated with 1 μg per 100 μl of peptides per well or glycopeptides in pure carbonate buffer 0.05 M (pH 9.6) and incubated at 4°C overnight. After five washes with saline containing 0.05% Tween 20, nonspecific binding sites were blocked by fetal calf serum, 10% in saline Tween 20 (100 μl per well) at room temperature for 60 min. Sera diluted from 1:100 to 1:100,000 were applied at 4°C overnight in saline/Tween 20/10% FCS. After five washes, we have added 100 μl of alkaline phosphatase conjugated anti-human IgM (diluted 1:200 in saline/Tween 20/FCS) or IgG (diluted 1:8000 in saline/Tween 20/FCS) (Sigma) to each well. After 3 h at room temperature incubation and five washes, 100 μl of substrate solution consisting of 1 mg/ml *p*-nitrophenyl phosphate (Sigma) in 10% diethanolamine buffer was applied. After 30 min, the reaction was stopped with 1 M NaOH (50 μl), and the absorbance was read in a multi-channel ELISA reader (Tecan Sunrise) at 405 nm. ELISA plates, coating conditions, reagent dilutions, buffers, and incubation times were tested in preliminary experiments.<sup>11</sup> The antibody levels are expressed as absorbance in arbitrary units at 405 nm (sample dilution 1:100).

Antibody affinity was measured by following the methods reported.<sup>25</sup> The semi-saturating sera dilution (1:600) was calculated from the preliminary titration curves (absorbance, 0.7). At this dilution, Abs were preincubated with increasing synthetic peptide antigen concentration (0; 7.68 E-11; 7.68 E-10; 7.68 E-09; 7.68 E-08; 7.68 E-07; 7.68 E-06; 3.84 E-05) for 1 h at room temperature. Unblocked Abs was revealed by ELISA, and the antigenic probe concentration-absorbance relationship was presented graphically.

### Electrochemical Apparatus

In a cyclic voltammetry (CV) experiment, the potentiostat applied a potential ramp to the working electrode to gradually change the potential and then reversed the scan, returning to the initial potential at a constant scan rate.

The electrochemical instrumentation includes an EG&G 283 potentiostat connected to a PC and the collected data were analyzed using a Princeton Applied Research Software, Power Suite.

A special electrochemical cell was used to handle only few microliters. The auxiliary electrode is a platinum wire and the reference is an Ag/AgCl electrode separated from the solution by a vycor tip. The active working electrode is a 1.6 mm diameter gold electrode (BAS) protected by 11-mercaptoundecanoic acid SAM from the ferrocenyl glycopeptide II. In the case of III and III', a mixture of 11-mercaptoundecanoic acid and decanethiol was used after immobilization of the ferrocenyl glycopeptides.

The electrochemical measurements have been realized in a 0.05% tween 20 solution containing LiClO<sub>4</sub> 0.1 M and potassium ferrocyanide (K<sub>4</sub>Fe(CN)<sub>6</sub>, Aldrich), 9 × 10<sup>-4</sup> M at room temperature. The concentration of Fc-CSF14(Glc) is 1.77 × 10<sup>-4</sup> M. Specific autoantibodies were diluted at 1:1000. All solutions were deoxygenated prior to experiments.

PAI Galilée N°11686QA (2006), MIUR (Italy), Ente Cassa Risparmio di Firenze, the Ministère de la Recherche et des Nouvelles Technologies (grant for AC) and the Burgundy Council are gratefully acknowledged.

### REFERENCES

- Roland, P.; Atkinson, J. A.; Lesko, L. *J Clin Pharm Ther* 2003, 28, 284–291.
- Baker, M. *Nat Biotechnol* 2005, 23, 297–304.
- Leslie, D.; Lipsky, P.; Notkin, A. L. *J Clin Invest* 2001, 108, 1417–1422.
- Doyle, H. A.; Mamula, M. J. *Trends Immunol* 2001, 22, 443–449.
- Lolli, F.; Rovero, P.; Chelli, M.; Papini, A. M. *Expert Rev Neurotherapeutics* 2006, 6, 781–794.
- Sebbag, M.; Simon, M.; Vincent, C.; Masson-Bessiere, C.; Girbal, E.; Durieux, J. J.; Serre, G. *J Clin Invest* 1995, 95, 2672–2679.
- Serre, G. *Joint Bone Spine* 2001, 68, 103–105.
- Schellekens, G. A.; de Jong, B. A.; van den Hoogen, F. H.; van de Putte, L. B.; van Venrooij, W. J. *J Clin Invest* 1998, 101, 273–281.
- Alcaro, M. C.; Lolli, F.; Migliorini, P.; Chelli, M.; Rovero, P.; Papini, A. M. *Chim Oggi* 2007, 25, 14–16.
- Vossenaar, E. R.; van Venrooij, W. J. *Clin Appl Immunol Rev* 2004, 4, 239–262.
- Lolli, F.; Mulinacci, B.; Carotenuto, A.; Bonetti, B.; Sabatino, G.; Mazzanti, B.; D'Ursi, A. M.; Novellino, E.; Pazzagli, M.; Lovato, L.; Alcaro, M. C.; Peroni, E.; Pozzo-Carrero, M. C.; Nuti, F.; Battistini, L.; Borsellino, G.; Chelli, M.; Rovero, P.; Papini, A. M. *Proc Natl Acad Sci USA* 2005, 102, 10273–10278.
- Lolli, F.; Mazzanti, B.; Pazzagli, M.; Peroni, E.; Alcaro, M. C.; Sabatino, G.; Lanzillo, R.; Brescia Morra, V.; Santoro, L.; Gasperini, C.; Galgani, S.; D'Elia, M. M.; Zipoli, V.; Sotgiu, S.; Pugliatti, M.; Rovero, P.; Chelli, M.; Papini, A. M. *J Neuroimmunol* 2005, 167, 131–137.

## SUPPLEMENTARY MATERIAL

13. Carotenuto, A.; D'Ursi, A. M.; Mulinacci, B.; Paolini, I.; Lolli, F.; Papini, A. M.; Novellino, E.; Rovero, P. A. *J Med Chem* 2006, 49, 5072–5079.
14. Mazzucco, S.; Matà, S.; Vergelli, M.; Fioresi, R.; Nardi, E.; Mazzanti, B.; Chelli, M.; Lolli, F.; Ginanneschi, M.; Pinto, E.; Massacesi, L.; Papini, A. M. *Bioorg Med Chem Lett* 1999, 9, 167–172.
15. Nuti, F.; Paolini, I.; Cardona, F.; Chelli, M.; Lolli, F.; Brandi, A.; Goti, A.; Rovero, P.; Papini, A. M. *Bioorg Med Chem* 2007, 15, 3965–3973.
16. Paolini, I.; Nuti, F.; Pozo-Carrero, M. C.; Barbetti, F.; Kolesinska, B.; Kaminski, Z. J.; Chelli, M.; Papini, A. M. *Tetrahedron* 2007, 48, 2901–2904.
17. Papini, A. M.; Rovero, P.; Chelli, M.; Lolli, F. Granted U.S.A. Patent and PCT Application WO 03/000733 A2.
18. Papini, A. M. *Nat Med* 2005, 11, 13.
19. Van Staveren, D. R.; Metzler-Nolte, N. *Chem Rev* 2004, 104, 5931–5985.
20. Chantson, J. T.; Verga Falza, M. V.; Sergio Crovella, S.; Metzler-Nolte, N. *Chem Med Chem* 2006, 1, 1268–1274.
21. Rizzolo, F.; Sabatino, G.; Chelli, M.; Rovero, P.; Papini, A. M. *Int J Pept Res Ther* 2007, 13, 203–208.
22. (a) Creager, S. E.; Radford, P. T. *J Electroanal Chem* 2001, 500, 21–29. (b) Radford, P. T.; French, M.; Creager, S. E. *Anal Chem* 1999, 71, 5101–5108. (c) Radford, P. T.; Creager, S. E. *Anal Chim Acta* 2001, 449, 199–209. (d) Bergren, A. J.; Porter, M. D. *J Electroanal Chem* 2006, 591, 189–200.
23. Colson, A.; Bayardon, J.; Rémond, E.; Lauréano, H.; Nuti, F.; Meunier-Prest, R.; Kubicki, M.; Darcel, C.; Papini, A. M.; Jugé, S. *J Org Chem*, submitted for publication.
24. Adamczyk, M.; Johnson, D. D.; Reddy, R. E. *Tetrahedron: Asymmetry* 2000, 11, 3063–3068.
25. Rath, S.; Stanley, C. M.; Steward, M. W. *J Immunol Methods* 1988, 106, 245–249.

MANUSCRIPT SUBMITTED

### Microwave-assisted Stereoselective Synthesis of $\alpha$ - and $\beta$ -linked Glucosyl Building Blocks useful for Solid-phase Peptide Synthesis

Feliciana Real-Fernández,<sup>1,2</sup> Francesca Nuti,<sup>1,2</sup> Mario Chelli,<sup>1,2</sup> Michael Chorev,<sup>3</sup> Paolo Rovero,<sup>1,4</sup> and Anna M. Papini<sup>1</sup>

<sup>1</sup>Laboratory of Peptide & Protein Chemistry & Biology, Polo Scientifico e Tecnologico, University of Firenze, I-50019, (FI) Sesto Fiorentino, Italy; <sup>2</sup>Dipartimento di Chimica Organica "Ugo Schiff" and CNR ICCOM, Via della Lastruccia 13, Polo Scientifico e Tecnologico, University of Firenze, I-50019, (FI) Sesto Fiorentino, Italy; <sup>3</sup>Laboratory for Translational Research, Harvard Medical School, One Kendall Square, Building 600, Cambridge, MA 02139, USA.

RECEIVED DATE (automatically inserted by publisher); E-mail: annamaria.papini@unifi.it

Carbohydrates are involved in different biological processes, e.g., recognition signal, cell adhesion, cell growth regulation, etc.<sup>1</sup> Naturally occurring *N*-glycoproteins and *N*-glycopeptides are usually reported to present as first sugar an *N*-acetyl glucosamine *N*- $\beta$ -linked to Asn side chain into the specific consensus sequence Asn-Xaa-Ser/Thr (where Xaa is any amino acid except Pro). The *N*-glycosidic bond links the glycan portion and the side chain of an asparagine residue. One exception is represented by nephritogenoside, a glycopeptide able to induce glomerulonephritis in its animal model,<sup>2</sup> where Asn at the *N*-terminal sequence Asn-Pro-Leu is modified by a trisaccharide with *N*- $\alpha$ -Glc as the first sugar moiety.<sup>3</sup>

Synthetic preparation of glycopeptides and glycoproteins, even if difficult, becomes more and more necessary. In glycopeptide synthesis, much attention has to be paid to the stereoselective formation of the glycosidic bond, which should survive during all the steps of peptide synthesis. In solid phase synthesis by the building block approach, preformed glycosylated amino acids<sup>4</sup> are employed in the stepwise assembly of the peptide backbone. The use of anomerically pure glycosylated building blocks in solid-phase glycopeptide synthesis (SPGPS) guarantees the presence of a stereoselective sugar linkage to the amino acid side chain.

A variety of syntheses leading to *N*- $\beta$ -linked amino acid building blocks are reported in the literature.<sup>5</sup> In particular, thanks to microwave energy, large-scale synthesis of  $\beta$ -linked glycans to Asn and Gln side chains were optimised in shorter time and higher yield compared to conventional approaches.<sup>6</sup>

On the other hand, the interest in developing a stereoselective synthesis of *N*- $\alpha$ -linked glycosylated asparagine prompted us to investigate several strategies. Up to now very few ones have been reported and none for the anomeric building block orthogonally protected for both Fmoc/tBu and Boc/Bzl SPGPS.

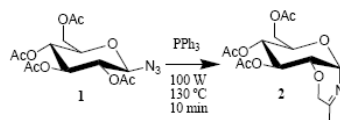
Recently, the use of glycosylazides as starting reagents has replaced the traditional glycosylamines, classically used in the synthesis of the  $\beta$ -anomer, as a consequence of poor final stereoselectivity.<sup>7</sup> A method for the stereoselective synthesis of *N*-glycosylated asparagine, based on the traceless Staudinger ligation of glycosyl azide with pre-functionalized phosphines, has been reported.<sup>8</sup> In this case, the  $\alpha$ -glycosyl amide could be obtained only when hydroxyl functions of the glycosyl moiety were benzyl-protected. This synthetic strategy required two more steps to change sugar hydroxyl protecting groups from benzyl to acetate.

Damkaci *et al* proposed a straightforward strategy to obtain acetylated *N*- $\alpha$ -glucosyl asparagine by controlling the

stereochemistry of the carbohydrate anomeric center via an isoxazoline intermediate.<sup>9</sup> We followed this strategy to try to obtain the desired building block Fmoc-Asn( $\alpha$ -GlcAc<sub>4</sub>)-OH orthogonally protected for SPGPS. First of all, we tried to improve the synthesis of the isoxazoline **3** by microwave (MW) technology.

While MWs are widely applied in other domains of organic synthesis, in the field of glycopeptide synthesis very few examples have been reported possibly because of the low stability of carbohydrates to thermal degradation.<sup>10</sup> Several results in other fields showed enhanced reaction rates and higher product yields as compared to conventional approaches.<sup>11</sup> Generally speaking, the MW energy should mainly be related to heat effects, and many reports have focused on "improvement of reactions".

The isoxazoline **2** was successfully synthesized under MW conditions at 100W and 130°C (Scheme 1). Thanks to MWs, the reaction time could be reduced from 15 h to only 10 min.

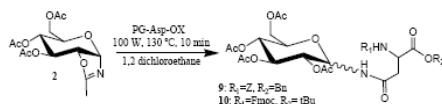


**Scheme 1.** MW-assisted synthesis of glucopyranosyl isoxazoline (**2**).

Damkaci *et al* reported the synthesis of *Z*-Asn( $\alpha$ GlcAc<sub>4</sub>)-OBn via acylation of the isoxazoline **2** leading to *N*- $\alpha$ -peracetylated glucosyl asparagine protected at the  $\alpha$ -amino function with a benzyloxycarbonyl group (*Z*) and at the  $\alpha$ -carboxyl function as benzyl ester (*Bn*). Unluckily, *Z*-Asn( $\alpha$ GlcAc<sub>4</sub>)-OBn is not a useful tool for SPGPS because *Z*/*Bn* are not orthogonal for solid phase strategy. This prompted us to perform several reactions to obtain *N*- $\alpha$ -glycosylated amino acids orthogonally protected for SPGPS, in particular Fmoc-Asn( $\alpha$ GlcAc<sub>4</sub>)-OtBu (**10a**). Finally, we succeeded in performing MW-assisted coupling reactions on differently protected aspartic acid derivatives (PG-Asp-OX) as acylating reagents (see Table 1) with the isoxazoline derivative **2** (Scheme 2). In fact, by MW irradiation (100 W), the reaction was complete in less than 10 min, maintaining the vessel temperature at 130 °C.

While *Z*-Asp(Spy)-OBn in the coupling reaction (Table 1) maintains a good stereoselectivity also under MW conditions, the use of Fmoc-Asp(Spy)-OtBu significantly decreased stereoselectivity and reaction yield. These results prompted us to develop a new strategy to obtain Fmoc-Asn( $\alpha$ GlcAc<sub>4</sub>)-OH.

## SUPPLEMENTARY MATERIAL



**Scheme 2** Coupling reaction of 3,4,6-tri-O-acetyl- $\alpha$ -D-glucopyranosyl isoxazoline **2** with PG-Asp-OX.

**Table 1** Coupling reaction conditions and reagents.<sup>a</sup>

PG-Asp-OX	equiv	$\alpha/\beta^b$	MW Protocol	Yield <sup>c</sup>
	3	No product	P = 100W T = 130°C Time = 10min	-
	3	53/47	P = 100W T = 130°C Time = 10min	32 %
	1	52/48	P = 100W T = 130°C Time = 10min	28%
	1.3 <sup>d</sup>	73/27	P = 100W T = 130°C Time = 10min	78%
	1.3 <sup>d</sup>	56/44	P = 100W T = 130°C Time = 10min	43%

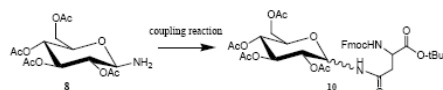
<sup>a</sup>All reactions were performed in a sealed vessel specific for the monomode microwave synthesizer CEM EXPLORER 48® in 1,2-dichloroethane using NMM, the coupling reagent DMT-NMM/BF<sub>4</sub>, and the acylating reagent PG-Asp-OX. Detailed protocol is reported in the Supporting material. <sup>b</sup>Calculated by HPLC analysis. <sup>c</sup>For isolated product. <sup>d</sup>CuCl<sub>2</sub>·2H<sub>2</sub>O was added as an additive. Syntheses of PG-Asp-OX **4**, **6**, and **7** are described in details in the Supporting material.

We previously reported a MW-assisted synthesis of Fmoc-Asn( $\beta$ GlcAc<sub>4</sub>)-OtBu coupling glucosylamine (1 equiv) to aspartic acid side chain (1 equiv) in the presence of NMM (1 equiv) and the new efficient triazine-based coupling reagent DMT-NMM/BF<sub>4</sub><sup>12</sup> displacing the equilibrium of the coupling reaction and favoring formation of the final product (Scheme 1).

Therefore, we developed a new MW-assisted strategy for the synthesis of the corresponding  $\alpha$ -glucosyl derivative Fmoc-Asn( $\alpha$ GlcAc<sub>4</sub>)-OH orthogonally protected for Fmoc/tBu SPGPS. We performed a series of coupling reactions changing different parameters (i.e., MW power, Temperature, and reaction time) to identify the optimal conditions leading to the *N*- $\alpha$ -linked glucosyl derivative **10a**. To the best of our knowledge, no data were reported on temperature effect influencing stereoselectivity of *N*-glycosidic bond formed between amino sugars and the side-chain carboxyl function of Asp.

The coupling reaction monitored by NMR and HPLC showed that in 5 min, at 70°C, and 100 W the *N*- $\beta$ -glucosyl derivative **10b** could be obtained and purified as a unique product (Table 2, entry 1). When temperature and MW power were increased, the  $\alpha$ -anomer **10a** started to form, with a maximum of  $\alpha/\beta$  ratio 87/13 at 150°C and 100 W (entry 5). Moreover, when MW power was increased from 100 W to 200 W (see entry 6) the  $\alpha/\beta$  ratio reached 92/8. By decreasing coupling reaction time to 1 min, it was possible to avoid N<sup>2</sup>-Fmoc deprotection possibly occurring because of high temperature.

All reaction conditions reported in Table 2 were also performed without microwave energy (data not shown). In that case only the *N*- $\beta$ -glucosyl anomer **10b** could be obtained.



**Scheme 3** Coupling reaction between 1-glucosylamine **8** and Fmoc-Asp-OtBu (**5**)

**Table 2** Comparative study of different coupling conditions for amide bond formation between 1-glucosylamine and aspartic acid side chain to obtain *N*- $\alpha$ - and/or *N*- $\beta$ -glucosyl derivatives **10a/10b**.

Entry	Temp <sup>a</sup> (°C)	Time <sup>b</sup> (min)	Power (W)	Yield <sup>c</sup> (%)	10 $\alpha$ /10 $\beta$ <sup>d</sup>
1	70	5	100	80	6/94
2	100	3	100	58	45/55
3	130	1	100	52	72/28
4	130	1	200	58	85/15
5	150	1	100	69	87/13
6	150	1	200	76	92/8

<sup>a</sup>All reactions were performed in a sealed vessel specific for the monomode microwave synthesizer CEM EXPLORER 48® in acetonitrile using Fmoc-L-Asp-OtBu, NMM, and the coupling reagent DMT-NMM/BF<sub>4</sub>. Protocol is described in details in the Supplementary material. <sup>b</sup>For coupling reaction. <sup>c</sup>At the temperature described. <sup>d</sup>For isolated product. <sup>e</sup>Calculated by HPLC analysis.

Considering that we achieved in a limited number of steps, with a very good yield Fmoc-Asn( $\alpha$ GlcAc<sub>4</sub>)-OH by microwave irradiation, we can hypothesize that the  $\alpha$ -anomer is the thermodynamically favored compound.

In any case, playing with microwave energy we can decide to obtain the  $\alpha$  or the  $\beta$ -anomer in high yield and short reaction time.

The *N*-glucosyl asparagine derivatives **10a** and **10b** could be successfully purified independently by Flash Column Chromatography. After deprotection of the  $\alpha$ -carboxyl function by a TFA solution in DCM we obtained the two anomeric pure building blocks useful for SPGPS, Fmoc-Asn( $\alpha$ GlcAc<sub>4</sub>)-OH (**11a**) and Fmoc-Asn( $\beta$ GlcAc<sub>4</sub>)-OH (**11b**), orthogonally protected for Fmoc/tBu strategy.

### References

- (1) (a) Varki, A. In: *Essentials of glycobiology*, ed. Cold Spring Harbor Laboratory Press, New York, 1999. (b) T. W. Rademacher, R. B. Parekh, R. A. Dwek. *Ann. Rev. Biochem.* 1988, 57, 785-838.
- (2) Shibata, S., Sakaguchi, H., and Nagasawa, T.; *Nephron*, 1976, 16, 241-245.
- (3) (a) Shibata, S.; Takeda, T.; Natori, Y. *J. Biol. Chem.* 1988, 263, 12483-12485. (b) Takeda, T.; Sawaki, M.; Ogiwara, Y.; Shibata, S. *Chem. Pharm. Bull.* 1989, 37, 54-56.
- (4) (a) M. Meldal. In: *Neoglycoconjugates: Preparation and Application*, ed. Y. C. Lee and R. T. Lee, Academic Press, Orlando, 1994, 145-198; (b) M. Meldal, *Cur. Opin. Struct. Biol.*, 1994, 4, 710-718; (c) M. Meldal, K. Bock, *Glycoconjugate J.*, 1994, 11, 59-63.
- (5) (a) Christiansen-Brans, I.; Meldal, M.; Bock, K. *J. Chem. Soc. Perkin Trans. 1*, 1993, 1461-1471. (b) Van Ameijde, J.; Albada, H.B.; Liskamp, R.; *J. Chem. Soc. Perkin Trans. 1*, 2002, 1042-1049. (c) Toshimi, I. 1994, *patent*: JP 93-77583 19930311. (d) Yang, L.; Liu, R.; Zhang, J.; Lam, K.; Lebrilla, C. B.; Gervay-Hague, J. *J. Comb. Chem.* 2005, 7, 372-384.
- (6) Paolini, I.; Nuti, F.; Pozo-Carrero, M.C.; Barbeti, F.; Kolesinska, B.; Kaminski, Z.J.; Chelli, M.; Papi, A.M. *Tetrahedron*, 2007, 48, 2901-2904.
- (7) (a) Staudinger, H.; Meyer, J. *Helv. Chim. Acta* 1919, 2, 635-646. (b) Gololobov, Y. G.; Kasukhin, L. F. *Tetrahedron*, 1992, 48, 1353-1407. (c) Kovacs, L.; Ösz, E.; Domokos, V.; Holzer, W.; Györgydeák, Z. *Tetrahedron* 2001, 57, 4609-4621.
- (8) Bianchi, A.; Bernardi, A.; *J. Org. Chem.* 2006, 71 (12), 4565-4577.
- (9) Dankaci, F.; DeShong, P. *J. Am. Chem. Soc.* 2003, 125, 4408-4409.
- (10) (a) Das, S. K.; Reddy, K. A.; Abbineni, C.; Roy, J.; Rao, K. V. L. N.; Sachwani, R. H.; Iqbal, J. *Tetrahedron Lett.* 2005, 44, 4507. (b) Oliveira, R. N.; Filho, J. R. F.; Srivastava, R. M. *Tetrahedron Lett.* 2002, 43, 2141. (c) Das, S. K.; Reddy, K. A.; Roy, J. *Synlett* 2003, 1607.
- (11) (a) Kappe, C.O. *Angew. Chem. Int. Ed.* 2004, 43 6250. (b) Kappe, C.O.; Dallinger, D. *Nat. Rev. Drug Disc.* 2006, 5, 51.
- (12) (a) Kaminski, Z.J.; Kolesinska, B.; Kolesinska, J.; Sabatino, G.; Chelli, M.; Rovero, P.; Blaszczyk, M.; Glowka, M.L.; Papi, A.M. *J. Am. Chem. Soc.* 2005, 127, 16912. (b) Kaminski, Z.J. *Int. J. Pept. Protein Res.*, 1994, 43, 312-319.







Vorrei ringraziare tantissimo la Prof.ssa Anna Maria Papini e il Prof. Paolo Rovero per offrirmi l'opportunità di portare avanti questo dottorato.

Grazie alla Prof.ssa Maria Rosa Moncelli per la sua collaborazione durante questi tre anni.

I would like to thank Prof. Sylvain Jugé and Dr. Rita Meunier-Priest of the University of Burgundy for their collaboration in this work. I thank all the people that received me at Dijon.

Ringrazio il Prof. Vincenzo Lombardi e il Prof. Mariano Venanzi. Grazie al Dr. Pasquale Bianco per svelarmi i segreti della trappola ottica.

Collaborare con tutti voi mi ha permesso costruire questo bellissimo progetto.

Grazie a tutto il gruppo "bioelectrolab", in particolare a Francesco per i suoi contributi a questo lavoro.

Non troverò mai le parole giuste per ringraziare Mario Chelli e Francesca Nuti. Lavorare accanto a voi è stato un vero privilegio.

Non vorrei dimenticarmi di Elisa e il suo « immuno-aiuto », grazie mille.

Cari ringraziamenti anche per Giuseppina, Fabio, Alexandra, Mari, Debora, Alessandro e Francis. Grazie alla mia prima compagna di cappa Fra Barbetti, a Ilaria, Claudia, Paolo F., Alessandra, Stefano, ai miei colleghi di dottorato Francesca Gori e Jalal; alle giovani Stefania e Virginia e a tutto il popolo peptidico che mi è stato vicino.

Devo anche ringraziare tutta la gente che durante questa esperienza mi ha accompagnato anche fuori dal lab, Riccardo e Diana, Paola con Margot e Moro, gli *sciupati*, ed in particolare Benedetta per essere stata una conquillina molto vicina durante tutto questo tempo.

Ringrazio Ildo e Graziella per farmi sentire sempre a casa. E soprattutto a te, Marco.



Esta tesis está dedicada a la memoria de David Real,  
Y a toda mi familia y amigos, el auténtico pilar de mi vida.